Riparian vegetation characterization of the Lower Santa Cruz River and Ciénega Creek through remotely sensed multi-sensor data fusion

September 30, 2013

Addendum to:

Historical Conditions of the Effluent-Dependent Lower Santa Cruz River (March 2013)

Tyson L. Swetnam[1,3], D. Phillip Guertin[1] , Akitsu Kimoto[2] and Evan Canfield[2]

[1] School of Natural Resources and Environment, The University of Arizona, Biological Sciences East Building, Tucson AZ 85721 USA

[2] Pima County Regional Flood Control District, 97 E. Congress St. Tucson AZ

[3] Corresponding Author: email: tswetnam@email.arizona.edu, phone: (520) 247-2293

Table of Contents

Figures 4
Tables 5
Executive Summary 7
1 Introduction 8
2 Vegetation Descriptions 9
2.1 Vegetation Types 10
2.1.1 Hydroriparian 10
2.1.2 Mesoriparian 11
2.1.3 Xeroriparian 11
2.1.4 Disturbed 11
2.1.5 Non-native 11
3 Passive and Active Remote Sensing 9
3.1 Multi-spectral vegetation indices 12
3.1.1 NDVI 13
3.1.2 Alternative vegetation indexes: the SAVI & EVI 19
3.1.3 Existing vegetation map products 19
3.2 Airborne Laser Swath Mapping 20
3.2.1 Horizontal and vertical uncertainty 23
3.3 Physical and Remote Sensing of Vegetation 24
3.3.1 Recommendation for future TVV monitoring 26
4 Standard Operating Procedure 28
4.1 Quality Control / Quality Assurance 29
4.2 Creating a FUSION Project 30
4.3 FUSION in Windows Command Line 31
4.3.1 Bare Earth Model 33
4.3.2 Canopy Height Model 34
4.3.3 GridMetrics 36
4.4 ArcGIS Tutorial 40
4.4.1 Merging FUSION ASCII tiles in ArcGIS 40
4.5.2 ArcGIS LAS Dataset Creation 42

4.5.3 ArcGIS *.ASC layers 43
5 Summary of the analyses and recommendations for future LiDAR acquisitions 43
5.1 Baseline assessment of vegetation change 43
5.1.1 Lower Santa Cruz 43
5.1.2 Ciénega Creek 52
5.1.3 Vegetation change in other tributaries of the Tucson Basin 56
5.2 Multi-spectral Ortho-photography and Satellite Imagery 60
5.3 Recommended Data Density 61
5.4 Priority Coverage Areas 66
5.5 Creation of a regional LiDAR Consortium 66
5.6 Benefit Cost Analysis 68
5.7 Awareness of National Standards 69
5.8 Software and Online Support Networks 73
Free Software 73
Commercial Software 74
General Resources & Vendors 74
Existing State Level LiDAR Consortiums 74
6 Data 75
6.1 Acronym descriptions 75
6.2 Definitions 75
6.3 File Tree 76
References 78

Figures

Fig. 3.1a Essential components for generating vegetation type models with remote sensing.

Fig. 3.1.1a Example of 1-meter resolution NDVI image over Black Wash TVV site, Avra Valley.

Fig. 3.1.1b Example NDVI and hill shade over Ciénega Creek at the Three Bridges / Gabe Zimmerman Trailhead.

Fig. 3.1.1c Example aerial LiDAR Canopy Height Model over Ciénega Creek at the Three Brides / Gabe Zimmerman Trailhead.

Fig. 3.1.1d Result of the NDVI logical surface being multiplied by the 2008 aerial LiDAR canopy model.

Fig. 3.2a Example of 2011 aerial LiDAR over Ciénega Creek with a corresponding photo point looking to the east.

Fig. 3.2b Map of Pima County LiDAR coverage for the years 2005, 2007, 2008, and 2011, over the Tucson Basin.

Fig. 3.3a Example of the aerial LiDAR data from 2008 over the Black Wash, TVV transect # 8.

Fig. 3.3b Example of aerial LiDAR paired with a photo point from the Canoa Ranch area.

Fig. 4 Process tree of input file types and output file types.

Fig. 4.1a Examples of the QA/QC output images (coverage, intensity, and density).

Fig. 4.2a Screenshot of FUSION/LDV Graphic User Interface

Fig. 4.3a Screenshot of how to open a command window for generating file lists and editing in TextPad.

Fig. 4.3.2a Three examples of canopy height models along the LSCR from 2005 to 2011, along with the associated bare earth surface changes.

Fig. 4.3.2b Example of 2-foot canopy height model (maximum) over Black Wash TVV site, Avra Valley.

Fig. 4.3.3 GridMetric at 10 m resolution for the mean canopy height over Black Wash, Avra Valley.

Fig. 4.4a Screenshot of file process for moving GridMetrics into ArcGIS 'Mosaic to New Raster'.

Fig 4.4b: ArcGIS example showing the entire 2007 RFCD data over the Sabino watershed.

Fig. 4.5.1a Screenshot of ArcGIS 10.1 *.LASD tile coverage.

Fig. 4.5.1b Screenshot of ArcGIS 10.1 LAS Dataset 3D View.

Fig. 5.1.1a Change in vegetation along LSCR years 2005 – 2011.

Fig. 5.1.1b Map of vegetation change along the LSCR years 2005 – 2011.

Fig. 5.1.1c Map of vegetation change 2005-2011 along Orange Grove, near former gravel pit.

Fig. 5.1.1d Vegetation change 2005-2011 north of the Ina Rd. wastewater treatment facility, up to Cortaro Rd.

Fig. 5.1.1e Vegetation change 2005-2011 north of the Roger Rd. wastewater treatment facility.

Fig. 5.1.1f Vegetation change 2005-2011 north of Curtis Rd up to Orange Grove Rd.

Fig. 5.1.2a Map of vegetation change 2005-2011 along the Ciénega Creek for both a bare earth and canopy height model.

Fig. 5.1.2b Vegetation change greater than 2 ft in the Ciénega Creek between 2005 and 2011.

Fig. 5.1.2c Change in vegetation along the Ciénega Creek between 2005 and 2011.

Fig. 5.1.3a Log-log scaling of the observed mean canopy height.

Fig. 5.1.2d Change in vegetation near the Pantano Jungle Restoration site, along the Ciénega Creek between 2005 and 2011.

Fig. 5.1.2e: Comparison of vegetation change along the Ciénega Creek and LSRC.

Fig. 5.1.3a Log-log scaling of the observed mean canopy height along the clipped and masked sections of the riparian zones across the LiDAR coverage area.

Fig. 5.1.3b Change in total vegetation volume across periods.

Fig. 5.3a: Example of the 2005 bare earth model (upper) and the 2011 bare earth model (lower) along Ciénega Creek. The total difference between 2005 and 2011 is shown on bottom.

Fig. 5.3b: Example of the 2005 bare earth model (upper) and the 2011 bare earth model (lower) along Ciénega Creek. The total difference between 2005 and 2011 is shown on bottom.

Tables

Table 3.2 Flight parameters and pulse density details of the LiDAR datasets used in this project.

Table 3.3.1 List of riparian areas in Pima County with LiDAR coverage and monitoring project data.

Table 4.3.3 List of GridMetrics (FUSION, McGaughey 2012):

Table 5.3 The cost and benefit of aerial LiDAR pulse densities.

Table 5.6a LiDAR Standards given by ASPRS, USGS, and FEMA

Table 5.6b Pre-flight Operations Plan (from FEMA 2010).

Table 5.6c Post-flight Aerial Acquisition and Calibration Report (from FEMA 2010).

Table 5.6d LAS classification codes.

Table 5.6e Establishing what will be delivered is an important part of the contract.

Table 6.1 Acronyms used in this document

Executive Summary

The authors were tasked by the Pima County Regional Flood Control District (RFCD) to characterize recent change [2005-2011] in vegetation canopy structure along the effluent-dependent Lower Santa Cruz River (LSCR). This study establishes baseline conditions along the LSCR in support of the Living River Project, an EPA-funded venture, and is an addendum to the 'Historical Conditions of Effluent-Dependent Lower Santa Cruz River' (March 2013).

Two wastewater reclamation facilities (WRF) on the LSCR are presently undergoing a $660 million dollar upgrade to improve water quality. Regulatory compliance date for expansion and compliance with the regulatory effluent quality requirements is January 30, 2014 for the Ina Rd. WRF and January 30, 2015 for the Roger Rd. WRF. Changes in wetland condition are expected following the upgrade. Baseline change in vegetation was measured by aerial Light Detection and Range (LiDAR) from datasets covering a significant portion of the LSCR effluent riparian zone and are available for three different dates over a range of six years (2005, 2008, and 2011). Aerial LiDAR presently cover ~2,400 mi^2 within Pima County, these areas include many of the tributaries of the Santa Cruz.

New aerial LiDAR is scheduled for summer 2015 and will be the third to fourth re-measurement of these ecosystems in a ten year period. We report on the cost and benefit of acquiring higher density aerial LiDAR in 2011 over the LSCR and the Ciénega Creek Nature Preserve, versus lower density data which was collected in 2005 and 2008 and make a recommendation for future aerial LiDAR collections.

At present there are no comprehensive vegetation monitoring strategies or reporting tools for tracking changes in vegetation structure along the LSCR or other waterways in Pima County. This report outlines a standard protocol for monitoring both vegetation structure along the LSCR and the other water courses flown with aerial LiDAR. This report also outlines a technique for fusing passive sensor multi-spectral vegetation indices such as the Normalized Difference Vegetation Index (NDVI) to the LiDAR data derivatives. This technique improves the classification of vegetation and helps to discriminate geologic and human features from the data in both complex terrain and the urban interface.

Both vegetation and channel morphology are highly dynamic along the LSCR and Ciénega Creek across the observation period. Riparian vegetation was heavily impacted in all major waterways by a meso-scale 2006 flood event, currently vegetation are recovering and increasing in size and distribution. Hydro-riparian vegetation in the LSCR is increasing at rates that far exceed other riparian areas in Pima County that do not have effluent discharge. Importantly, these new effluent supported ecosystems are unlikely to survive future significant flood events, such as witnessed in 1983, 1993, and 2006. This result suggests benefits gained by restoration efforts to sustain or improve these systems have uncertainty in both the present and long term because the quantifiable ecological changes are transient.

Keywords: Lower Santa Cruz River, LiDAR, vegetation, monitoring, biomass, effluent, wetlands

1 Introduction

The characterization of vegetation at ecosystem scale is a classic problem for ecological monitoring and land management decision making. The cost of physically inventorying an entire ecosystem is both prohibitively expensive and physically impractical. One compromise to this scale problem has been to conduct statistically robust field campaigns where field data are collected at strategic locations and extrapolations of those data are used to estimate the properties of the entire ecosystem. Remote sensing can improve on field data and allow extrapolation across landscapes through regression modeling for areas of similar digital number values to those sampled in the field. Here we deploy one such technology, called aerial Laser Swath Mapping (ALSM), which we will refer to generically as aerial Light Detection and Ranging (LiDAR). In the last decade such active-sensor remote sensing technology has become both commercially available and readily affordable. Aerial LiDAR accurately measures vegetation, topography, and infrastructure with precision that surpasses most traditional survey measures, and does so at orders of magnitude greater resolution – taking millions to billions of point observations, versus the few hundred points typical of a traditional surveyor project.

The Lower Santa Cruz River (LSCR) is the longest effluent dependent river in Arizona. The effluent water from two wastewater reclamation facilities (WRF) in Metro Tucson has created approximately 200 acres of wetland habitat beginning north of the Roger Rd. facility on up through the town of Marana. The current $660 million dollar upgrades to the two wastewater treatment facilities are expected to be completed by early 2014 for the Ina Rd. WRF and early 2015 for the Roger Rd. WRF and will bring these treatment plants into full compliance with EPA regulations. These upgrades will substantially reduce nitrogen and other nutrients, as well as suspended solids loads. Subsequent changes are anticipated that will affect wetland health of the LSCR including riparian vegetation on the river.

Pima County through the Regional Flood Control District (RFCD), Regional Wastewater Reclamation Department (RWRD), and the Office of Sustainability and Conservation (OSC) have also initiated an EPA-funded project called: *The Living River – Charting the Wetland Health of the Lower Santa Cruz River.* The intent of this study is to establish ecosystem vegetation baseline conditions and report on vegetation change prior to the upgrade in support of *The Living River* project. This study was funded with RFCD tax levy funds as cost-share for an EPA Wetlands Grant awarded to Pima County to monitor changes in wetland health in the effluent dependent LSCR following upgrades to the treatment plants.

Here we assess the physical characteristics of woody plants along the riparian corridors of the Tucson Metro Area, with major foci on the LSCR and Ciénega Creek Nature Preserve. We conduct a change analysis of vegetation along the waterways with repeat LiDAR coverage and show how vegetation has changed over the baseline period [from 2005 – 2011]. In addition, we

make a recommendation for future ortho-photography and aerial LiDAR acquisitions, and provide a standard operating procedure for assessing vegetation structure with open-source LiDAR software and industry standard commercial software [e.g. ArcGIS (ESRI 2012)].

The sections of this report are divided into six sections:

1. This section
2. Brief description of riparian vegetation communities along the LSCR.
3. Methods for identifying and characterizing vegetation from passive (ortho-photography and satellite imagery) and active sensor (e.g. LiDAR) remote sensing.
4. A standard operating procedure for processing aerial LiDAR data sets.
5. Summary of analyses and recommendations for the 2015 aerial LiDAR acquisition.
6. Description of the data and of the deliverables file tree.

Each section has short summaries of the steps involved in characterizing the data in either a geographic information system (GIS) or from the field to the model process.

2 Vegetation Descriptions

Complete vegetation descriptions of both the past and present conditions on the LSCR are given in the *Historical Conditions Report 4 Historical Conditions of Vegetation* (Pima County 2013 pp. 4-1 to 4-12) and in Webb et al. (2013). In 2005 as part of the Watercourse and Riparian Habitat Protection and Mitigation Requirements Ordinance, the Pima County Board of Supervisors revised a regulatory Riparian Classification Map (RCM). Riparian habitat classifications in eastern Pima County are viewable here: http://gis.pima.gov/maps/mapguide/. The RCM was updated due to the inadequacies of the original 1994 maps, which did not cover all of eastern Pima County and used only multi-spectral LANDSAT data collected during the early 1990s. The 2005 RCM maps considered water availability, species composition, and structure for differentiating hydromesoriparian habitat from xeroriparian habitat. The classification of xeroriparian habitat into four subgroups relied on new NDVI from LANDSAT bands 3 and 4 using a natural breaks algorithm based on a review of the distribution (Fonseca and Regan 2002).

The absence of specific tree species, with a certain canopy volume or height does not define an area as one or another type of hydromesoriparian vegetation. Because riparian ecosystems are constantly in a state of flux, either from recent disturbance [e.g. flood scour or drought] or in a state of secondary succession, the use of volume or height categories as classified by LiDAR or Total Vegetation Volume (TVV) transect data does not qualify an area as being mesoriparian or hydroriparian. First principle measures of topography, including the presence of surface water or shallow groundwater, distance from channel, and location within the 100-year flood plain must also be taken into account when defining the potential natural vegetation type of any

section of the riparian zone. To be clear, indicator species like cottonwood or willow may be used to help differentiate hydromesoriparian from xeroriparian areas, but their absence does not disqualify a site from being suitable habitat for such.

However, for on-site or off-site mitigation purposes, replacement vegetation volumes for impacts to regulated riparian areas of unincorporated Pima County are defined in the Regulated Riparian Habitat Mitigation Standards and Implementation Guidelines (RFCD 2010). Xeroriparian vegetation volume standards are specified for four proportionate cover settings from most to least dense. City of Tucson uses slightly different vegetation volumes (TSMS 2013) for regulatory purposes. This LiDAR study combines elements of the RFCD and City of Tucson vegetation volume standards to classify riparian vegetation according to Table 2.1. and as further described below.

Table 2.1 Reference values for riparian habitat used in total vegetation volume (TVV) estimates of vegetation characteristics and species as described in RFCD Regulated Riparian Habitat Mitigation Standards and Implementation Guidelines (2010), maximum height estimates are from TSMS Vegetation Volume Classification scheme.

Habitat Class	TVV (	Height Range (ft & m)	Indicator Species	Structure
Hydroriparian	N/A	0-70 (ft) 0-22 (m)	Fremont cottonwood, black willow, ash, netleaf hackberry, Mexican elder, Arizona sycamore.	Gallery forest, closed canopy structure, little understory.
Mesoriparian	N/A	0-70 (ft) 0-22 (m)	Velvet mesquite, desert hackberry.	Bosque along flood channels
Xeroriparian High (A)	>1.26 (TSMS) >0.85 (RFCD)	16-20 (ft) 5-7 (m)	Velvet mesquite and blue palo verde	Open cover, scattered or heterogeneous assemblage.
Xeroriparian Intermediate (B)	>1.03 (TSMS)0.675-0.85 (RFCD)	6-15 (ft) 2-5 (m)	Velvet mesquite, white thorn acacia, blue palo verde, and desert broom	"
Xeroriparian Low (C)	>0.63 (TSMS) 0.5-0.675 (RFCD)	<6 (ft) <2 (m)	white thorn acacia and creosote	"
Disturbed and Xeroriparian Sparsely Vegetated (D)	<0.63 (TSMS) <0.5 (RFCD)	<3 (ft) <1 (m)	Invasive trees, plants, grasses, and weeds, N/A.	Sparse or absent due to recent disturbance

2.1 Vegetation Types

2.1.1 Hydroriparian

Hydroriparian is the least common and possibly most valuable riparian vegetation type in southern Arizona. Obligate species assemblages include Fremont Cottonwood (*Populus fremontii*), Arizona Sycamore (*Platanus wrightii*), black (Goodding's) willow (*Salix gooddingii*), coyote willow (*Salix exigua*), and netleaf hackberry (*Celtis reticulata*). Cottonwood-willow gallery forests and mesquite bosques are observed along the Ciénega Creek study area.

The hydroriparian zone in the LSCR driven by effluent, contains several native species, including the Gooding willow, and Fremont cottonwood; as well as and Athel woodland associations of Athel Tamerisk (*Tamarix aphylla*) (Historical Conditions Report, Pima County 2013). Riparian marshes or wetlands, '*ciénegas'* in Spanish, require perennial water or near surface ground water. Ciénegas were more common in the historical period before local agriculture diverted the Santa Cruz's ephemeral surface water and lowered the water table (Webb et al. 2013). There is still perennial surface water present in several locations around Pima County, including: the Ciénega Creek, Upper Sabino Creek, Agua Caliente Park, Rincon Creek, Tanque Verde Creek, and Upper Honey Bee Canyon. Riverine woodlands, referred to by the Spanish name '*bosque'* are also common along most of the intermittent streams (in Spanish '*arroyo'*) in southern Arizona.

2.1.2 Mesoriparian

Areas characterized as mesoriparian are typically made up of mesquite bosque. Mesoriparian areas typically include native species assemblages of trees and shrub that may not be obligate of surface water (Regulated Riparian Habitat Mitigation Standards and Implementation Guidelines, RFCD 2010; Historical Conditions Report, Pima County 2013, Webb et al. 2013). Facultative (not-required for survival) species in the mesoriparian include velvet mesquite (*Prosopis velutina*) which flourishes under riparian conditions when not out-competed by the obligate species. Webb et al. (2013) consider those community assemblages to be 'pseudo-riparian'.

2.1.3 Xeroriparian

Beyond the channelized hydroriparian waterway and mesoriparian bank habitats, are the ephemeral stream xeroriparian vegetation types. Xeroriparian is further subdivided into four classifications A through D, where A is the most dense category, and D is sparsely dense (RFCD 2010).

The xeroriparian vegetation in the Santa Cruz Valley is typical of Sonoran upland groups (RFCD 2010, Historical Conditions Report Pima County 2013, Webb et al. 2013) to the western Altar Valley with an increasing mix of Chihuahuan desert types along the eastern edges of the Rincon Valley.

2.1.4 Disturbed

Areas that are disturbed no longer exhibit characteristics of native vegetation and are either devoid of vegetation or include non-native species.

2.1.5 Non-native

In addition to the natural landscapes there are also large parcels of agriculture along the LSCR. There are several large groves of pecan trees, near the confluence of the Canada del Oro, and

north of Tucson in Marana are fields that rotate between alfalfa, cotton, corn, sorghum, and winter wheat.

There are also invasive communities of Athel Tamarisk along the riparian effluent corridor north of Roger Rd. Bamboo (*Bambuseae spp.*) is also present in some riparian drainages in the surrounding watersheds including in the Sabino Creek and Rincon Creek. Johnson Grass (*Sorghum halepense*) is also common along irrigation canals and the LSCR.

3 Passive and Active Remote Sensing

Passive and active remote sensing allows us to characterize ecosystem phenomena through analyses of observed spectral and spatial values compared to ecosystem measures. Passive remote sensing is dependent upon illumination of a surface target by the sun. Active remote sensing on the other hand uses its own light to illuminate a target. The aerial LiDAR discussed here uses an infrared laser beam to illuminate targets and record the distance from the sensor, which is then computed to derive the target's spatial location.

The fundamental limits of remote sensing are spatial, spectral and temporal resolution, and are dependent upon the type of sensor used (Ridd 1995, Huete et al. 1998, 2002, Lefsky et al. 2002, Kerr et al. 2003). For example, aerial photography has a high spatial resolution [< 1 meters (m)] but a narrow spatial coverage (the flight area), a long temporal scale (repeated annually or less than annually), and is generally limited to 3 to 4 spectral bands. Satellite data on the other hand have repeated measurements of hours to weeks, have global coverage, and dozens of spectral bands, but have a spatial scale of 900 m^2 (30 m pixel) to 1,210,000 m^2 (1.1 km pixel) due to the extreme distance of the sensor above the Earth's surface. Typically the resolutions of satellite data are too coarse for monitoring vegetation characteristics at local scale [the individual or patch level]. The availability of suitable remotely sensed data fundamentally limits (1) the ability to characterize phenomena at the individual level [e.g. trees or shrubs], and (2) tracking changes in vegetation over time.

3.1 Multi-spectral vegetation indices

Here we use four spectral band National Agricultural Imagery Program (NAIP) imagery (Boryan et al. 2011) [available over Tucson for the years 2005, 2007, and 2010: http://sco.azland.gov/imagery.htm] to create a vegetation index that helps to characterize the vegetation in the LiDAR structural data.

In order to accurately predict vegetation from other features [rocks, cliffs, houses, power-lines, etc.] that are present in the LiDAR we utilized a common technique for characterizing vegetation from remotely sensed data, the NDVI (Normalized Difference Vegetation Index). There were two available NAIP imagery collections with the required 4 spectral bands, from the

years 2007 and 2010. The 2007 image is two years after the 2005 LiDAR and one year before the 2008 LiDAR; the 2010 image is from 1 year before the 2011 LiDAR. We use the 2007 NDVI for the 2008 LiDAR and the 2010 NDVI for the 2011 LiDAR. Optimally, future LiDAR collections should be done at the same time as the ortho-photography to ensure the best possible alignment of vegetation with the LiDAR.

In order to determine what is vegetation versus what is geological or human built structure requires more than just LiDAR (Fig. 3.1).

Fig. 3.1 Essential components for generating vegetation type models with remote sensing.

3.1.1 NDVI

The NAIP ortho-photograph from 2007 covers most of the Pima Association of Governments (PAG) 2008 LiDAR acquisition including the LSCR and Ciénega Creek. The four bands are: Near Infrared (NIR), Red (R), Green (G), and Blue B. The NDVI requires the NIR and R bands for its calculation:

NDVI which supports an alternate threshold value because of differences in the time of day, the time of year, and the local growing conditions at the time the ortho-photo was acquired. Because the threshold for vegetation changes with vegetation type, and the range of values used in the 4-band ortho-photograph varied by scene, using a single cut-off threshold for the NDVI across the entire Tucson Basin is not possible or advisable. It is recommended the analyst determine a unique cut-off parameter for their project area based on the particular digital number values in the NAIP image under analysis before doing attempting any clipping of the LiDAR with the NDVI.

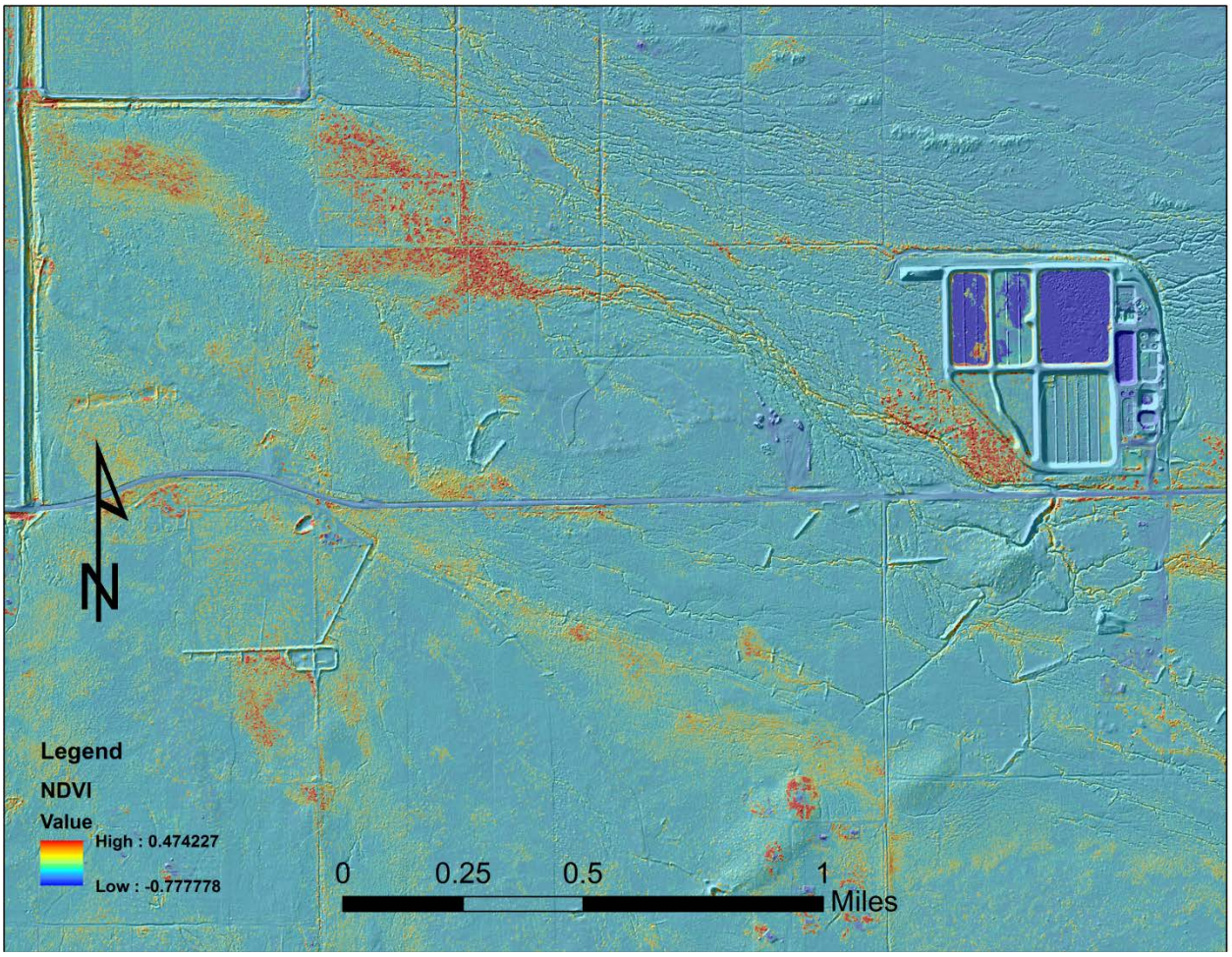

Fig. 3.1.1a 1 m^2 resolution NDVI over the Black Wash TVV site, Avra Valley.

The LANDSAT series of satellites use a combination of two bands for the NIR (Band 4) and R (Band 3) to derive NDVI:

LANDSAT data are available over the LSCR for an extended period covering the last 30 or so years. LANDSAT data have a spatial resolution of 900 m^2 (30 m) making them useful for characterizing communities of vegetation but not individual organisms.

Case Study: Davidson Canyon and Ciénega Creek at the Three Bridges

The area around the Gabe Zimmerman Memorial Trailhead [along the Ciénega Creek Nature Preserve] near Davidson Canyon off Marsh Station Rd is a good place to demonstrate the utility of NDVI for correcting error in a LiDAR canopy height model (CHM) (Fig. 3.1.1c). The vegetation along this section of the Ciénega Creek is characterized as hydroriparian with Cottonwood-willow gallery forest along the creek, mesoriparian within the flood plain, and xeroriparian along the toe slopes of the canyon and along the ridges above the creek. The 'Three Bridges' cross Ciénega Creek and are for two railroads and one for passenger vehicle bridge (Figure 3.1.1b).

The 2007 NDVI image was generated in ArcGIS using the Raster Calculator with the equation given above. The observed point at which the NDVI appeared to respond to visible vegetation in the ortho-photography over the xeroriparian areas was $\geq$0.014. After establishing a break value we suggest reclassifying the NDVI by a logical (0 or 1) value in ArcGIS using a Boolean expression in Spatial Analyst's Raster Calculator. Next, use the Raster Calculator to multiply the CHM by the logical – for example, if the logical value is 0 the canopy height data are removed from the product, if the logical value is 1 the CHM value is retained.

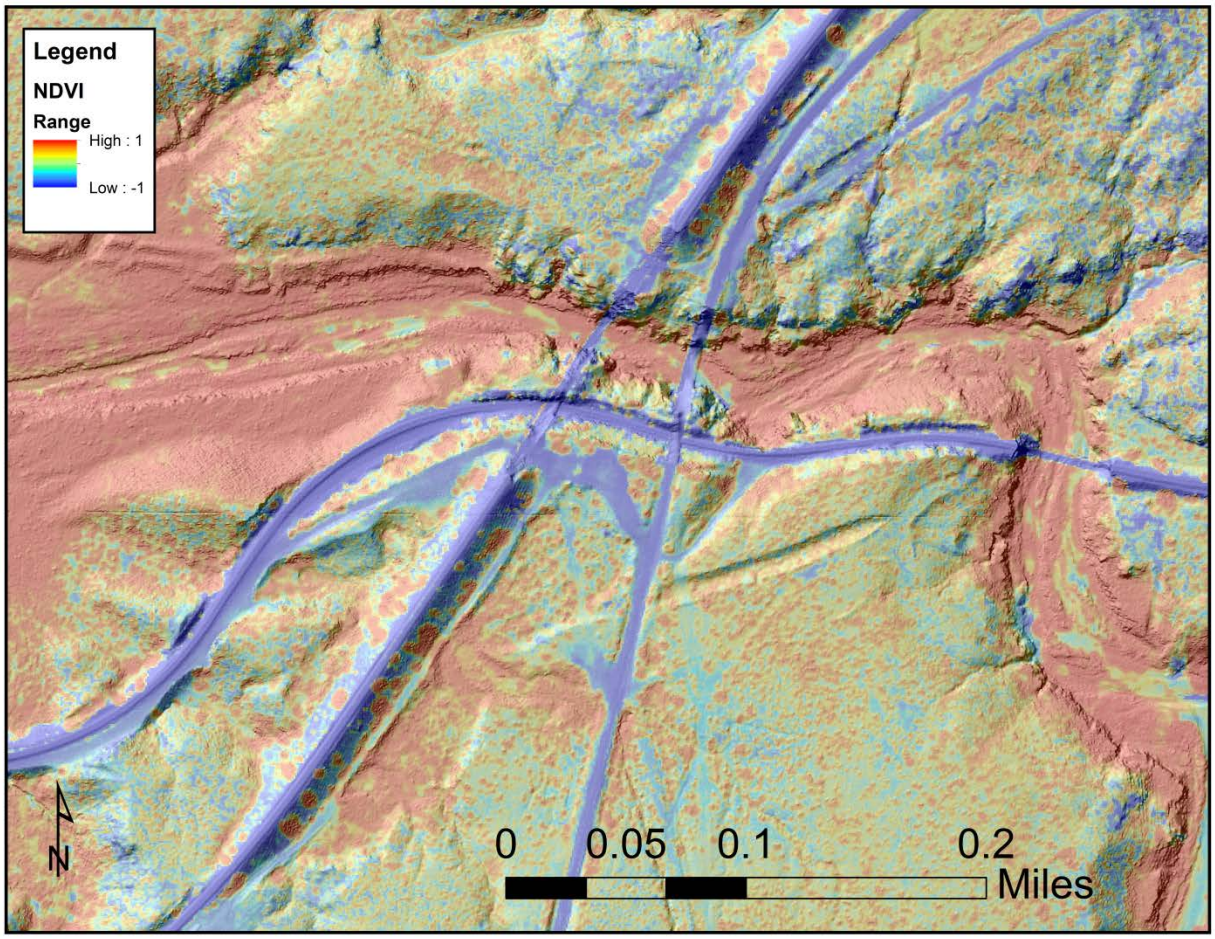

Fig. 3.1.1b A hillshade produced from the 2 ft resolution bare earth model, colored by the 2007 1 m NAIP NDVI. Positive values are from green vegetation (red = +1) and negative values are non-vegetated surfaces (blue = -1).

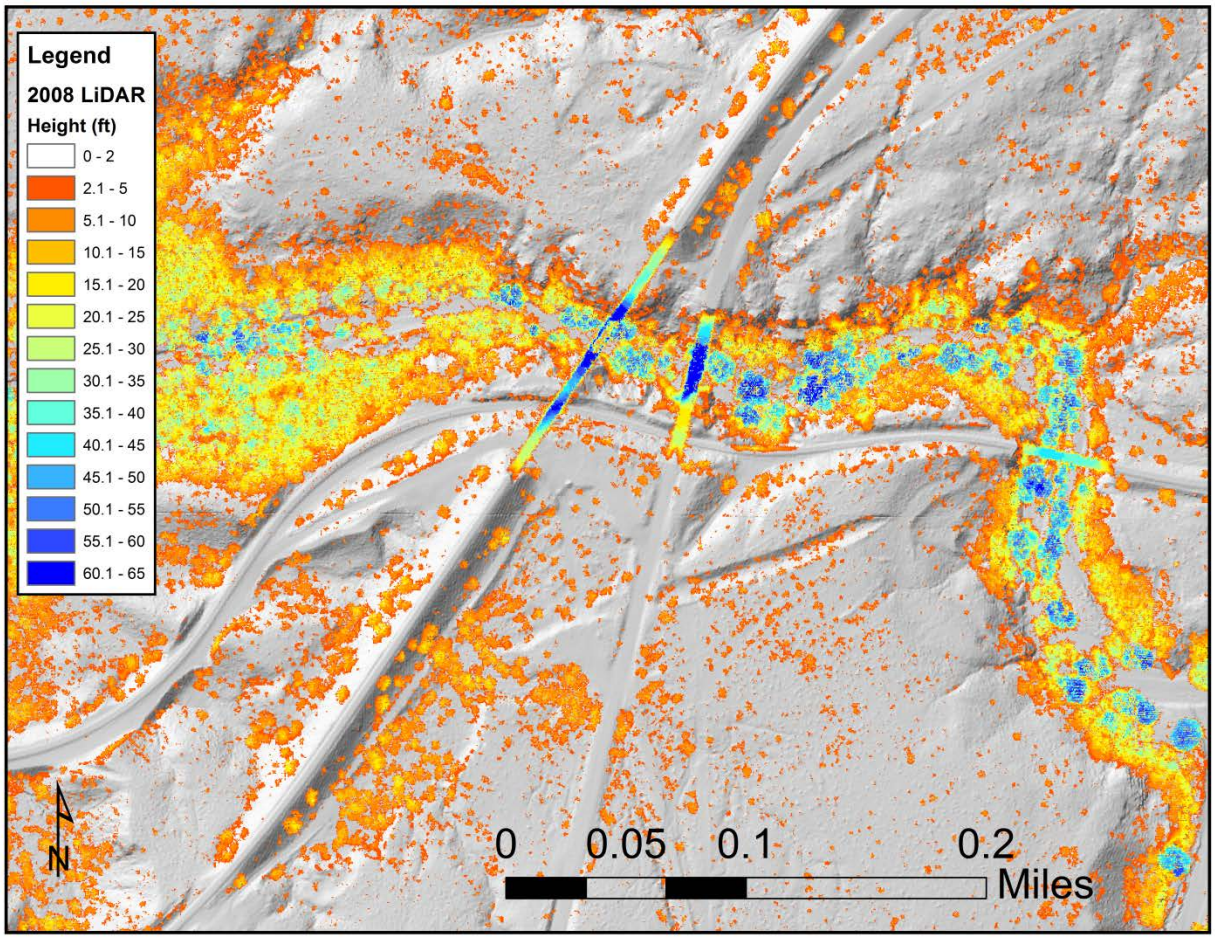

Fig. 3.1.1c The 2008 aerial LiDAR canopy height model at 2 ft resolution shows the three bridges over the canyon (light blue and darkest blue). The same type of modeling error is as likely for any structure or house seen across the Tucson Metro basin in the canopy height model.

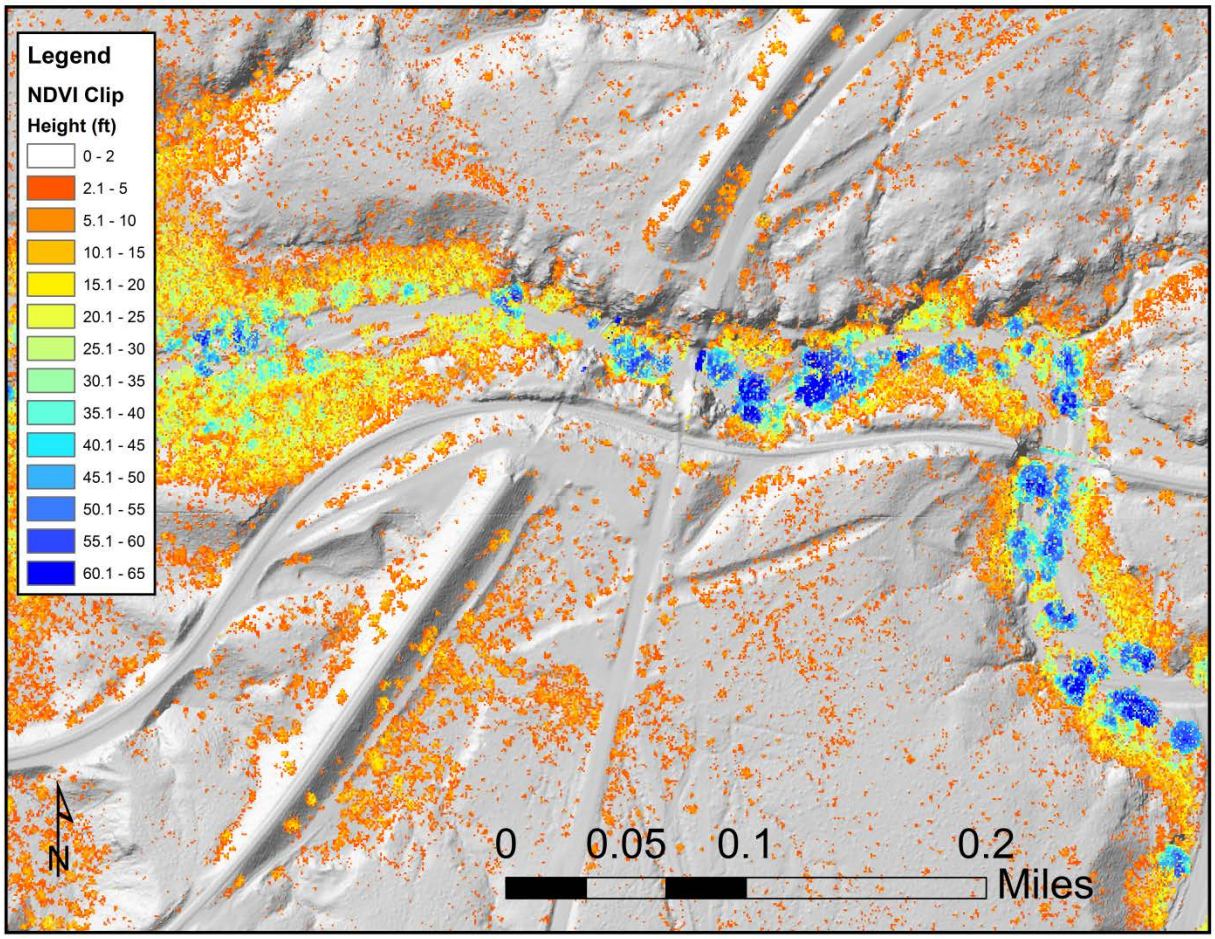

Fig. 3.1.1d Result of the NDVI logical surface being multiplied by the 2008 aerial LiDAR canopy model. The three bridges have been removed as have some features along the edges of the Ciénega Creek canyon wall.

3.1.2 Alternative vegetation indexes: the SAVI & EVI

Two additional alternative vegetation indices which may be calculated from multi-spectral imagery include the Soil Adjusted Vegetation Index (SAVI) (Huete 1988) or Enhanced Vegetation Index (EVI) (Huete et al. 2002, Jiang et al. 2008). We did not conduct either a SAVI or EVI in our analysis but we present the equations here in support of future end users.

Large areas of Pima County exhibit relatively little vegetative cover (<30% by total area) suggesting that a SAVI may be useful for correcting the reflectance of light in the red and infrared spectrum:

and surrounding Sky Islands (LANDFIRE 2010). Regional scale vegetation mapping products available include the LANDFIRE existing vegetation type maps (EVT) (LANDFIRE 2010). The LANDFIRE vegetation types were determined during a series of professional workshops in the early 2000's, the EVT layer was derived from remote sensing and ecological model data fusions that relied on LANDSAT imagery; thus the data resolution is set to the 30m pixel scale. The LANDFIRE EVT map can be used as a tool for selecting vegetation types from developed, urban, cropland, and mining at the 30 m scale.

The University of Arizona with the Nature Conservancy, USDA Forest Service, DOI BLM and National Park Service are engaged in a vegetation characterization and mapping project as part of the Arizona FireScape (www.AZFirescape.org). The various FireScape landscapes are located in Southeastern Arizona's Sky Islands. The Santa Catalina/Rincon FireScape extends close to the Ciénega Creek, Rincon Creek, Rillito, Canada del Oro washes. While these vegetation types do no not explicitly overlap the study areas here, they support the same communities of vegetation, and are considered to be equivalent and could potentially be extended to include these areas at a future date.

3.2 Airborne Laser Swath Mapping

The initial collection of aerial LiDAR data by PAG in 2005 was the largest, with ~2,340 mi^2 flown. In 2007, following the meso-scale flood event in 2006 which saw unprecedented flooding off the Santa Catalina Mountains and the destruction of several bridges and roads in the Sabino Canyon area, the Pima County RFCD contracted a flight over the entire Sabino Watershed. In 2008 PAG acquired a re-flight of most of the 2005 area with some additional new coverage (total area 1,787 mi^2), a partial re-flight of the previous areas plus more additional area not yet obtained in either flight was flown in 2011 [582 mi^2] (Table 3.2). In 2011 a special emphasis was placed on vegetation characterization for the LSCR north of Roger road where 9 mi^2 of moderate density [4-8 pulses per $meter^2$ (ppsm)] LiDAR was collected; over the Ciénega Creek Natural Preserve the highest density dataset was collected [>12 ppsm].

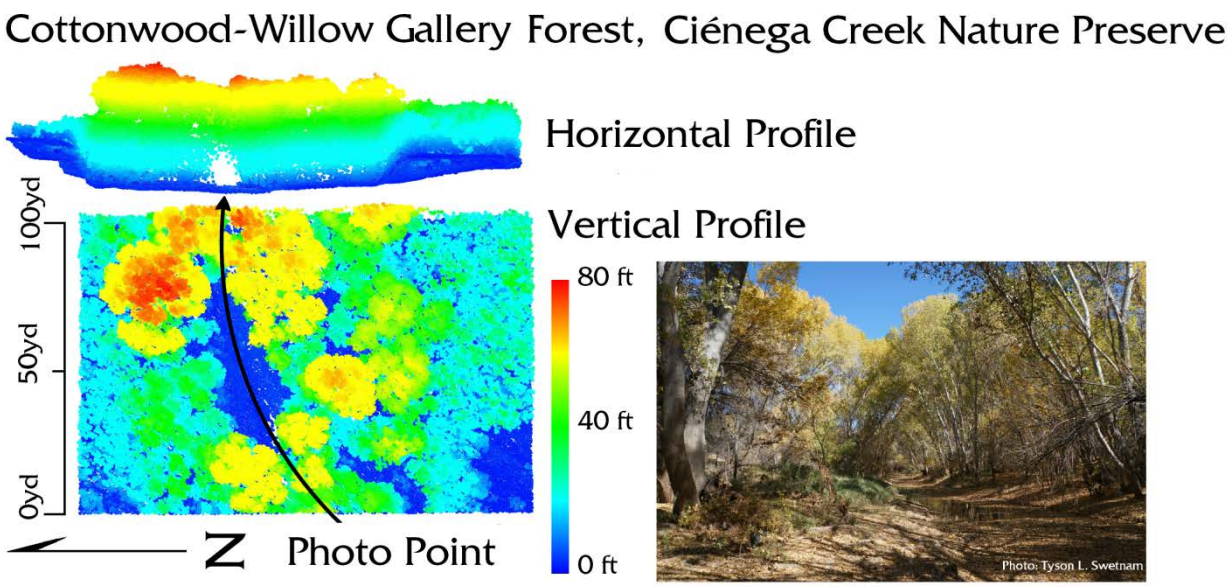

Fig. 3.2a Example of 2011 aerial LiDAR over Ciénega Creek with a corresponding photo point looking to the east.

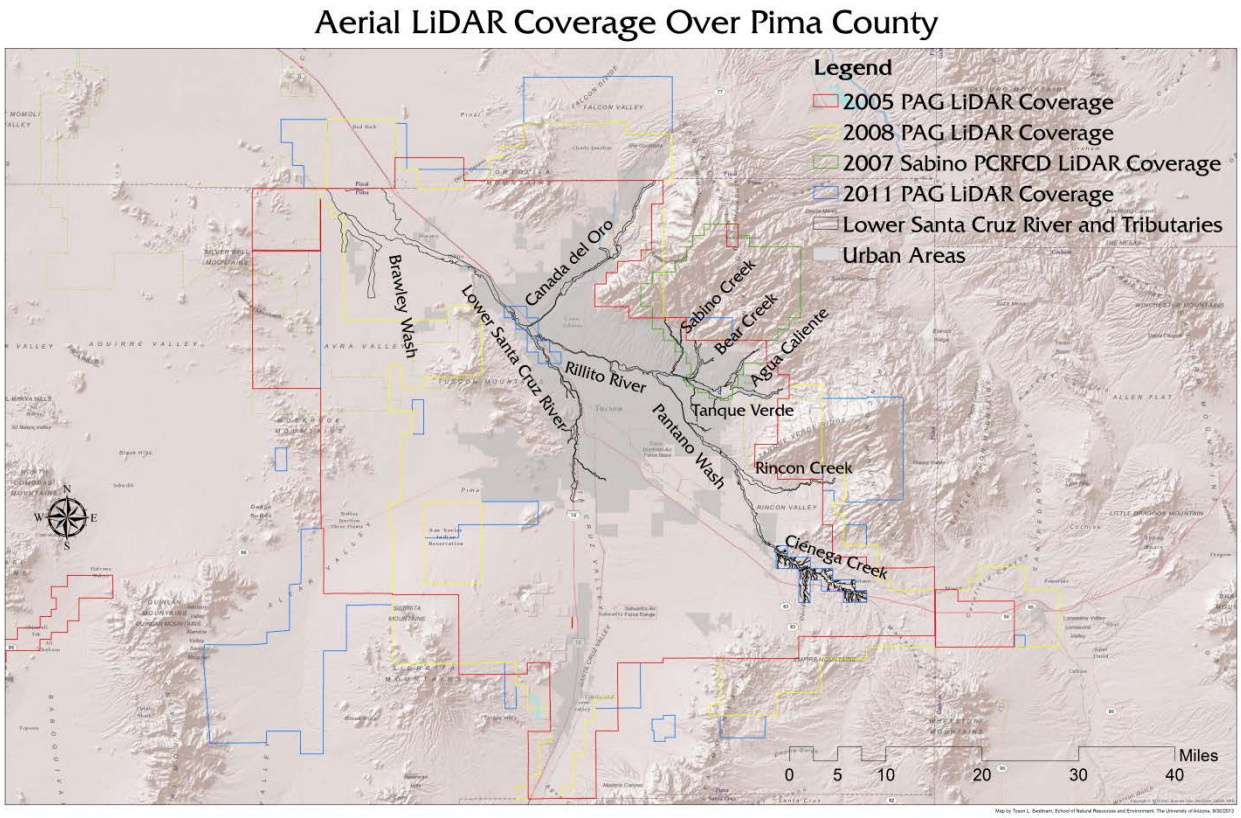

Fig. 3.2b Pima County LiDAR Coverage from PAG. The red tiles represent the 2005 flight mostly over-lapped by the 2008 repeat coverage (green tiles), the 2011 LiDAR flight (blue tiles) are mostly along the fringes of the 2008 flight, plus repeat in the two project areas along the LSCR around the water treatment facilities and along the Ciénega Creek. The tiles are mostly divided by township and range sections (=1 square mile). The gray color represents the urban Tucson Metro area. The black poly-lines are the riparian areas and tributaries of the Santa Cruz in the Tucson basin.

Table 3.2 Flight parameters and pulse density details of the LiDAR datasets used in this project.

	2005 (PAG)	2007 (PCRFCD)	2008 (PAG)	2011 (PAG)
Vendor	Sanborn Inc.			
Acquisition Dates (Julian day)	Est. May (N/A)	March 25-27 (84-86)	February 21 - March 13 (52-72)	April 10-16, 22-25
LiDAR Scanner	Optech ALTM 2050	Optech ALTM 2050	Leica (L) ALS-50 Optech (O) ALTM 2050	Leica ALS-50
Airspeed (knots)	N/A			120
Pulse Rate	50kHz	50kHz	73.5 kHz (L), 50 kHz (O)	48-104.2 kHz
Scan Frequency	31Hz	31Hz	42 Hz (L), 34 Hz (O)	30-44 Hz
Maximum returns per pulse	1,2, Intensity	1,2, Intensity	1,2, Intensity	1-4, Intensity
Scan Angle (degrees°)	±16°	±16°	±20°	±11-20°
Uncertainty (Vertical/Horizontal)	±15-37 cm/±100 cm ± 6 – 15 in / ± 39.4 in	±18 cm/±100 cm ±7 in / ±39.4 in	±15-37 cm/±100 cm ± 6 – 15 in / ± 39.4 in	±13.44 cm/±50 cm ±5.3 in / ±19.7 in
Flight above ground level	~1,700 m ~5577 ft	~1,700 m ~5577 ft	1,000m (O), 1500 m (L) 3280 ft (O), 4921 ft (L)	900 - 8,000 m 2,952 – 26,246 ft
Flight line sidelap	<50%	<50%	<50%	>50%
Average LiDAR pulse-return spacing	1.8 ppsm 2.15 ppsyd	3.44 ppsm 4.11 ppsyd	2.66 ppsm 3.19 ppsyd	Med:7.1 ppsm 8.49 ppsyd High:12.5 ppsm 14.95 ppsyd
Average Ground point-density ppsm	>1	>1	>1	>3
Area in acres (ac) (hectares Ha)	605,005 ha 1,495,000 ac	31,792 ha 78,560 ac	465,420 ha 1,150,080 ac	155,400 ha 384,000 ac
Number of tiles	2,349	150	1,787	583
Total Number of Pulse Returns	10,423,276,685	1,153,550,429	12,922,422,098	8,595,563,057
Units	International Feet			
Projection, Datum	Central Arizona State Plane, NAD89-92, NAVD88			
.LAS Version	1.0	1.1	1.1	1.2

3.2.1 Horizontal and vertical uncertainty

The horizontal uncertainty of the LiDAR is ±1 m (Sanborn Inc. 2009, 2011). This means that co-rectification of the ortho-photography will result in an error ±1 m on the horizontal plane for the actual object location.

When we conducted the NDVI classification we observed that along the edges of tall trees the NDVI did not always overlap the data exactly. This is the consequence of the orthogonal angle at which the ortho-photography was collected and not with the LiDAR observation. We recommend that the analyst check the alignment in the GIS before clipping data using the NDVI threshold technique. If there appears to be a large proportion of misalignment between the two data products the analyst may consider using the 'Shift' function in ArcGIS to move the

image or CHM to better align the two data products. Importantly, after a Shift has been done the data may not align elsewhere and may no longer be consistent enough for other mapping purposes.

The vertical uncertainty of the LiDAR also varies between the four flights (Sanborn Inc. 2007, 2009, 2011). Field spot characterization for the 2005 and 2008 flights indicate that the 2005 is 42 cm (15 in) contour interval compliant (CIC), 2008 was 15 cm (6 in) CIC, and 2011 was 13.5 cm (5.3 in) (Sanborn Inc. 2009, 2011).

3.3 Physical and Remote Sensing of Vegetation

Pima County uses a consistent classification scheme referred to as Total Vegetation Volume (TVV) for characterizing its riparian vegetation communities. Conceptually, TVV is estimated as the total volume (

Example of aerial LiDAR along the Black Wash (Avra Valley) TVV Monitoring Site

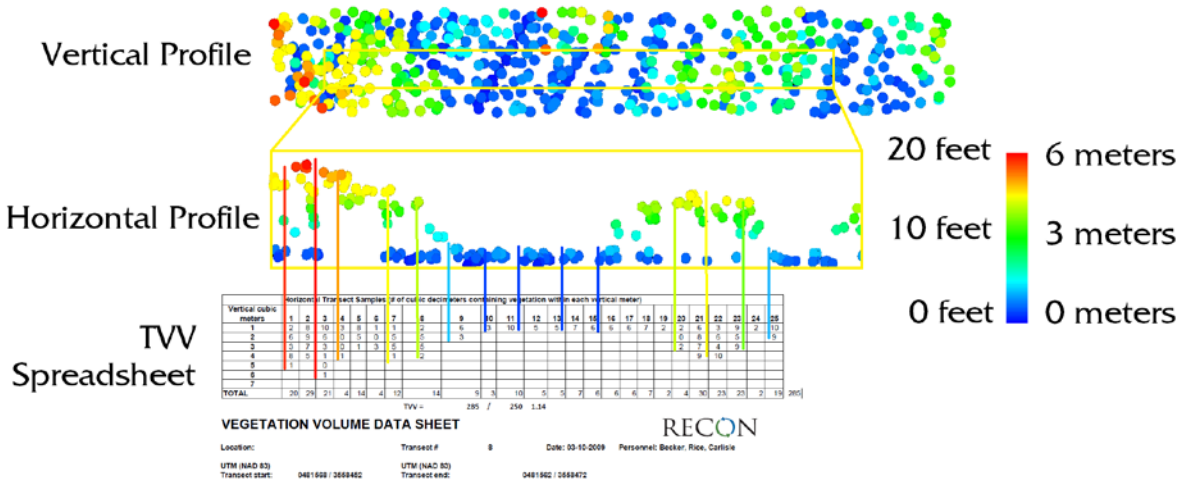

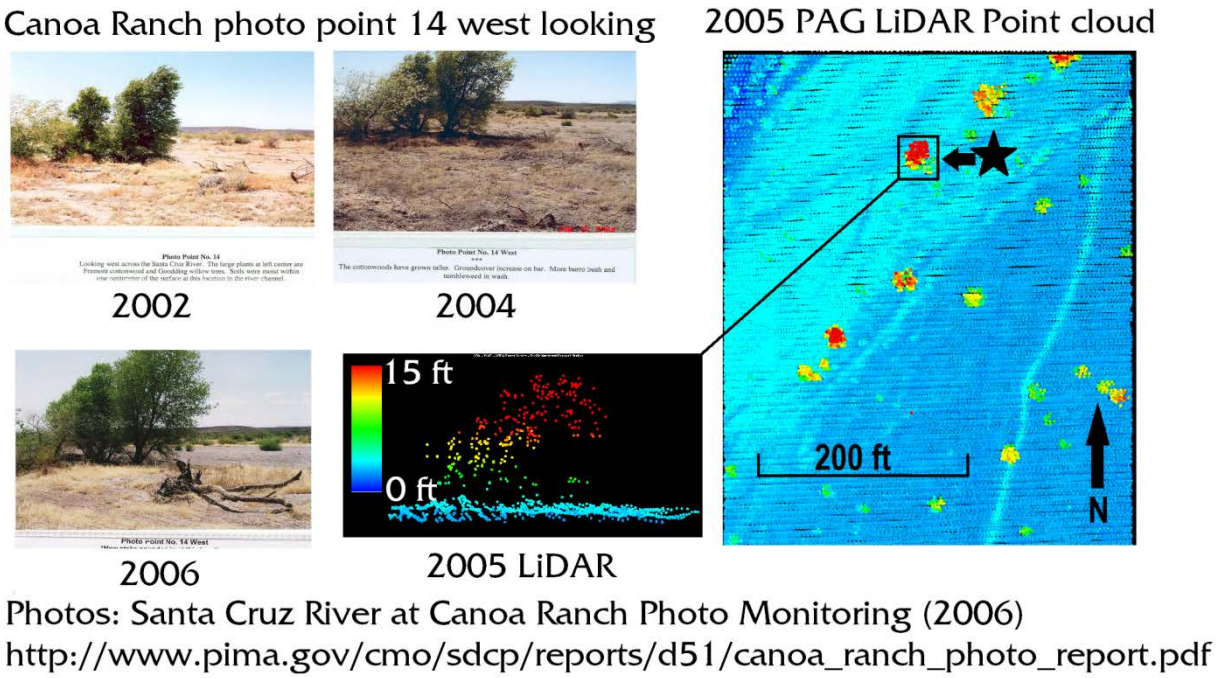

Fig. 3.3b Example of aerial LiDAR paired with a photo point from the Canoa Ranch area.

Because the period of time to measure vegetation in the field [in validation of the LiDAR] has long passed we instead looked for existing field data from the Pima County RFCD, and Pima County Office of Conservation (Table 3.2) collected on or around the dates of the LiDAR acquisitions. These surveys were mostly conducted by the third-parties: RECON Environmental, Inc. (RECON), The WLB Group, and Westland Resources, Inc. Several of the surveys took place along the LSCR and Ciénega Creek, but did not include TVV data. In Fig. 3.3b (above) we show a single cottonwood tree in the Canoa Ranch area that has a repeat photo point series taken of it. The shape of the cottonwood is clearly apparent in the 2005 LiDAR versus the 2004-2006 photo points, also an example of the density of the LiDAR points inside the canopy is apparent – for this low density LiDAR there are several points from the top of the canopy and enough points around the tree to make out its shape, but there are few points within the canopy for estimating its leaf area.

To maximize the production value of this study, we did not attempt a robust validation of the TVV to the aerial LiDAR. Because of uncertainty involving the geo-referencing precision of the TVV we determined it to be cost-prohibitive spending the inordinate amount of time required to accurately align TVV transects and measure the correlations of the LiDAR pulses to the observed field data. As we discuss briefly in the following sub-section: aerial LiDAR has been shown repeatedly to measure vegetation with precision that far exceeds human ability, making this validation unnecessary.

3.3.1 Recommendation for future TVV monitoring

To maximize the utility of the LiDAR for monitoring vegetation across large areas the collection of field observations should be timed as close as possible to the LiDAR acquisition to ensure physical characteristics can be compared to the vegetation before it grows, or is diminished, or is removed by a subsequent disturbance. To be clear, LiDAR measures vegetation height with a high level of precision and accuracy, and is repeatedly demonstrated across vegetation studies globally (Ustin and Gamon 2010, Van Leeuwen and Nieuwenhuis 2010). It is the authors' opinion that it is a waste of valuable field resources to take measures of vegetation height or volume in an effort to determine whether LiDAR is physically accurate for measuring vegetation height – the overwhelming consensus is that LiDAR measures the physical world in a way that far exceeds human measured precision. We recommend the focus of field crew surveys be on what LiDAR does not measure: the health of individual plants, species specific traits [such as whether a community of plants are in a leaf-on or leaf-off condition at the time of the LiDAR acquisition], and the overall species diversity of a site. Studies quantifying the biomass of individual trees should consider taking diameter measurements of the trees or shrubs at base height or breast height; biomass can be readily estimated by bole diameter and height measurements [obtained from the canopy height model] once an allometric biomass model for a particular species is established (Jenkins et al. 2004). Studies interested in quantifying biomass across space should quantify the total vegetation biomass in the field and conduct a regression analysis based on the LiDAR canopy height metrics (Asner et al. 2011b).

Importantly, a field survey of the individual plant at its X and Y [latitude and longitude] location, utilizing either an existing canopy height model as a stem-map, or by taking back azimuth distance and bearing observations with a compass and laser range finder from a known survey point will establish [for the life of that particular plant or tree] its absolute location, allowing simple future re-measurement with LiDAR. A full inventory of plant community diversity cannot be resolved by aerial LiDAR alone yet important physical metrics taken by LiDAR and other spectral data may increase the sensitivity of species diversity models that use LiDAR metrics. All vegetation monitoring plots must be geo-referenced either with a high resolution GPS using differential correction technology or take a back azimuth angle with survey grade equipment from known a benchmark location. In an urban area this can be any identifiable feature such as a road feature, a power pole, a dwelling, or in a natural setting a geologic feature or a single tree that is easily distinguished from the stem-map.

In the San Pedro watershed Farid et al. (2006, 2008) found that a combination of terrestrial laser scanning (TLS) and aerial LiDAR accurately characterized desert riparian vegetation. The LiDAR in that study was similar in density to the 2005 and 2008 LiDAR; anecdotally suggesting the results discussed in this report have comparable confidence intervals. TVV is closely related

to Leaf Area Index (LAI) which is measured similarly (

4 Standard Operating Procedure

Here we define a standard operating procedure for analyzing discrete return LiDAR datasets for vegetation characteristics in both (1) USFS FUSION/LDV (McGaughey 2012) for the *.LAS, and (2) ArcGIS 10.1 (ESRI 2012) for ortho-photography (Fig. 4). Typically, when a new LiDAR dataset is delivered from a vendor it will come with a campaign report which explains many, but potentially not all, of the relevant details pertaining to the LiDAR acquisition. Conducting a 'quality assessment and quality assurance' (QA/QC) on your dataset is a useful first step toward ensuring the vendor has delivered on the contract [e.g. meeting required coverage areas and density specifications]. FUSION's QA/QC produces several other useful features such as coverage and intensity images for helping to visualize the data. In this standard operating procedure we outline how to (1) run FUSION's QA/QC on a new dataset, (2) create a FUSION/LDV project, (3) execute FUSION's command line batch processes; and (4) create an ArcGIS project with *.LAS LiDAR data (Fig. 4).

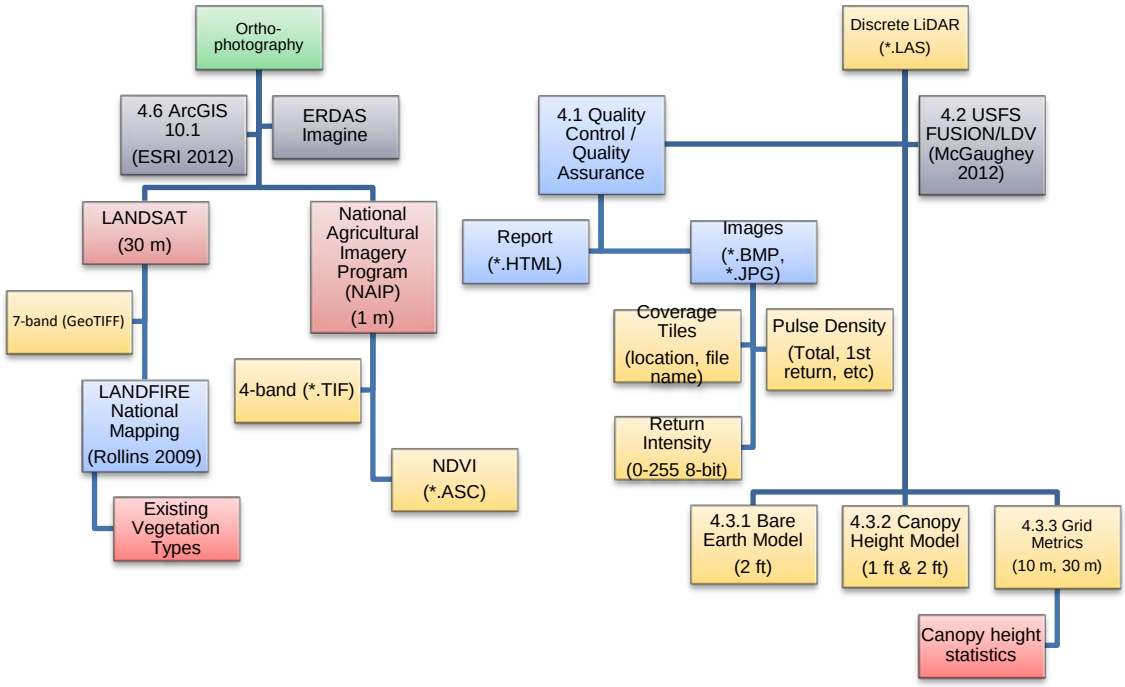

Fig. 4 Process tree of input file types and output file types, identifiers before name (e.g. 4.3.3) refer to a section in this Standard Operating Procedure where each process is discussed.

The discrete pulse return *.LAS data delivered by the vendor, in the cases of the PAG and RFCD LiDAR, are already classified. The data are coded into one of three classes: unclassified = 0, processed not classified = 1, and bare earth = 2(ASPRS 2011). The bare earth classified points can be used to create a bare earth surface model, or digital terrain model (*.DTM).

In general *.LAS data and derivatives delivered by the vendor include:

1. The full point cloud – either unfiltered or filtered. Filtered data are what the vendor has produced in a proprietary software suit [typically TerraSolid and TerraScan (http://www.terrasolid.fi/)]. Remember, the original data were saved as flight lines, these filtered *.LAS data are processed to remove overlapping points, outliers, and other geo-referencing problems; finally the data are chopped up like brownies into either square or rectangular tiles along a coordinate axes (in the case of the PAG data – Arizona State Plane, International Feet, HARN projection, along the Arizona Township and Range Section Grid).
2. .LAS Bare Earth – This *.LAS file contains only the vendor's classified bare earth elevation points. These files are suitable when a user is not interested in any further classification of surface features. Be aware these surfaces were produced with a (possibly unknown) set of parameters representing a 'best fit' of the data. These data may be incomplete or incorrect in areas with very steep or broken topography, or in areas with very dense vegetation cover.
3. ASCII Bare Earth – *.ASC, *.TXT, *.CSV, and *.XYZ. These are digital elevation model grid raster produced from the *.LAS data. These data are no longer in a vector format. These layers are useful if you are not interested in further classification of the surface. They are also appropriate for users who are not able to work in FUSION or other LiDAR software; these data are ready for import into a GIS platform, such as ArcGIS 10.1 (ESRI 2012).

4.1 Quality Control / Quality Assurance

Before beginning analyses of new a LIDAR project it is advisable to run a QA/QC on the *.LAS data. FUSION/LDV (McGaughey 2012) supports a QA/QC module called 'Catalog' which produces a descriptive report in *.HTML format, the QA/QC describes important characteristics of the data after the user establishes which features they are interested in by turning on a set of '/switch' functions in a command line batch process. Catalog can generate images of (1) a coverage file which identifies the location of each tile by name, (2) the intensity of pulses, and (3) the density of pulse returns (Fig. 4.1a). These images are geo-referenced to the data and can be loaded into FUSION/LDV to help view the data.

We used the QA/QC to determine the density of first returns and total return pulses across the entire flight area for our study. We also produced a catalog file list image which shows us where all of the LiDAR tiles are located. The QA/QC reporting includes the average and range of pulse return density across the flight area as defined by the user.

The FUSION manual (McGaughey 2012) contains an in-depth explanation of how to run the QA/QC and produce images and tables. The QA/QC outputs are saved in an .HTML file format which hyperlinks to the various image files (density, intensity, and coverage) in a single

directory. These image files can also be opened in FUSION/LDV in replacement of an orthophotograph.

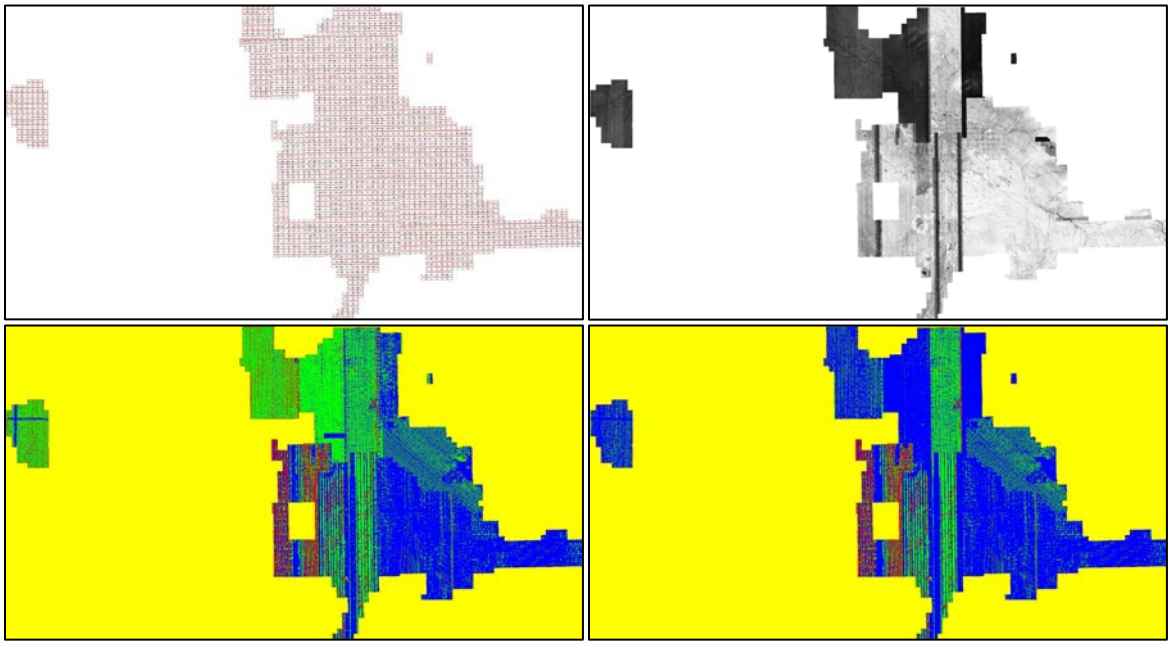

Fig. 4.1a The Catalog function output for the entire PAG 2008 acquisition. The upper left panel is the coverage identifying the individual tiles [each tile is approximately equal to 1 square mile] by identifier file name; the upper right panel is the intensity (white = high, black = low) of the pulse returns, importantly these data are not normalized; the lower left panel is the density of first returns (<1 ppsm = red, 1 – 2 ppsm = green, >2 ppsm = blue, yellow = no data); and the lower right panel shows the density of all returns in the data data, scaled the same as the lower left.

4.2 Creating a FUSION Project

FUSION/LDV is an open-source LiDAR data analysis tool provided by the US Forest Service (McGaughey 2012). It can be downloaded from a portal website with a series of web-based tutorials:

Introduction to FUSION Launch Page: http://www.fs.fed.us/eng/rsac/fusion/
"The Latest Version": http://forsys.cfr.washington.edu/fusion/fusionlatest.html
"The Manual": http://forsys.cfr.washington.edu/fusion/FUSION_manual.pdf

In FUSION (Fig. 4.2a) a Project File (*.DVZ) can be created to save time when opening the required files to build a project; this is equivalent to the *.MXD file in an ArcGIS project. The files necessary for a working FUSION project include the:

Image… can be an aerial photo, a CHM, or intensity image projected in the same coordinate system as the LAS data. File types: *.JPG, *.BMP, and *.TIF.

Raw Data… *.LAS or *.LDA tiles of study area (can be point cloud or bare earth)

POI… Points of interest, a *.SHP file of either points or polygons.

Bare earth… the *.DTM elevation model.

Canopy… the *.DTM surface height model.

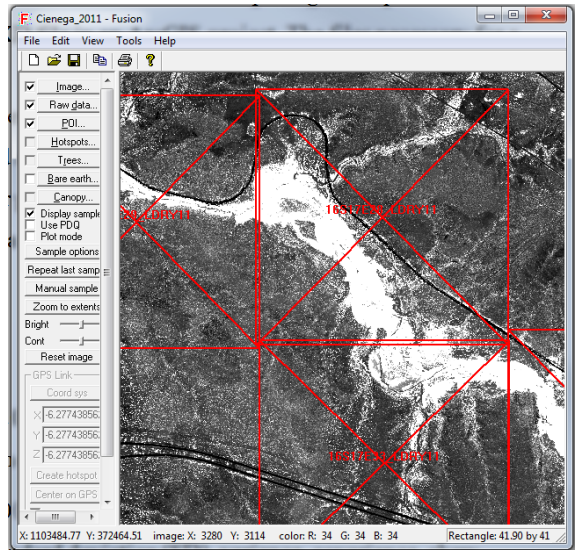

Fig 4.2a: FUSION graphic interface.

Hotspots… the Hotspot file is generated in 'Catalog' during the QA/QC – when loaded it will display as an icon which can be clicked upon to see the meta-data for the particular tile.

Trees... options are for generating forest based analysis;

Further details can be found in the FUSION/LDV Manual (McGaughey 2012).

4.3 FUSION in Windows Command Line

FUSION has both a graphic user interface, shown above right (Fig. 4.2a), as well as an extensive command line functionality built into it. The user can create command line batch (*.BAT) files which call executable programs (*.EXE) in FUSION's home directory folder [e.g. C:\FUSION\]. Individual tiles can be called by their directory location in the *.BAT file – or alternatively a file list *.TXT file can be created that calls all of the files in the list. Importantly, FUSION can only load ~2 GB worth of data into RAM because of its 32x architecture. FUSION is unable to process an entire large acquisition in RAM at one time. Alternatively, the 'Call' *.BAT file executes a for-loop statement that repeats itself on individual tiles sequentially from the filelist *.TXT file. [Note, all of the command statement is written on one line without any carriage returns]. We have colored the statements to reflect where each relates to the *.EXE or file structure:

```
for /F "eol=; tokens=1* delims=,. " %%i in
(E:\PimaCounty_rivers_project\Santa_Cruz_river\GridMetrics\2005filelist.txt) do call santa_cruz_gridmetrics_2005
%%i
```

The orange text represents the 'for loop' of the Call *.BAT. The red text is the drive letter and folder where the file list *.TXT is kept, the dark blue text is the *.BAT file containing the

executable command. The batch command grabs each file sequentially from the file list ('2005filelist.txt'):

```
I:\PAG_2005\11S14E02_LDRY05.las
I:\PAG_2005\11S14E01_LDRY05.las
I:\PAG_2005\11S14E03_LDRY05.las
…
I:\PAG_2005\19S13E32_LDRY05.las
```

McGaughey (2010, personal communication) recommends editing the list to remove the drive letters to make the commands more portable (for example an external hard drive with an unassigned drive letter). To produce a file list of a large LiDAR dataset follow these instructions:

1. Open a command prompt window and navigate to the drive letter and folder containing the LIDAR point data files the current folder (use the CD command)

    a. Click on the Windows Home button and type 'cmd' in the interface box:

    b. Type in the Drive Letter, e.g. 'I:'

    c. Select the folder e.g. 'cd\PAG_2005\'

    d. Type: 'dir /b /s *.las > filelist.txt'. This produces a .TXT file in the folder with a list of the files that have the suffix '.las' with the drive letter and subfolders identified.

    e. A text file has now been generated in the folder called 'filelist.txt', open the directory where the .LAS data are held and look for it (Fig. 4.3a).

    f. If desired, you can edit the filelist.txt in Windows NotePad (we recommend using TextPad). This can be useful when files change directories later in the processing, or if you are interested in changing the file format to the .DTM or .ASC type, and to alter the folder path. An easy way to do this in TextPad is to select the 'Replace…' command under the 'Search' tab.

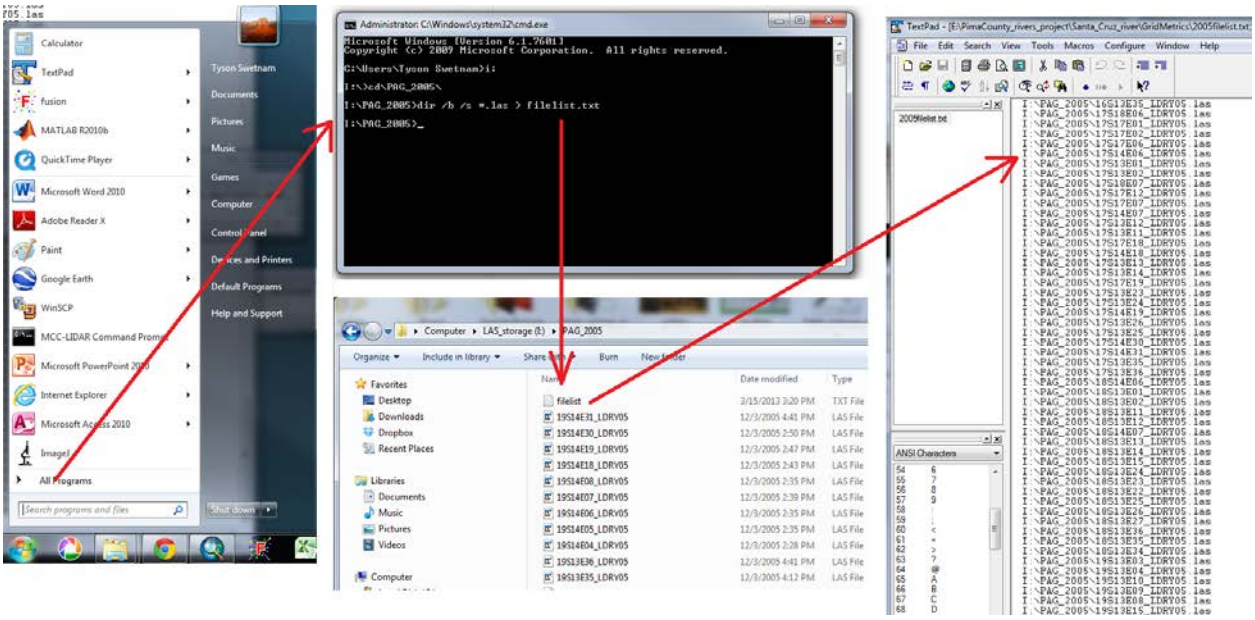

Fig. 4.3a Example of how to open a command window, generate a file list text file, and view the in TextPad.

4.3.1 Bare Earth Model

If the bare earth points in the *.LAS were not defined by the vendor a classification of ground points by Kriging the point cloud (Kraus and Pfeifer 1998) can be done in FUSION with the GroundFilter.EXE. Because the vendor has already classified the bare earth returns in the PAG data we did not conduct this procedure. If the user does not agree with the bare earth returns classified in the *.LAS they can parameterize GroundFilter with a more or less aggressive set of parameters to generate a new set of bare earth surface pulses [see McGaughey (2012) FUSION manual or Kraus and Pfeifer (1998) for complete details on the Kriging technique].

Assuming the data were delivered in both point cloud (*.LAS) and raster file types (*.ASC, *.TXT, *.XYZ) the user will need to create a bare earth layer either (1) from the *.LAS or (2) by converting the *.ASC bare-ground grids into a Digital Terrain Model (*.DTM) that can be accessed by FUSION. This step can be done either with ArcMap (3-D Analyst) or with FUSION's 'ASCII2DTM.EXE' in the command line:

```
ASCII2DTM G:\PAG2008\ASC\16S13E35.ASC  G:\PAG2008\DTM\16S13E35.DTM
```

The red text ASCII2DTM is the *.EXE, the blue text is the input file and the green text is the output file. ASCII2DTM generates the *.ASC in the same folder as the *.DTM.

To generate a new bare earth surface from the *.LAS we used FUSION's GridSurfaceCreate.EXE:

```
GridSurfaceCreate /median:5 /smooth:5 G:\PAG2008\DTM\%~n1.dtm 2 f f 2 0 2 2 %1.las
```

The *.DTM bare earth model we generated was 2 ft, the units of the PAG LiDAR are in international feet. We applied a 5 unit by 5 unit /median and /smooth switch to remove dimpling across the surface.

Before generating a Bare Earth Model several considerations should be made before leaving the point cloud environment:

- Will the data need any interpolation - such as smoothing or filtering?
    - We smoothed our surface model to remove any dimples or pits in the surface.
    - In some cases a jagged surface may be preferable, such as in complex terrain.
    - Sub-meter models will likely require smoothing to reduce the presence of 0 or NoData values.
    - Ordering of script for the median and smooth switches in FUSION will modify the output suface.
    - *.LAS point spacing is a primary measure for the need potential for smooth or median filtering.
    - What is the best neighborhood size of the smoothing or filtering?
        - The larger the neighborhood the greater the impact of the spline on the model.
- Do you want to keep the local maxima/minima?
    - Keeping minima and maxima in a bare earth surface will create pimples, dimples, or pock marks in the final surface. Typically the best option is to smooth the data with a 3x3 or 5x5 neighborhood filter. This function becomes more important when you are working in neighborhoods where roof-tops have likely been classified as non-ground points in the LAS cloud by the vendor, rendering the footprints of houses as empty spaces; when the footprint of a house becomes larger than the size of the spline used to create the bare earth surface a pit will result in the final model.
    - The density of the LAS data should tell you a bit about what the minimum scale will be of the .DTM product. The PAG data for 2005 and 2008 had at least 2 pulses per square yard and at least 1 pulse per square meter at ground level; this supported a 2 ft canopy height model, while the 2011 flight supports a 1 ft model.

4.3.2 Canopy Height Model

Canopy height models are generated when you difference the bare earth elevation from the maximum elevation of the pulses [for our models we used 2 ft canopy height model resolution (Fig 4.3.2a, Fig 4.3.2b)]. When running CanopyModel you must establish whether you want a canopy surface model [units in elevation above mean sea level], or a canopy height model

[units in elevation above bare earth]. Here is an example, of the script we used to generate the canopy height models:

```
CanopyModel /ground:G:\PAG2011\DTM\%~n1.dtm /outlier:-1,100 G:\PAG2011\CHM\%~n1.dtm 2 f f 2 0 2 2
%1.las
```

In this example we used a bare earth model: G:\PAG2011\DTM\%~n1.dtm, the %~n1 calls a particular file name from the filelist.TXT and assigns the *.DTM extension. We set outliers at -1 ft and 100 ft above ground level: /outlier:-1,100. We set the outliers at these levels because we knew a priori the largest cottonwoods in the riparian areas were no greater than 90-feet in height. It is important to establish the outlier parameter based on expected maximum heights. In tiles with little or no tall vegetation (e.g. xeroriparian) the outlier might better be set at 45 to 60 feet.

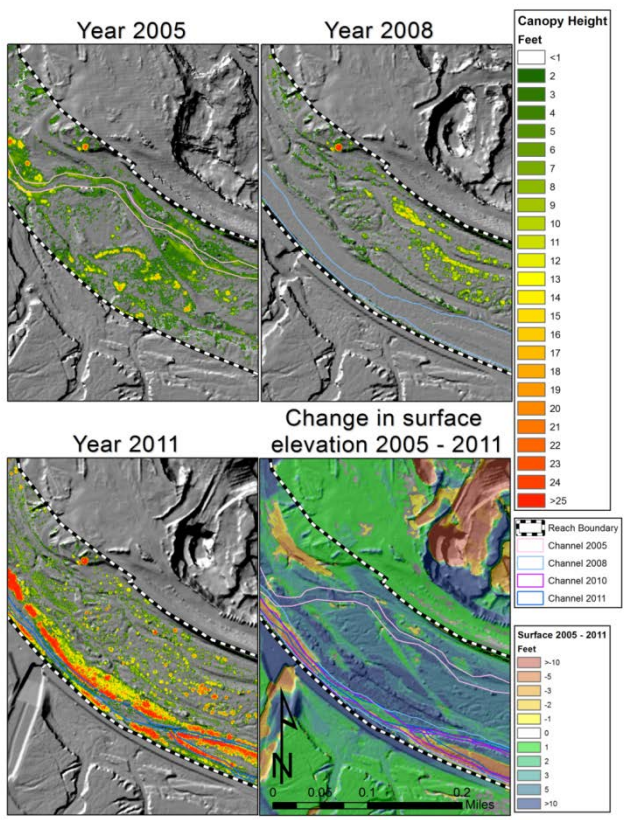

Fig. 4.3.2a A bare earth hill shade (in gray scale), canopy height model (green to red), and bare earth differencing of the years 2011 minus 2005 (red to blue). Examples are of the same section of the LSCR near Orange Grove Rd for the years 2005, 2008, and 2011 [two top panels, lower left panel]. The active channel in each year is shown with two colored lines that represent the banks (Historical Conditions Report, Pima County 2013). Some major earth moving was conducted both north [in a gravel pit] and south [the creation of flood control features] of the Reach Boundary between 2005 and 2011 [lower right panel].

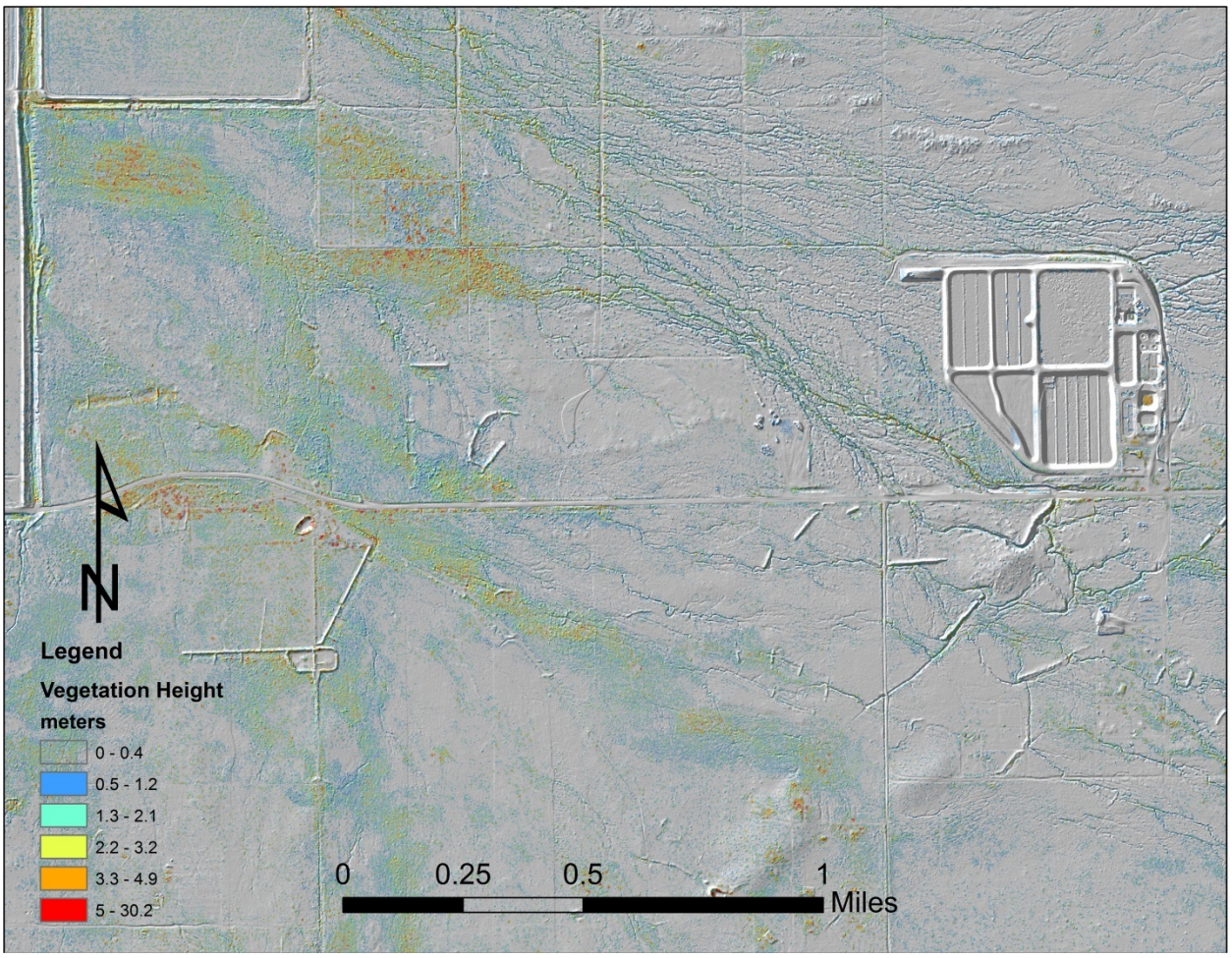

Fig. 4.3.2b Example of 2-foot canopy height model over Black Wash TVV site, Avra Valley.

4.3.3 GridMetrics

In FUSION (McGaughey 2012) the LiDAR point cloud statistics were calculated across a grid scale. The 'GridMetrics.EXE' process outputs multiple statistics which can be turned on or off by a /switch command. Each statistic is output as a *.ASC or *CSV file that is ready to be projected in a GIS. Unlike CanopyModel which typically uses only a single maxima pulse return to generate a surface height value, GridMetrics takes the statistic of the cloud within a much larger footprint. From the *.LAS data we processed 10 m and 30 m grid metrics which included forty statistics (Table 4.3.3). The statistics were generated using the points >3.2808 feet (1 m) above ground level [as defined by the bare earth *.DTM model] to avoid biasing the statistic with surface returns in low vegetation cover percentage cells.

The FUSION/LDV 'GridMetrics' (McGaughey 2012) command function can be run for any size grid the user chooses. For this study GridMetrics were run at 10 m (Fig. 4.3.3) and 30 m cell size [to allow pyramiding with LANDSAT imagery]. The intensity values of the point cloud data were

also processed for the same statistics as the height values, though those results are not discussed further as the intensity data are not normalized.

Importantly, the larger the grid cell size the less its statistical uncertainty becomes - as the error is proportionate to the

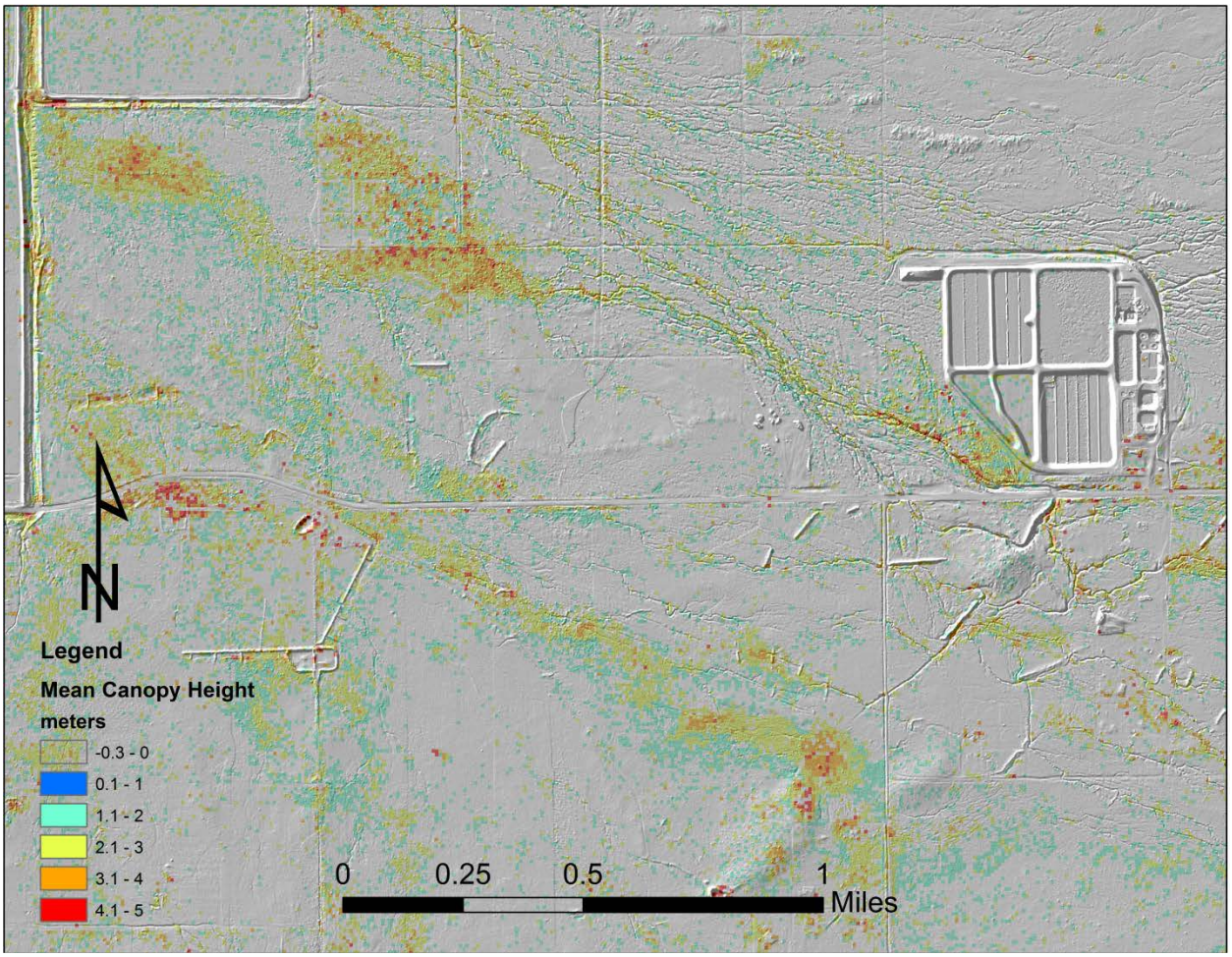

GridMetrics /outlier-3.2808,147.64 /diskground /ascii /minht:3.2808 /first /raster:densitytotal,min,max,mean,mode,stddev,variance,cv,cover,abovemean,abovemode,skewness,kurtosis, AAD,p01,p05,p10,p20,p30,p40,p50,p60,p70,p80,p90,p95,iq,90m10,95m05,allcover,afcover,allcount,allabovemean,afabovemean,fcountmean,allcountmean,totalfirst,totalall G:\PAG2005\DTM\%~n1.dtm 32.8084 32.8084 E:\PimaCounty_rivers_project\Santa_Cruz_river\GridMetrics\2005\10m\%~n1.csv %1.las

Viewed in the command line, each individual .LAS file is executed by the '**GridMetrics.EXE**' for the **santa_cruz_gridmetrics_2005.bat**. Each file LAS is called by the file list where **%1** is the parameter extension syntax for a path and file name, and **%~n1** expands to just the file name. The green text with '**/**' are switches that are programmed into FUSION, turning on a **/switch** causes a new set of rules to be applied to the function. For further details of the output properties see the FUSION/LDV User Manual (McGaughey 2012).

Here we have colored the command lines to help in explaining each of their properties

The **dark red color** calls the executable command **GridMetrics.exe**.

The **green color** are the switches used by **GridMetrics**, although some switches are common to other commands in FUSION. We removed the outlier pulse returns with the **/outlier** switch; the values are in the units of the data; here in feet below and above the bare earth surface (**-3.2808 feet and +147.64 feet**) which are equal to -1 m and +45 m; we use a negative valued minima to ensure that small pits or cliffs are not removed. We did not load the surface model into memory by switching on **/diskground**, this slows the process, but ensures that we do not run out of RAM (FUSION is 32-bit and has a maximum RAM of 3GB). The distributed processing method used here calling individual tile DTMs saved on memory usage. The **/ascii** switch produces outputs in .ASC format in addition to the .CSV format, which allows us to import them into ArcGIS directly. We used a minimum height 1 m above ground **/minht:3.2808**. This was to ensure that we removed any scan-line problems that might have occurred from the surface layer generation and uncertainty with the sensor. This is less of a problem with the 2011 flight than with the 2005 (the older sensors had greater uncertainty).We only used first returns **/first** for this process to ensure we estimated values equally across the surface where dense vegetation may have had multiple second return values. Next, the long list of classes **/raster:densitytotal, …, totalall** are the actual GridMetrics that produced (Table 4.3.3). A full description of each statistic can be found in the FUSION/LDV manual.

The **orange color** represents the surface model that was used to normalized the data. In this case we are querying the identifier from the filelist.txt, i.e. **11S14E02_LDRY05** and changing the suffix from **.las** to **.dtm** by using the script **%~n1** called from the filelist.txt.

The grey color is the size of the output pixels that we intend to generate. Because the PAG data are all in standard units (International Feet), we set the size of the gridmetric to 32.8084 ft 32.8084 ft (=10 m pixels).

The light blue is the name of the directory where the output data are generated.

The **dark blue** is the file input that the executable receives from the Call batch command, originating from the filelist.txt.

Table 4.3.3 List of GridMetrics (FUSION, McGaughey 2012):

count	point counts per cell
densitytotal	total counts per cell used for calculating cover
densityabove	counts per cell for points above heightbreak
densitycell	Density of returns used for calculating cover
min	minimum value for cell
max	maximum value for cell
mean	mean value for cell
mode	modal value for cell
stddev	standard deviation of cell values
cv	coefficient of variation for cell
skewness	skew computed for cell
kurtosis	kurtosis computed for cell
AAD	average absolute deviation from mean for the cell
cover	cover estimate for cell
p05	5th percentile value for cell (must be p05, not p5)
p10	10th percentile value for cell
p20	20th percentile value for cell
p25	25th percentile value for cell
p30	30th percentile value for cell
p40	40th percentile value for cell
p50	50th percentile value (median) for cell
p60	60th percentile value for cell
p70	70th percentile value for cell
p75	75th percentile value for cell
p80	80th percentile value for cell
p90	90th percentile value for cell
p95	95th percentile value for cell
iq	75th percentile minus 25th percentile for cell
90m10	90th percentile minus 10th percentile for cell
95m05	95th percentile minus 5th percentile for cell

Examples of two GridMetrics statistics:

Mean Canopy Height

Height indices of LiDAR from vertical profiles are proven to be strongly correlated to above ground biomass (Lefsky et al. 1999,2002a,2002b, Drake et al. 2003, Popescu et al. 2004, Asner et al. 2009). The mean canopy height (MCH) is calculated as:

where CHP is canopy height profile at height *i* above ground to a maximum height *h* (Lefsky et al. 1999). MCH is shown elsewhere to be the most representative metric of forest biomass by several studies (Asner et al. 2009, 2010, 2011a, 2011b, 2012, Hudak et al. 2012).

Mean Canopy Cover

GridMetrics can be applied to estimate the vertical canopy cover (VCC) and the angular canopy cover (ACC), canopy gap fraction, and leaf area index (LAI). Because the LIDAR directly measures canopy surfaces, the gaps between and within canopies are well suited for measuring VCC. The simplest way to calculate VCC is to calculate the proportion of canopy hits above a specified height threshold – we discussed this procedure for the SAVI and EVI equations in Section 3.1.2 where L is the cover percentage:

To merge the files in ArcGIS, open a new ArcGIS project and use the search feature or navigate through: **ArcToolbox → Data Management Tools → Raster → Raster Dataset → Mosaic to New Raster**.

Next, click the start button and open an instance of Windows '**Computer**' and navigate to the directory where the GridMetrics files are located. For example: I:\PAG2005\GRIDMETRICS\10M\

In these folders are the ~80 different GridMetrics statistics: 40 elevation based metrics and 40 laser intensity based metrics. It is likely users will only want the elevation metrics. It is recommended that users use 'Search Computer' to search for the file names of the metric you wish to mosaic in ArcGIS.

To search for a certain type of metric use the end of the file name identifier, i.e. type 'elevation_mean.asc' in the upper right corner Search Computer box. This will bring up all of the GridMetric files with the searched text highlighted as: '#####_first_returns_all_metrics_elevation_mean.asc' where ##### is the township and range or UTM tile identifier. Next, select all of the files in the folder (Fig. 4.4a, below right side).

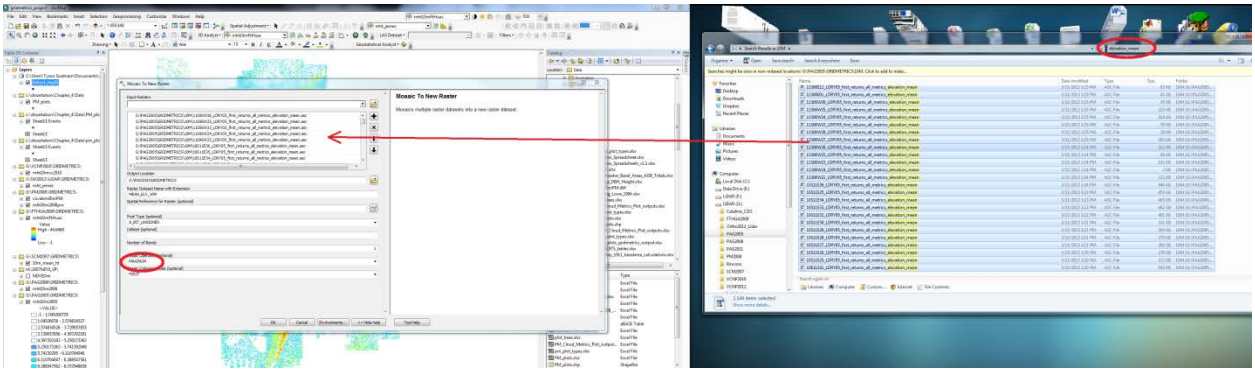

Fig. 4.4a Example of dragging files into ArcGIS to save on time.

Once users all of the files are selected drag them into ArcGIS's 'Mosaic to New Raster' input Raster menu (see the red arrow). This is much easier than loading the tiles one at a time – especially since there are thousands of tiles in the full data sets.

After the user has chosen a new directory for the output location and given the new raster dataset a name with an extension, set Number of Bands to '1', and the Mosaic Operator to the 'MAXIMUM' value (see red circle above left).

Users need to set the operator to 'MAXIMUM' because GridMetrics will have saved no-data values as negative numbers in the files, if the 'mean' or the 'last' operator is used the values along the edges of tiles will be averaged, causing a seam-line.

Run the 'Mosaic to New Raster' function, the output should load into ArcGIS. View the data to make sure that it is complete. (Fig. 4.4b, below, the 2007 Santa Catalina LiDAR over the Sabino Watershed)

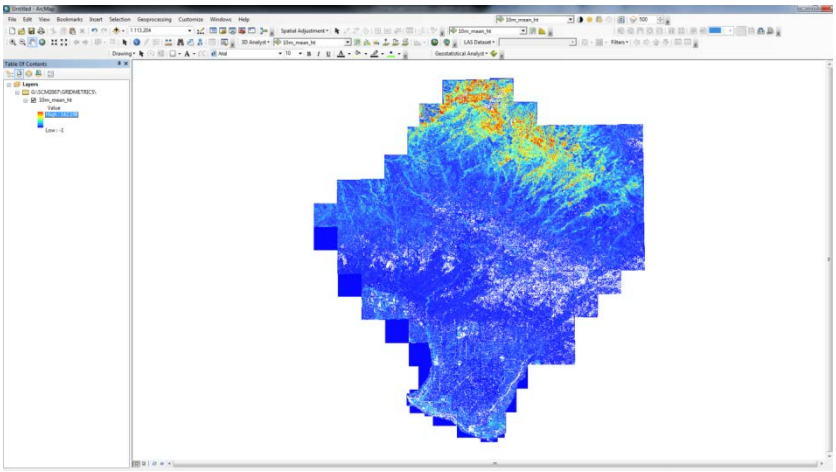

Fig 4.4b: ArcGIS example showing the entire 2007 RFCD data over the Sabino watershed.

4.5.2 ArcGIS LAS Dataset Creation

An easy way to view the *.LAS data are to load the tiles into an ArcGIS 10.1 LAS dataset.

Open the **ArcGISToolbox → Data Management Tool → LAS Dataset → Create LAS Dataset.**

Navigate to the folder where the *.LAS files are saved and select the entire list and import into **Create LAS Dataset**. Save the ArcGIS LAS Dataset (*.LASD) file to an appropriate project folder or database. Set the Projection Coordinate System to NAD 1983 HARN State Plane Arizona Central International Feet.

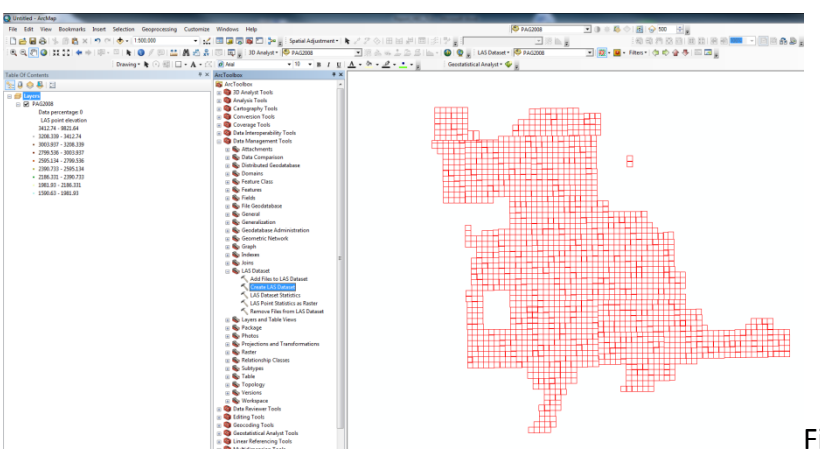

Fig 4.5.1a ArcGIS LAS Dataset

The entire extent of the *.LASD should now be visible as a set of square polygon files. (Fig. 4.5.1a, right, the PAG 2008 LiDAR *.LAS tile coverage in ArcGIS):

When you zoom to a single tile ArcGIS will begin to draw the point cloud (Fig. 4.5.1b, right panel). You can specify whether you want to look at all of the points, or the points by their classification [Elevation, Classification, Return].

You can open a LAS Dataset 3D View or a Profile view to look at the point cloud data:

While this is superficially useful for examining the data cloud – this tool does not analyze the statistics of the LiDAR dataset.

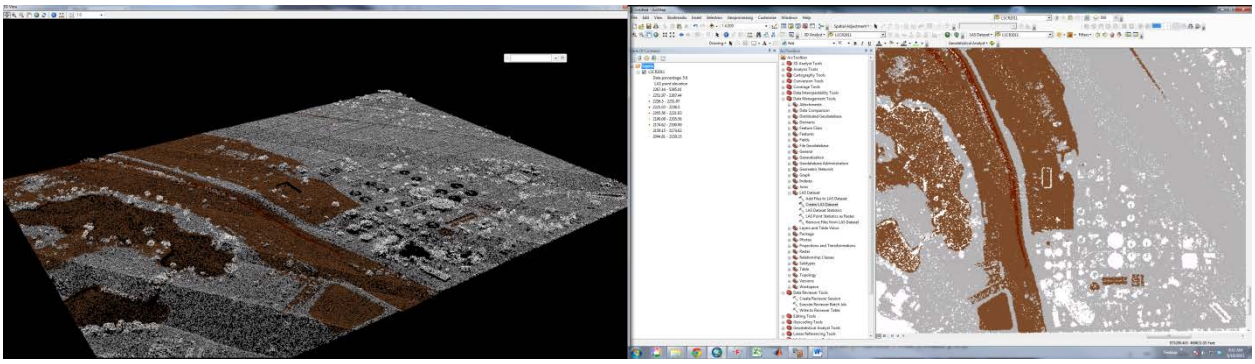

Fig. 4.5.1b The Roger Rd. Treatment plant and nearby Silverbell Park Lake seen in in the 2011 *.LAS data with ArcGIS 3D View. The colors are scaled by elevation (brown = lowest, white = highest).

4.5.3 ArcGIS *.ASC layers

The data products [CHM, DTM, and GRIDMETRICS] can all be opened directly into ArcGIS 10.1 (ESRI 2012). Presently the tiles have not had any ArcGIS associated files generated [their projections and datums are not defined]. When the *.ASC files are opened in ArcGIS it is important that the user set the projection and datum to the correct setting. For all of the PAG and PCRFCD LiDAR the projections are the same and are given in Table 3.2.

5 Summary of the analyses and recommendations for future LiDAR acquisitions

Here we report our findings, along with recommendations for future LiDAR acquisition in the riparian vegetation along the LSCR and its tributaries.

5.1 Baseline assessment of vegetation change

5.1.1 Lower Santa Cruz

Following the 2006 meso-scale flood event much of the vegetation observed in the 2005 LiDAR canopy height model was scoured away, as seen in the 2008 LiDAR canopy height model. Additionally, the effluent dependent channel shifted in some stretches within the greater flood controlled river (Historical Conditions Report, Pima County 2013)(Fig. 4.3.2). In 2008 the initial response in the hydroriparian vegetation was (1) a general decrease in vegetation in locations

where the channel had shifted but not scoured the vegetation by the flooding, (2) a complete denudation in locations where the vegetation was scoured by the flood waters, and (3) secondary succession beginning to set in with small patches of newly established vegetation taking root. By 2011 vegetation had recovered significantly across most locations including areas away from the 2011 channel. Overall, 70% of the area showed no significant changes [±1 ft change - within the vertical uncertainty of the LiDAR], 19.5% of the area was negatively impacted with >2 ft negative change, and 10.5% increased >2 ft in height. The results suggest that overall the vegetation in the LSRC in 2011 was still recovering from the 2006 flood event relative to the vegetation that existed in 2005 [which had likely re-generated after the 1993 flood event]. If we break the vegetation up into height classes, however, by 2011 vegetation along the effluent dependent zone had increased from 2005 level across the tallest height categories (Fig. 5.1.1a) signifying large woody vegetation along the channel had recovered to pre-2006 levels. Shorter height classes [e.g. herbaceous and shrub cover] across the larger flood controlled channel had not yet fully recovered in 2011 (Fig. 5.1.1a). The slower recovery in the mesoriparian or xeroriparian sections of the flood plain suggest these vegetation are not benefiting from the effluent saturated soil water due to their distance from the current channel. The years following 2006 have included regional drought conditions which have also likely slowed vegetation establishment and growth in areas far from the current channel.

The areas along the 2011 channel with the largest growth, including new tall woody vegetation [primarily Gooding Willow and Athel tamarisk] were all located within 30 yards of the effluent driven channel. Notably, from the ortho-photography in the years 2005, 2008, 2010, and 2011 the effluent driven channel is observed to have meandered in each year (Historical Conditions Report, Pima County 2013). These shifts are the result of either man-made action along the river to help promote infiltration or natural shifts following seasonal rain events.

Remarkably, a former gravel pit that was filled with water near Orange Grove Rd, last visible in the 2005 ortho-photography, had been completely emptied after the 2006 flood event wiped out its berm to the northwest, as seen in the 2008 ortho-photograph (Fig. 5.1.1c). The active effluent driven channel continued to flow north of the pit a little more than a hundred yards away, although it too has meandered into a new channel. By 2011 the pit had begun to grow a large quantity of Athel tamarisk (Historical Conditions Report, Pima County 2013), meanwhile the rest of the river bed remains barren between the former pit and the 2011 channel. Further, the 2005 channel has filled with new vegetation in the former bed (Fig. 5.1.1c). The deposition of water-borne seeds over time into the pit and along the 2005 channel prior to and during the flooding is one possible mechanism for sowing future vegetation. One other mechanism may be that fine sediments deposed over time create a more productive nutrient bed with increased soil water retention versus the sandier substrate nearby. These mechanisms should be studied

further as they likely play a key role in facilitating vegetation regeneration after flooding in the flood plain.

Along the effluent dependent reach of the LSCR where LiDAR data are available for all three periods (2005-2011) vegetation is highly dynamic and responds rapidly to shifts in the channel morphology following seasonal flooding. Note that in Fig 5.1.1c in the 2011 images the channel along the upper-right side has moved, and the vegetation in 2005 has been destroyed and new vegetation has grown adjacent the new channel; the body of water present in 2005 has also been destroyed over which new vegetation has grown. In the lower panel we show the change in vegetation height between 2005 and 2011. The hot colors (yellow to red) represent negative change in vegetation height [e.g. trees that have been destroyed due to the 2006 flooding, or have died and fallen]; the cool colors [light blue to dark blue] represent positive change in vegetation height [e.g. trees that have established and grown in since the 2005 LiDAR flight].

The vegetation regrowth in the effluent dependent zone north of Roger Rd. and Ina Rd. wastewater treatment facilities by far outstrips growth to the south of the Roger Rd. treatment facility. Because the 2011 acquisition did not fly over any of the non-effluent dependent channel we cannot make a direct observation of the relative increase in vegetation elsewhere. Importantly, these new effluent supported ecosystems are unlikely to survive future significant flood events, such as witnessed in 1983, 1993, and 2006. Any ecological benefits gained by restoration efforts to sustain or improve these systems are uncertain, and will be at continued risk from future significant flood events.

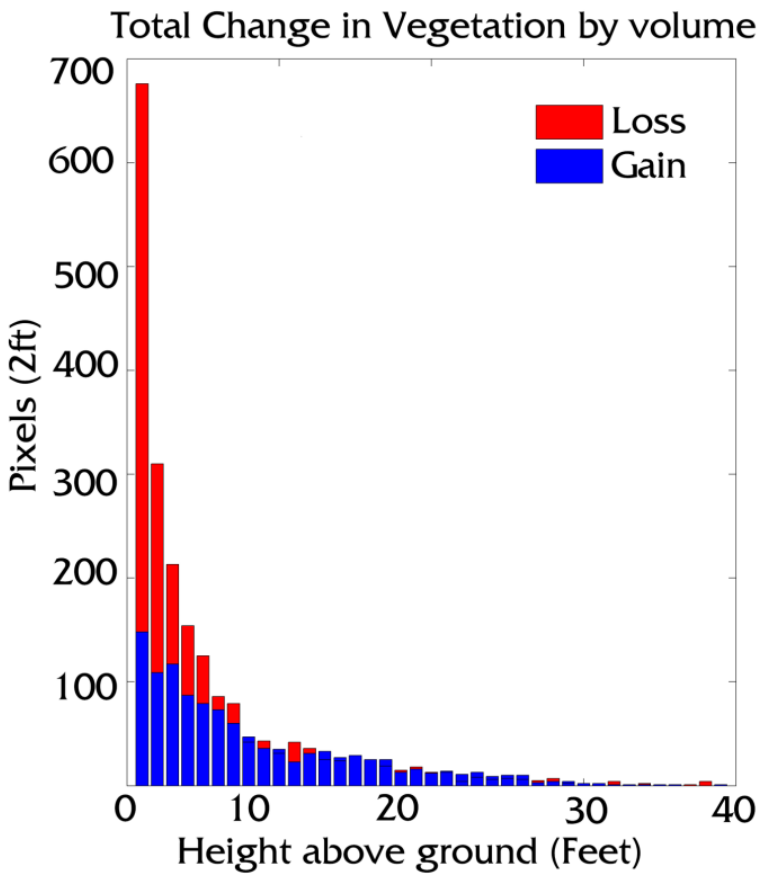

Fig. 5.1.1a Vegetation change in the 50-year flood control reach of the LSCR between Roger Rd. and Cortaro Rd. for the years 2005 to 2011.

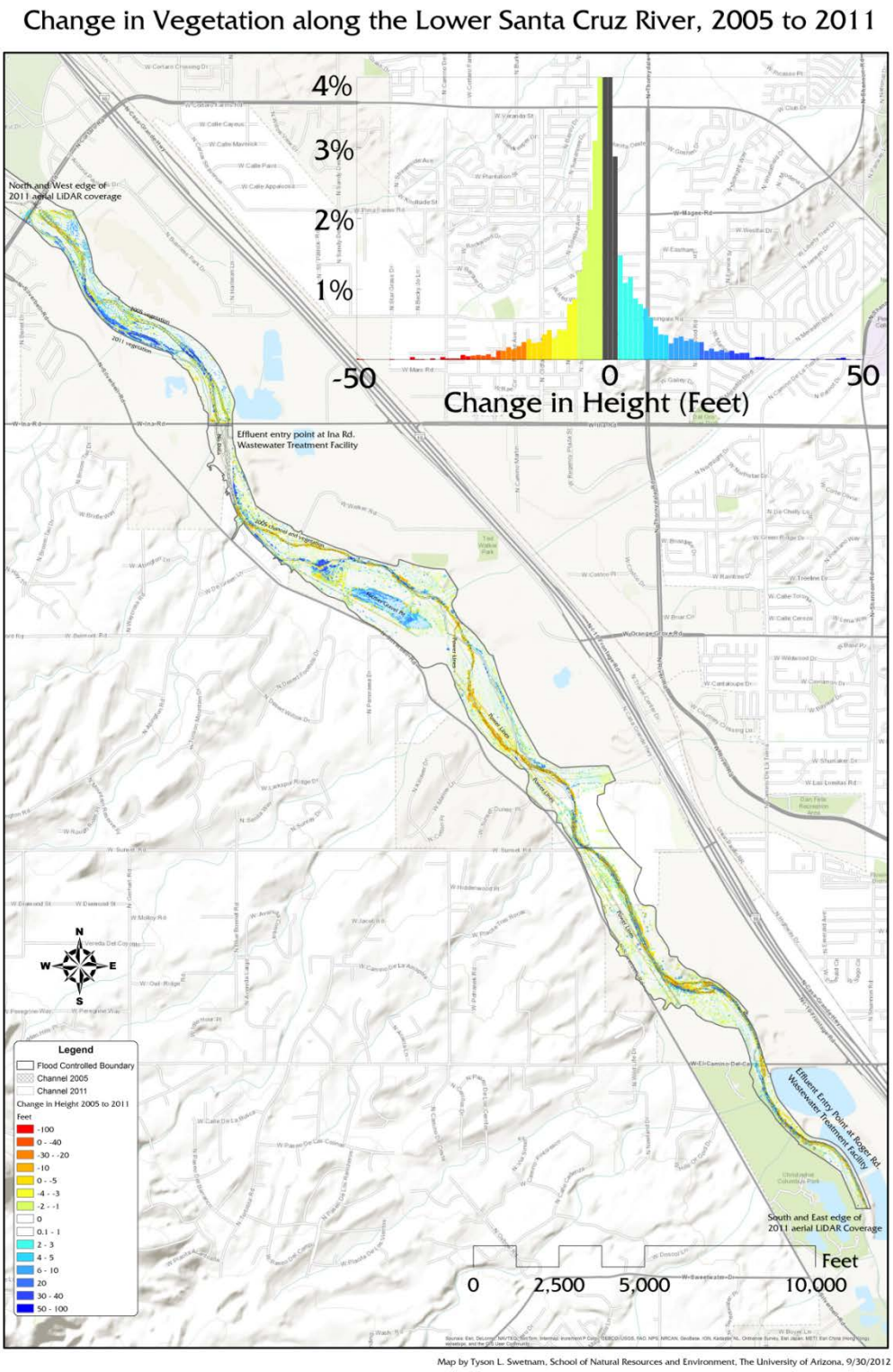

Fig. 5.1.1b Map of vegetation change along the LSCR from the Roger Rd. Treatment Facility to the Ina Rd. Treatment Facility, to Cortaro Rd, 2005 – 2011.

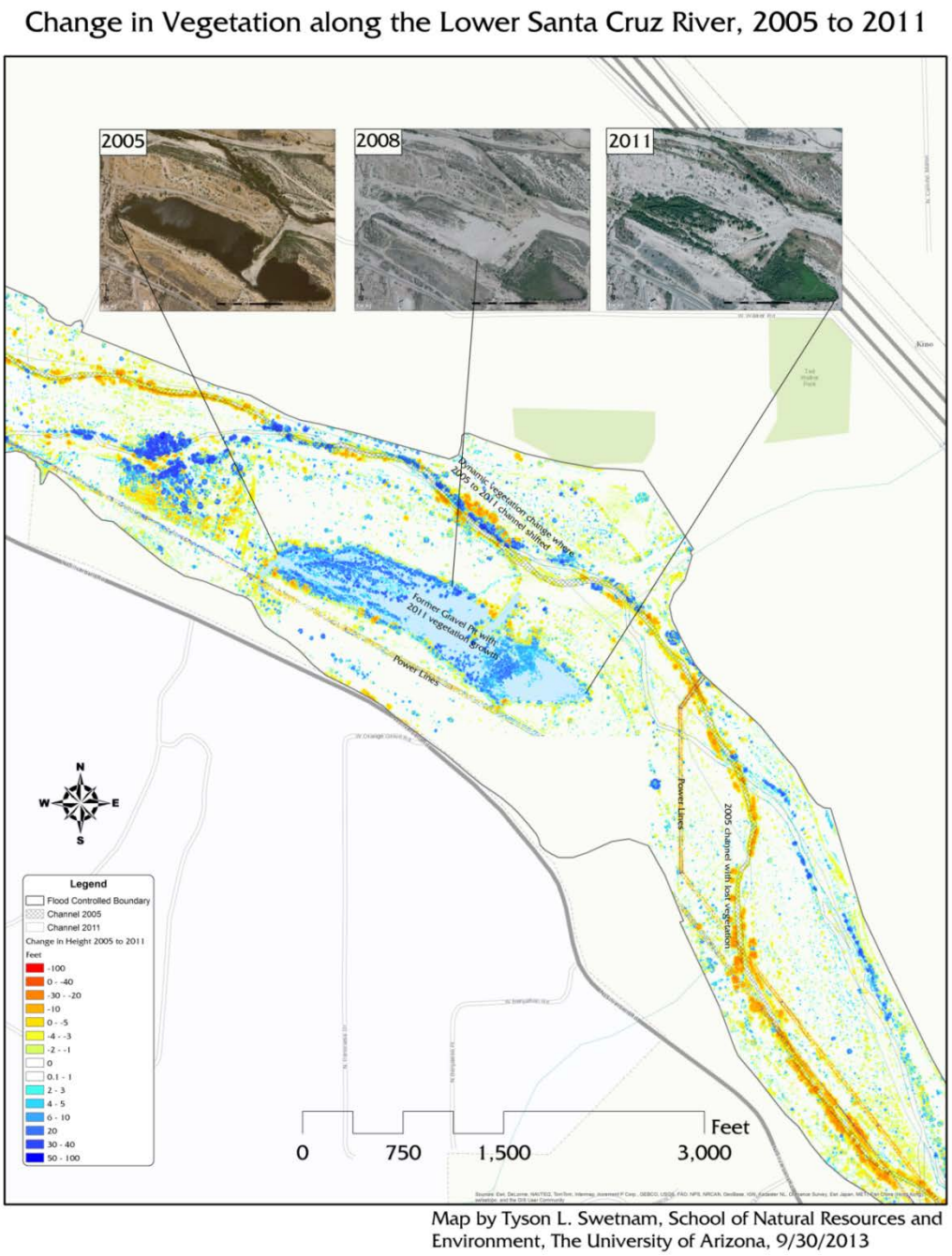

Fig. 5.1.1c Aerial photographs from 2005 and 2011 showing former gravel pit that had filled with water along the Santa Cruz near Orange Grove Rd. (top two panels).

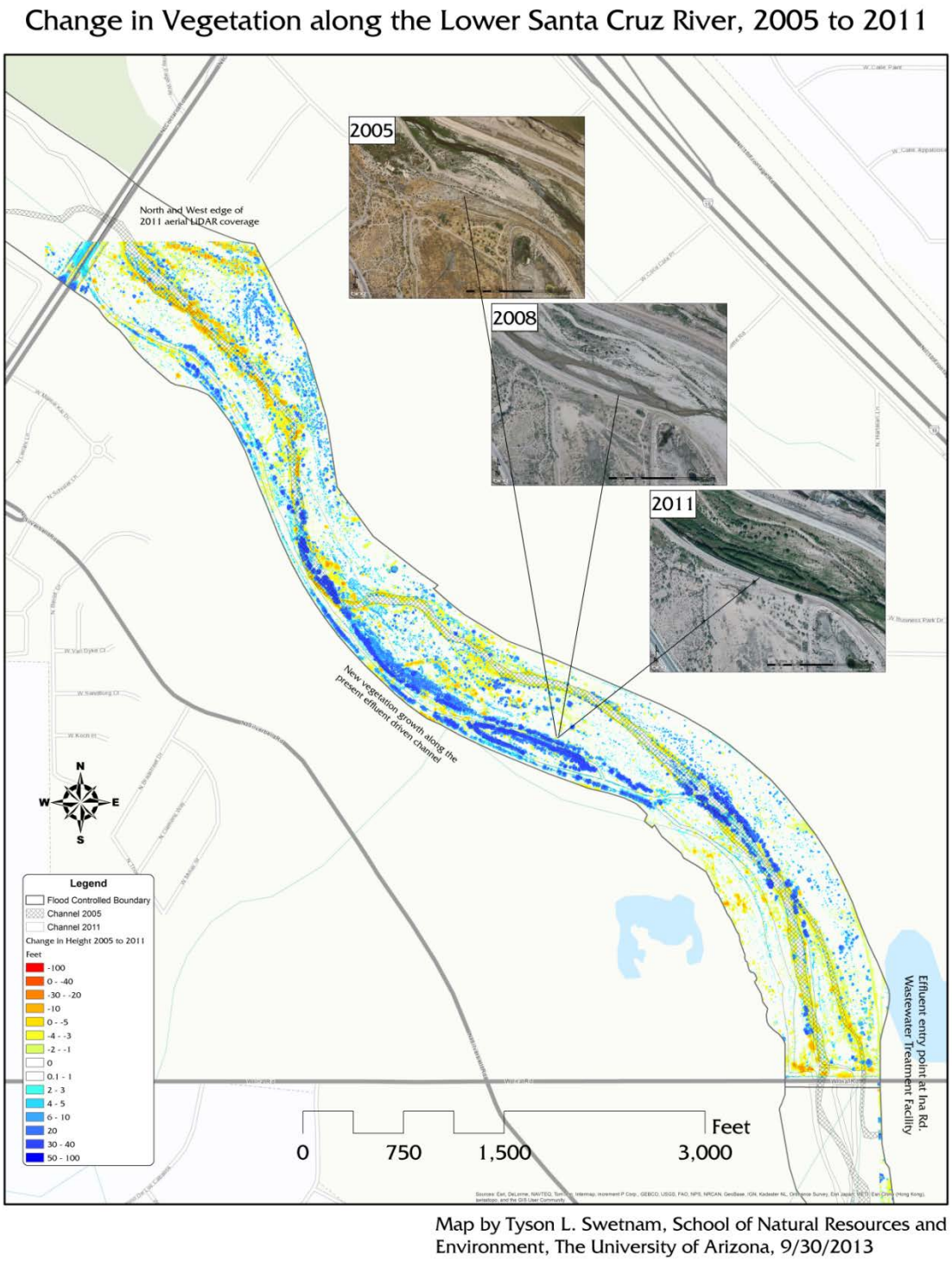

Fig. 5.1.1d Vegetation change north of the Ina Rd. wastewater treatment facility, up to Cortaro Rd.

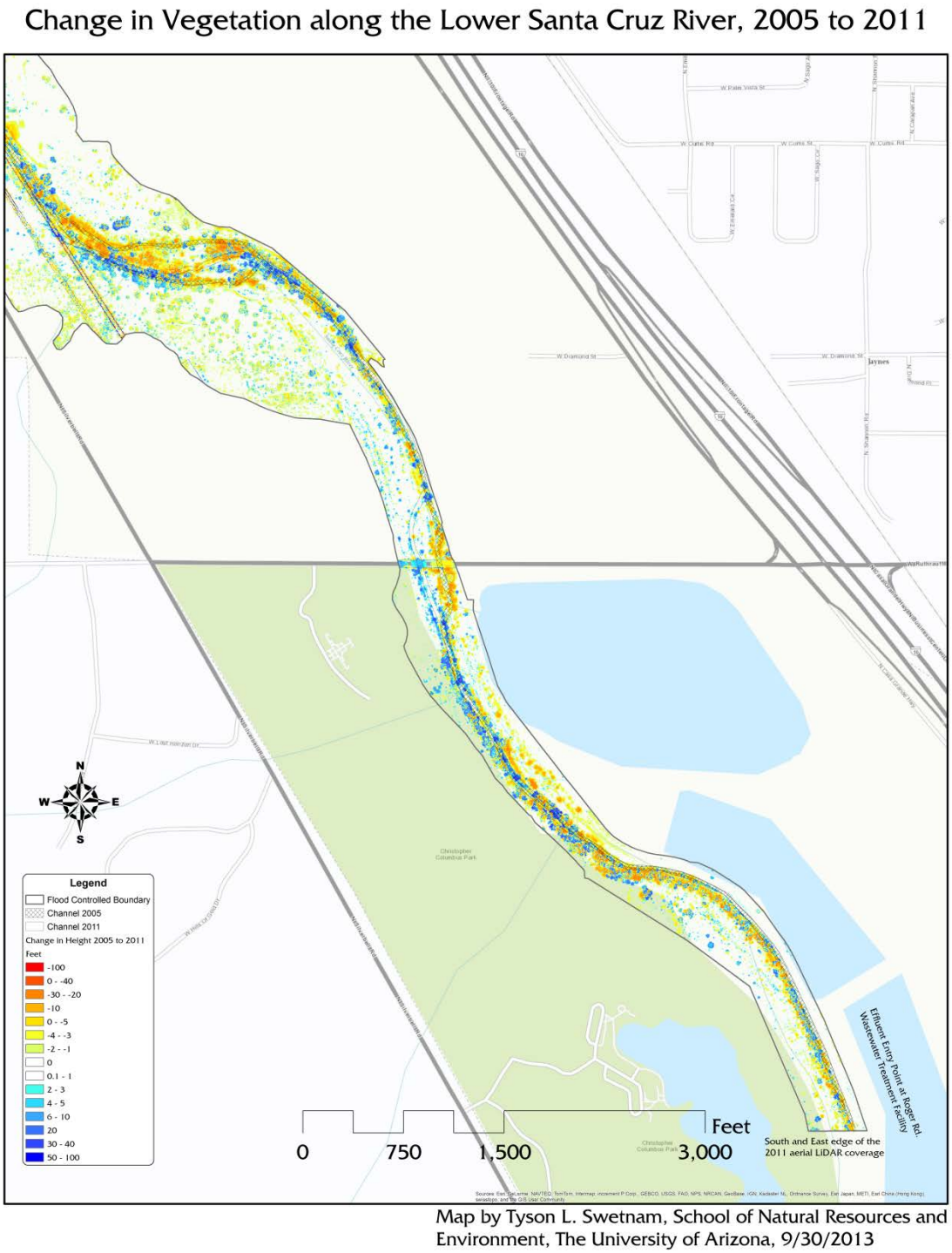

Fig. 5.1.1e Vegetation change north of the Roger Rd. wastewater treatment facility.

Change in Vegetation along the Lower Santa Cruz River, 2005 to 2011

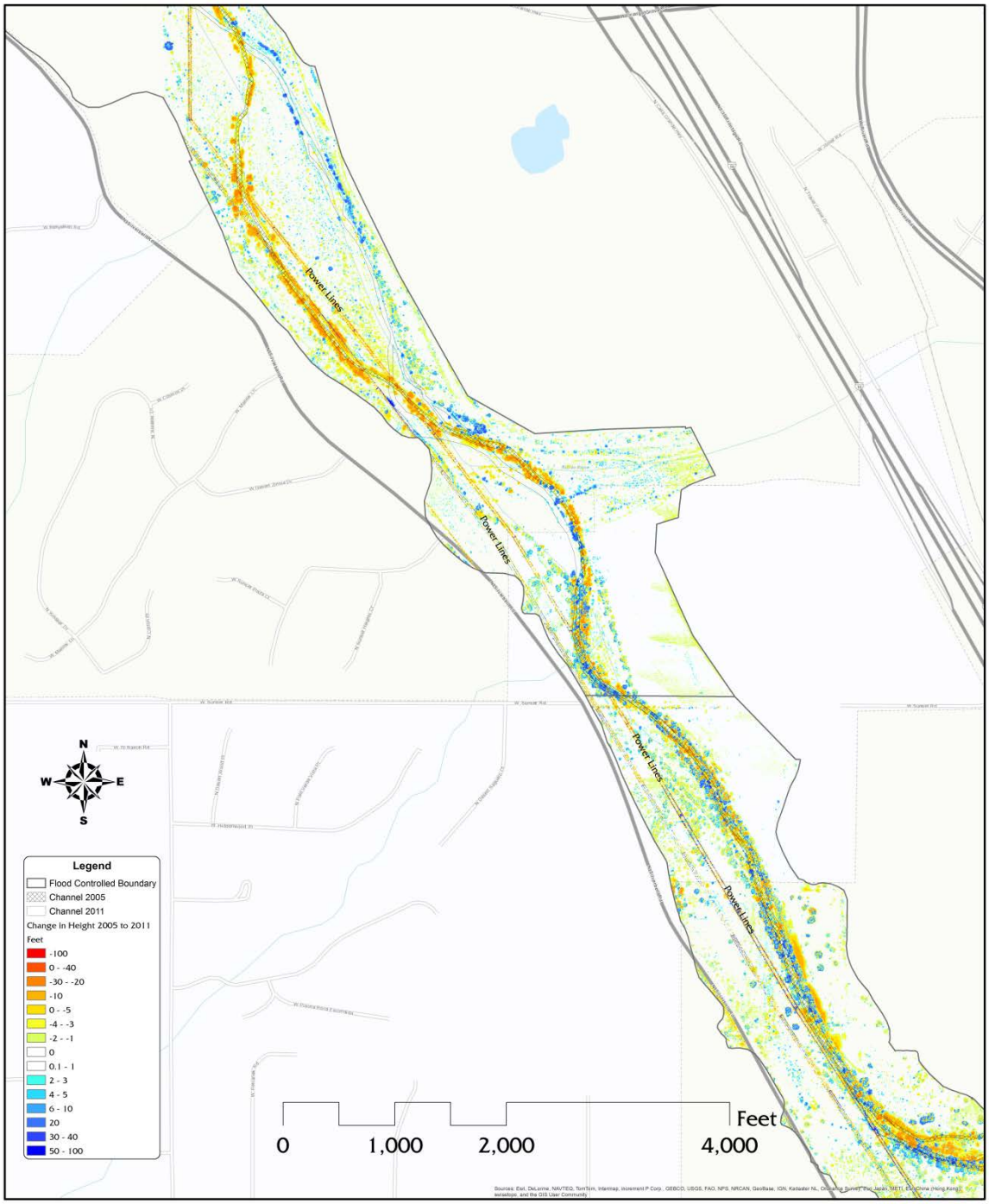

Map by Tyson L. Swetnam, School of Natural Resources and Environment, The University of Arizona, 9/30/2013

Fig. 5.1.1f Vegetation change north of Curtis Rd up to Orange Grove Rd.

5.1.2 Ciénega Creek

Hydroriparian vegetation in Ciénega Creek Nature Preserve was deeply impacted by the 2006 meso-scale flooding (Griffiths et al. 2009) (Fig. 5.1.2a - Fig. 5.1.2d). Channel morphology also changed along stretches of Ciénega Creek following the 2006 flood (Fig. 5.1.2a). The rate of change in both vegetation and channel morphology from 2005-2008 vs. 2008-2011 has decreased, suggesting the period of instability is slowing down across the system and is returning to changes experienced by annual flooding. In several locations where the creek naturally meanders large trees were destroyed by the flooding where the overflow destroyed banks and rechanneled the creek (Fig. 5.1.2a, Fig. 5.1.2c, Fig. 5.1.2d).

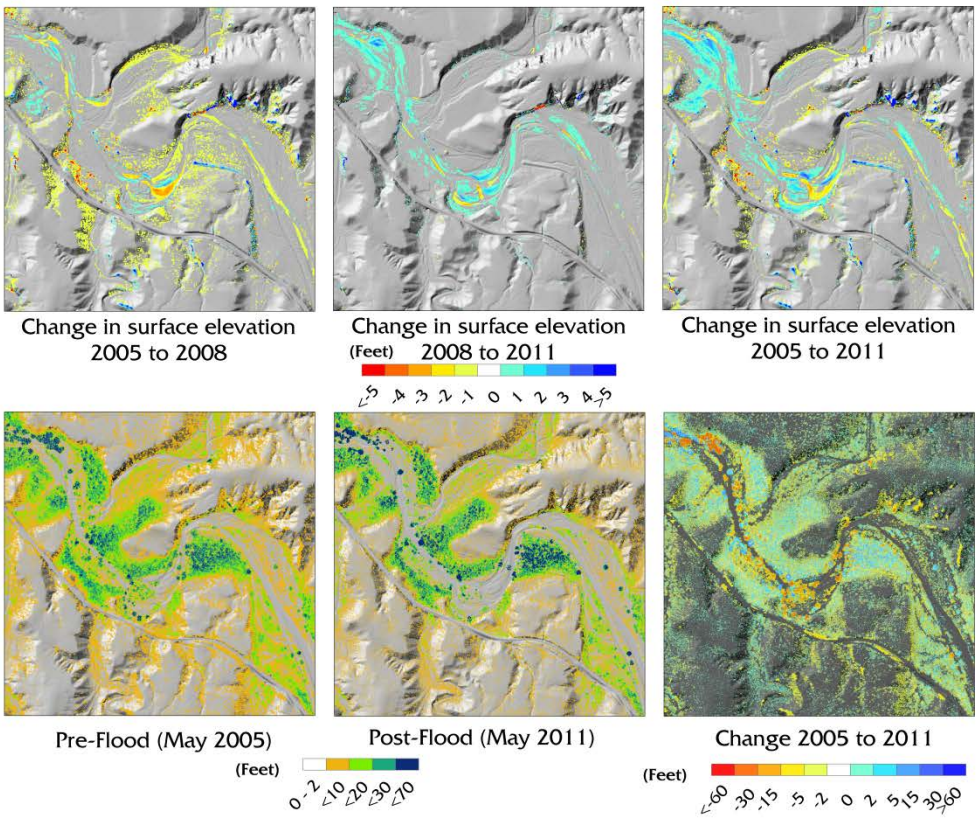

Fig. 5.1.2a Map of vegetation change along the Ciénega Creek in the surface height model between 2005 and 2008 (upper-left), 2008 and 2011 (upper-middle), and 2005 to 2011 (upper-right). The pre-2006 flood canopy height model as seen in 2005 (lower-left), the vegetation post-flood in 2011 (lower-middle), and the total change in vegetation between 2005 and 2011 (lower-right).

Vegetation along Ciénega Creek is very different than along the LSCR, exhibiting late-stage mature Cottonwood-Willow gallery forest. Ciénega Creek is a perennial water source, one of the few locations in Pima County with surface water besides the effluent dependent Santa Cruz. The maturity of the cottonwood-willow gallery forest suggests the system has been established

for a long period of time. The magnitude of the 2006 flooding in Ciénega Creek was far less than what is experienced in the larger LSCR drainage, thus damage to vegetation following flooding did not affect Ciénega Creek in the same way. For example, in the LSCR nearly all of the vegetation was scoured away in 2006, resulting in a log-log linear decrease in vegetation across the area of interest (Fig. 5.1.2e). On the other hand, in Ciénega Creek, the flooding affected smaller portions of the channel, mostly along the turns in the river where creek side banks were eroded away (Fig. 5.1.2a). The observed decrease in coverage of shorter class vegetation across the Ciénega Creek (Fig. 5.1.2b) was more likely the result of the ongoing drought conditions decreasing total foliage in the xeroriparian and mesoriparian bosque trees. The same change is not seen in the 10 m mean canopy height grid metric statistic (Fig. 5.1.2e), suggesting the difference in Fig. 5.1.2b is nullified at the community scale [e.g. vegetation structure is still there, canopy cover has simply decreased].

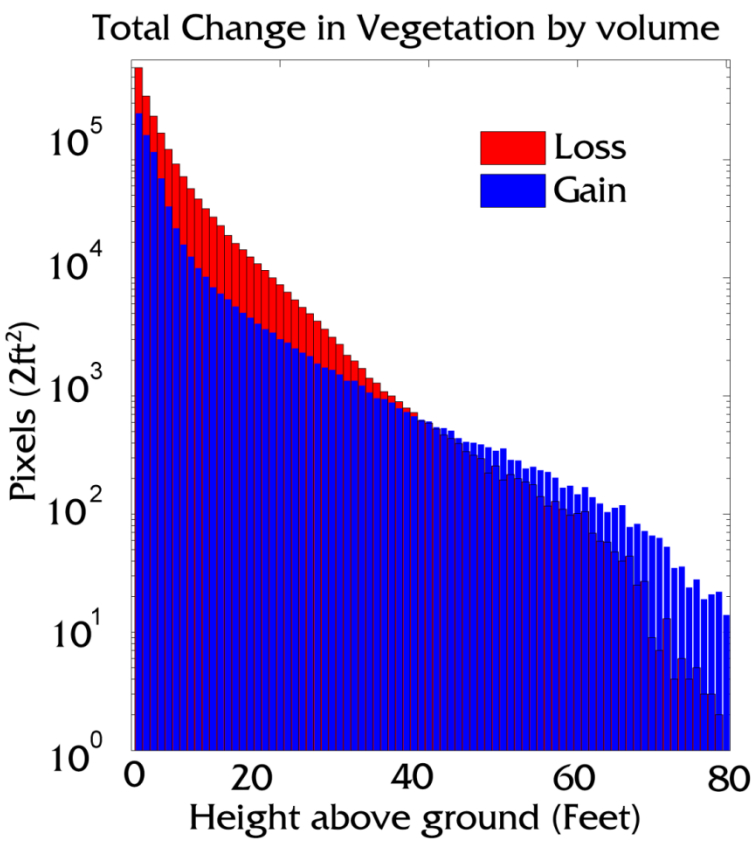

Fig. 5.1.2b Vegetation change greater than 2 ft in the Ciénega Creek between 2005 and 2011. Note: the y-axis is on log-scale due to the wide variation in height classes. Importantly, the increase in large trees is due to existing Hydroriparian trees broadening their canopies and growing taller, while the larger scale impact was in the negative changes in height across Xeroriparian woody and herbaceous cover due to the ongoing drought condition.

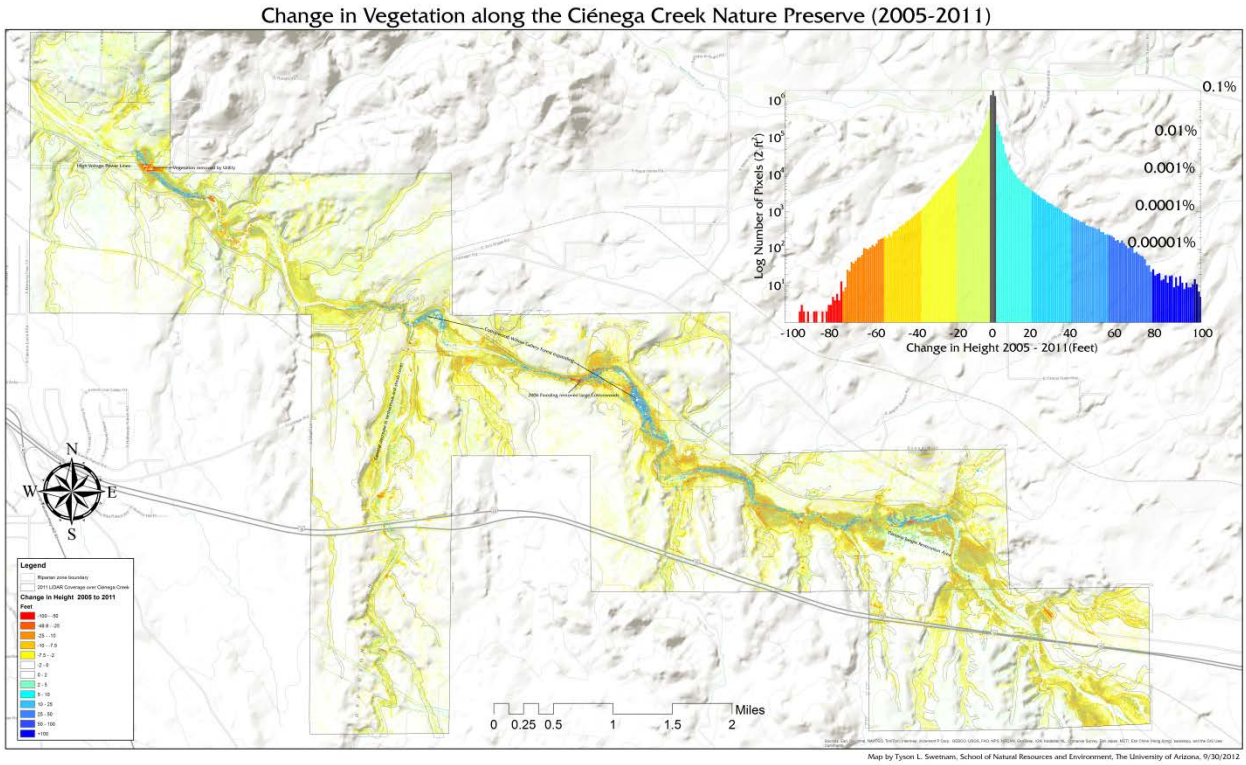

Fig. 5.1.2c Change in vegetation along the Ciénega Creek between 2005 and 2011.

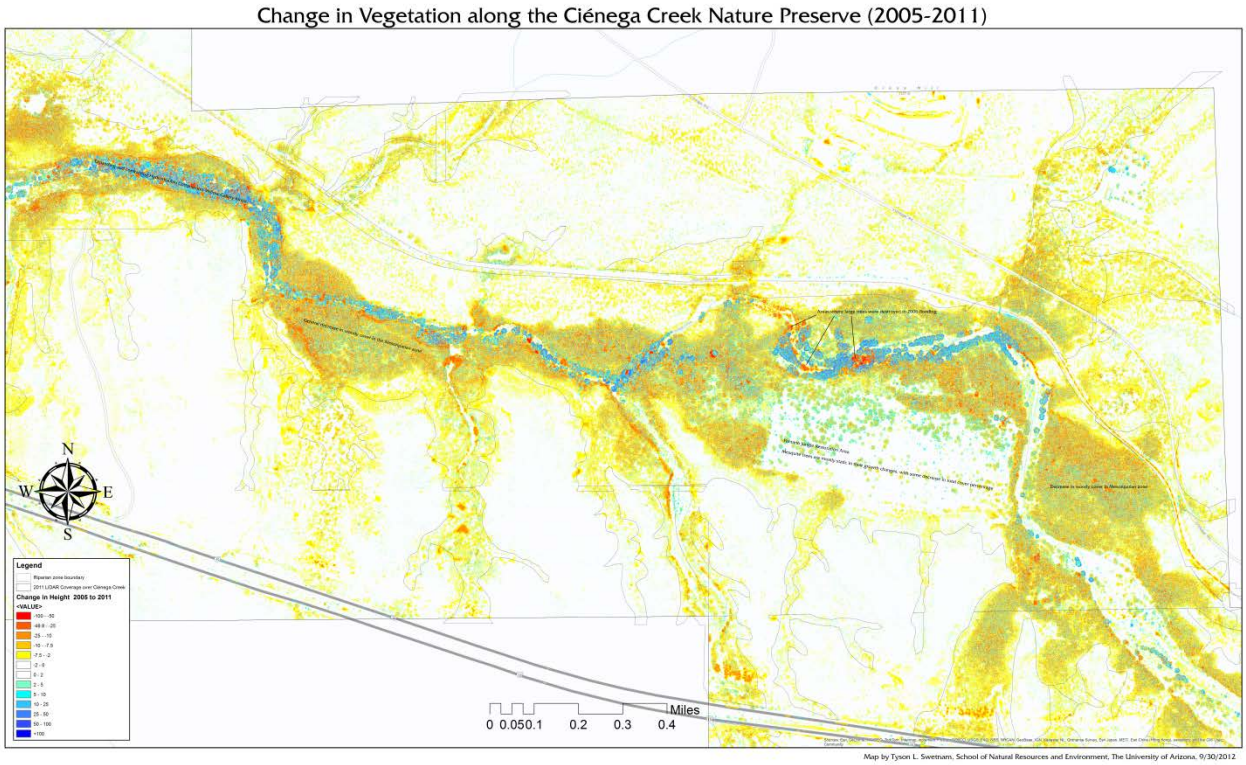

Fig. 5.1.2d Change in vegetation near the Pantano Jungle Restoration site, along the Ciénega Creek between 2005 and 2011.

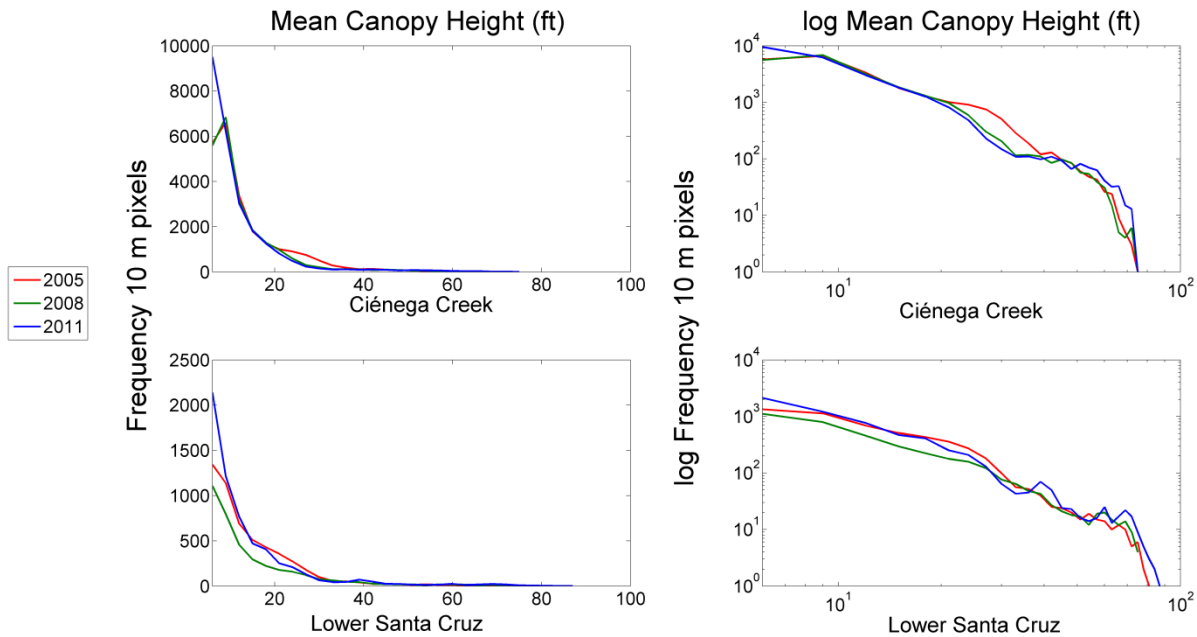

Fig. 5.1.2e: Comparison of vegetation change along the Ciénega Creek and LSRC. Note that the largest change in vegetation height class for the 10m GridMetric pixels in Ciénega Creek is in the 20 to 40 ft average height class range. On the other hand, in the LSCR the vegetation is decreased log-log linearly across most of the height distribution following the flooding less than 40 ft average height. After 2008, [represented by the blue line for 2011] there is a jump in the total proportion of very tall vegetation in Ciénega Creek for trees 50 to 80 feet, this is in response to the increasing canopy diameters of large cottonwoods along the hydroriparian zone. In the LSCR there is also an increase in trees 30 to 50 feet in height suggesting the effluent-dependent channel is supporting a new hydroriparian community not present in 2005.

5.1.3 Vegetation change in other tributaries of the Tucson Basin

In areas with two or more LiDAR acquisitions we were able to conduct change analyses of vegetation both by differencing the canopy height model (as shown above in sections 5.1.1 and 5.1.2) and by differencing the canopy height grid metric statistic [e.g. the mean canopy height] at a larger community scale. The grid metric is statistically more robust for measuring change across a community of vegetation; rather than changes within a single individual, as is possible with the canopy height model. The grid models shown here were sampled at 10 m in FUSION/LDV 'GridMetrics' and output as .ASC raster files to ArcGIS where they were mosaicked together. The layers were then clipped along the NRHI riparian zone boundary (Fonseca and Regan 2002) for each watershed and differenced across years with the ArcGIS Raster Calculator [e.g. CHM(2008) – CHM(2005) = CHM(

The impact of the 2006 meso-scale flood (Webb et al. 2008, 2013, Griffiths et al. 2009) on vegetation is apparent in all of the tributary watersheds of the LSCR, as well as the LSCR itself. The impacts to vegetation vary based on (1) the size of the catchment, and (2) the different types of vegetation in those riparian areas. Importantly, we must consider the extent of pre-2006 vegetation in any given area had already been impacted by the repeated floods in 1983 and 1993. Most of these system have been 'reset' at least once by these recent repeated flood events. Although bare in 2005 and 2008 these sites are better considered 'disturbed' or in an early stage of secondary succession rather than classified as a less productive vegetation type [e.g. xeroriparian which are in fact mesoriparian].

Notably, the vegetation size frequency distributions for most of the riparian zones analyzed appear to follow power law log-log linear scaling where large areas were evaluated (Fig. 5.1.3a, Fig. 5.1.3b).

In the LSCR, mean canopy height decreased across all height classes less than 30 ft tall log-log linearly following the 2006 event, there was also significant changes in mean height greater than 30 feet following the event. Conceptually, the scale and type of disturbance regime in the LSCR can be characterized as large flash flooding. These events have the same impact as a high severity forest fire – all individuals in the ecosystem are destroyed within the boundary of the event. When a large enough area is disturbed all of the various vegetation stages are impacted equally, the result is a log-log linear decline in vegetation height (Fig. 5.1.3a, Fig. 5.1.3b).

In the Black Wash there was very little change between 2005 and 2008, reflecting the small size of this TVV monitoring site (Fig. 5.1.3a, Fig. 5.1.3b).

In the Canada del Oro, one of the largest tributaries besides the Rillito feeding into the LSCR the changes in vegetation are similar to those in the LSCR, a log-log linear decrease across all size classes from 2005 to 2008 (Fig. 5.1.3a, Fig. 5.1.3b).

In the Ciénega Creek the impacts are very different; there is less change in the shorter height classes relative to the LSRC. There is a large impact in the average height between 20 and 40 feet from the 2006 flood, and there is a significant increase in the extent of very tall tree (>40 ft) by 2011 (Fig. 5.1.3a, Fig. 5.1.3b).

Rincon Creek was only flown in 2005 and 2008; there was significant flooding along the Creek, where some large mesquite trees were destroyed. Unlike nearby Ciénega Creek, Rincon Creek does not have a tall, mature, Hydroriparian gallery forest, although there are cottonwoods and willows throughout the drainage.

The Rillito River was flown in 2005 and 2008. The Rillito is like the Canada del Oro and LSCR with flood controls on either bank. The Rillito is also one of the largest waterways feeding into

the LSCR. The impact of the 2006 flooding is similar to these other two large systems: large vegetation >10 feet in height was negatively impacted by the flooding.

In the mouth of Sabino Canyon, a site of major flooding in 2006, average vegetation height 10 ft to 50 ft decrease following the flood (Fig. 5.1.3a, Fig. 5.1.3b). Sabino canyon was partially flown in 2005 and 2008, with the entire watershed flown in 2007 in response to the flooding. By 2008 the vegetation appears to have increased in the shorter classes, but there is a further decrease in vegetation 17 to 40 ft in height (Fig. 5.1.3a, Fig. 5.1.3b). This continued decrease may have been from continued erosion and loss of bank side vegetation following the major flooding as the new channel continued to scour the banks into 2008.

Agua Caliente and Tanque Verde washes also exhibit a similar response to the flooding as Sabino Creek and Ciénega Creek: a decrease in large vegetation 20 to 40 ft mean canopy height, with continued decreases into 2008 in the large height classes, and a slight increase in the recovery of short vegetation types.

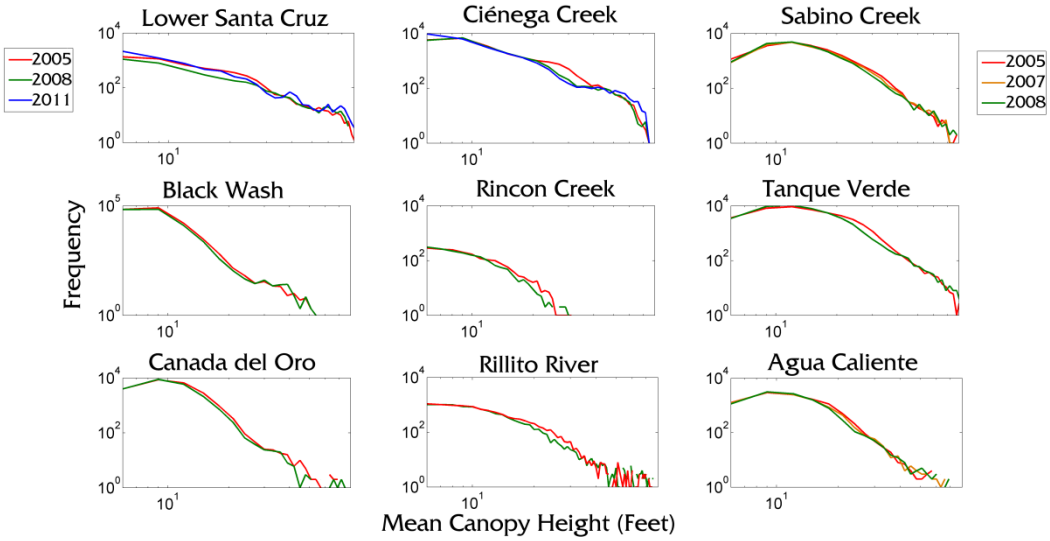

Fig. 5.1.3a Log-log scaling of the observed mean canopy height along the clipped and masked sections of the riparian zones across the LiDAR coverage area. There are four different dates in which LiDAR data was available (2005, 2007, 2008, and 2011), most locations had at least one repeat date, with multiple locations having two repetitions out of the four dates. Notably, all of the vegetation height distributions appear to follow a power law for parts of their scaling distribution. Change in vegetation along the Ciénega Creek and LSCR [for which there are three different collection dates (2005, 2008, 2011)]. After the meso-scale 2006 flood event there is a marked decrease in the average height of vegetation (red line = 2005, green line = 2008); by 2011(blue) there is a pulse of new vegetation with shorter height, but the taller height classes have not yet recovered. In both Ciénega Creek and LSCR the increase in individuals at very large size can be attributed to a bulk increase in canopy cover in large trees.

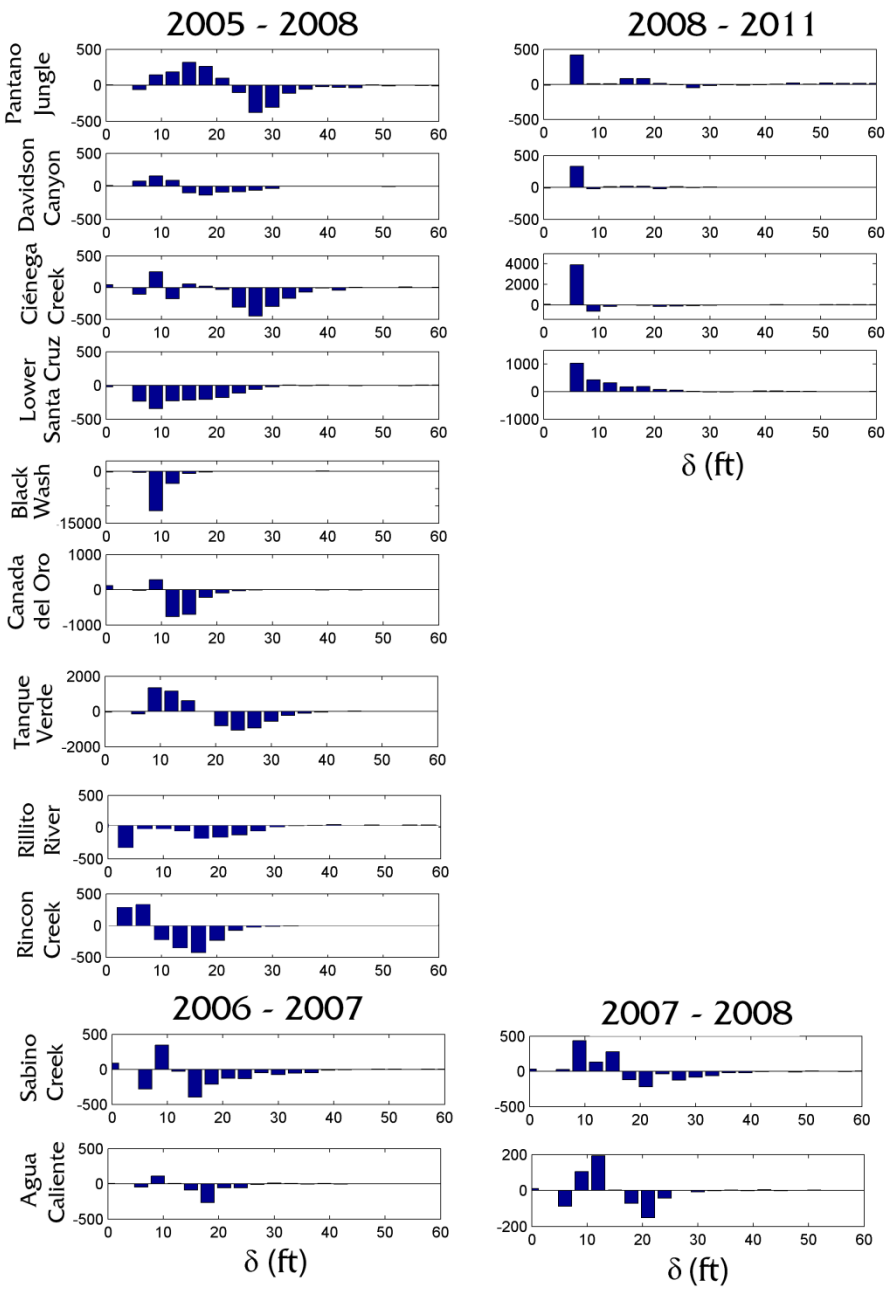

Fig. 5.1.3b Change in total vegetation volume across periods. On the x-axis are change in mean canopy height (10 m), and on the y-axis are the total number of pixels in the area. Importantly, in all areas the 2006 meso-scale flooding appears to have knocked back the vegetation total across all size classes for the 2005 to 2008 period, particularly in the 20-30 ft classes in the upper tributaries and the 10-30 ft class in the LSCR. In the 2008 to 2011 period all locations appear to be recovering with the smallest height classes increasing the fastest.

5.2 Multi-spectral Ortho-photography and Satellite Imagery

The technique we demonstrated here: creating an NDVI from a 4-band multispectral image, is one of the simplest techniques for characterizing vegetation from digital imagery. The NDVI threshold method (Carpenter 2012) was very useful as a first order approximation of what 'is' vegetation and what 'is not' for discriminating structure in a canopy height model. An important point about setting NDVI thresholds for vegetation is the seasonality and variation in vegetation greenness – NDVI images taken at different times of day, on different dates, in different years will have different threshold values. We suggest moving the threshold up and down and comparing those results to a known target until the NDVI threshold best aligns with the target. More advanced techniques that require additional spectral bands and include the creation of classification and regression tree (CART) models for computer vision and learning algorithms have already been demonstrated by Hartfield et al. (2011) using the PAG LiDAR.

The NAIP imagery are not the only multi-spectral data with dates close to the LiDAR collections. There are privately held data available for purchase, such as from Digital Globe Inc., which support a 1 m 8-band multi-spectral satellite product over Pima County. However, those data were outside the budget consideration of this project at this time. Measuring benefits gained from high resolution multi-spectral imagery was not possible in this study; however other studies using object-based image analysis (OBIA)(Ke et al. 2010, Guo et al. 2011, Nordkvist et al. 2012) which paired imagery and aerial LiDAR all report significant improvements in classification accuracy.

The availability of temporally correct multi-spectral aerial and satellite imagery was one problem identified in this study. The rapid changes in vegetation structure observed along the LSCR following the 2006 flood event are an important example of the need for having paired imagery and LiDAR. The coincidence of the NAIP imagery along dates close the aerial LiDAR acquisition helped us pair the two data sets but left some margin for error as the LiDAR is typically flown during 'leaf-off' conditions to ensure penetration of the laser through the canopies of vegetation, and the NAIP is flown during 'leaf-on' conditions to ensure the best estimate of vegetation health.

A second problem we identified in attempting to filter the LiDAR canopy height model with the NDVI revolved around the removal of the power lines in the canopy height model over the 50-year flood plain. Because the NDVI is generated from an orthogonal image it still has some horizontal error associated with it. This problem was particularly apparent when we tried to align the NDVI over the canopy height model – the power lines, being 20 or more feet off the ground are visibly offset in the ortho-photograph relative to their true location. This made their removal impossible with the unsupervised NDVI threshold technique– and likely increased the

error of omission of actual vegetation which grows adjacent to the power lines. To solve this problem we filtered the raw *.LAS data before generating a canopy height model. By running the 'FilterData' process (McGaughey 2012) in FUSION/LDV we removed returns that were above the mean elevation plus a filter parameter multiplied by the standard deviation of the elevations.

5.3 Recommended Data Density

Based on three levels of data density from the years 2005, 2008, and 2011, we report both significant benefits to increased density, as well as non-significant differences. Importantly these differences are based on the level of inference in which we are interested in observing vegetation structure. One non-significant observation was: at the 30 m grid metric level there is little to no change in the grid metric statistic value [mean canopy height or canopy cover %] with an increase in data density. The lack of change in grid metric statistics over simple structured vegetation, on flat terrain [e.g. single layer xeroriparian vegetation] suggests there is no clear benefit to having a higher density LiDAR dataset for 'community scale' vegetation characterization in the xeroriparian vegetation types. For more rigorous measures of canopy structure [i.e. canopy base height, canopy bulk density (i.e. total vegetation volume), leaf area index, and individual plant segmentation], on the other hand, the higher density LiDAR is clearly superior. This is due to the fact low density LiDAR data fails to penetrate individual tree canopies producing enough returns to derive robust canopy-based statistic. The acquisition of medium to high LiDAR data could potentially replace the need for conducting further TVV studies in Pima County. Any decrease in quality of a LiDAR data set versus transect-level TVV is far outweighed by the global coverage of a LiDAR acquisition.

In areas with complex terrain and closely placed structures [e.g. housing developments], the delineation of vegetation from geologic and human structure and the production of an accurate bare earth surface becomes tenuous. Anecdotally, neighborhoods of tightly packed houses or downtown buildings are like slot canyons where the local site conditions are modified by the buildings. In complex urban settings with trees, or in areas with complex terrain with dense vegetation cover, we recommend that data density be increased to ensure a usable number of returns can be generated to create (1) suitable bare earth surfaces, (2) defined building outlines, and (3) robust vegetation models.

The 2011 high density LiDAR allowed us to define 'individual scale' objects, like shrubs and cacti at approximately 1 ft resolution, whereas the low density 2005-2008 data was limited to 2 ft resolution. Importantly, some of the increases in precision gained from the newer data are from the advancement of the LiDAR technology: newer sensors take more accurate measurements and better algorithms for filtering and correcting the raw data now exist which further reduce uncertainty while remaining at the same point density.

Medium density data over the LSCR from 2011 are superior to the low density data available from 2005 and 2008, this is in agreement with other aerial LiDAR-based research that suggests a minimum pulse return density of at least 4 ppsm for identifying vegetation, and >8 ppsm for characterizing vegetation structure (Gatziolis and Anderson 2008, Mitchell et al. 2012). In a 2013 white paper (http://www.watershedsciences.com/about/news/lidar-pulse-densities-comparison-white-paper), Watershed Science Inc. suggest a modern standard of data usability requires LiDAR densities ≥15 ppsm; this suggestion is however based on results of studies conducted in the Pacific Northwest where vegetation is much taller and in general tree cover is higher. We cannot dismiss this recommendation out of hand; the fact that some of our vegetation communities are very small suggest an increase in precision and density may in fact improve the accuracy of both the bare earth surface models and improve our the ability to monitor desert vegetation communities.

In areas with increasingly complex vegetation where large trees are growing, such as in the Hydroriparian Cottonwood-Willow gallery forest along the Ciénega Creek and [at least for the present] in the LSCR effluent dependent zone, there were measurable benefits to the higher density LiDAR. Benefits include: (1) the ability to quantify the three dimensional vegetation structure [e.g. canopy volume and canopy base height –which are complimentary to Pima County's TVV protocol], (2) penetration [i.e. illumination] of enough laser pulses through the canopy to the surface level for the production of an accurate bare earth model (Fig. 5.3a, Fig. 5.3b), and (3) characterization of small vegetation which may play a significant role in creating habitat for wildlife. The difference in the 2005 and 2008 LiDAR (low density = 1.3 ppsm) and 2011 LiDAR (medium to high density= 4.0 - 12.5 ppsm) for bare earth modeling in the Ciénega Creek is apparent in Fig. 5.3a. The 2005 bare earth model was rather coarse and did not pick up the fine scale variability of either the stream morphology or the canyon sides, particularly in areas with densely covered vegetation. The results in the image are areas along cliffs and in the stream where geological features were miss-classified as vegetation. The 2011 bare earth model, on the other hand, supports an order of magnitude increase in spatial resolution (1 ppsm to 12 ppsm), and reveals fine detail features including channel morphology not visible in the previous LiDAR models.

In Table 5.3 we offer a brief list of benefits added and the recommendations for considering future acquisition densities.

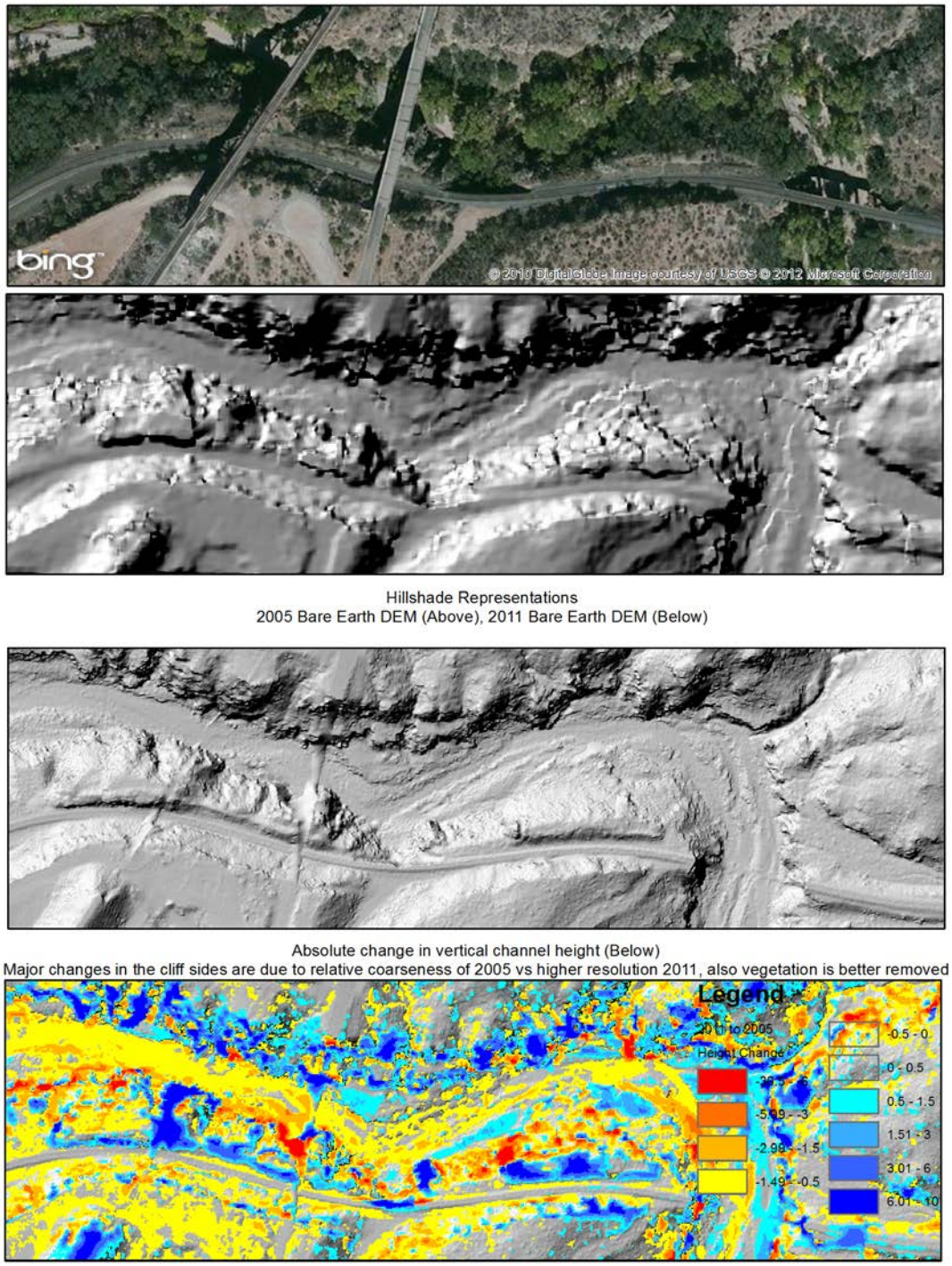

Fig. 5.3a: Example of the 2005 bare earth model (upper) and the 2011 bare earth model (lower) along Ciénega Creek. The total difference between 2005 and 2011 is shown on bottom.

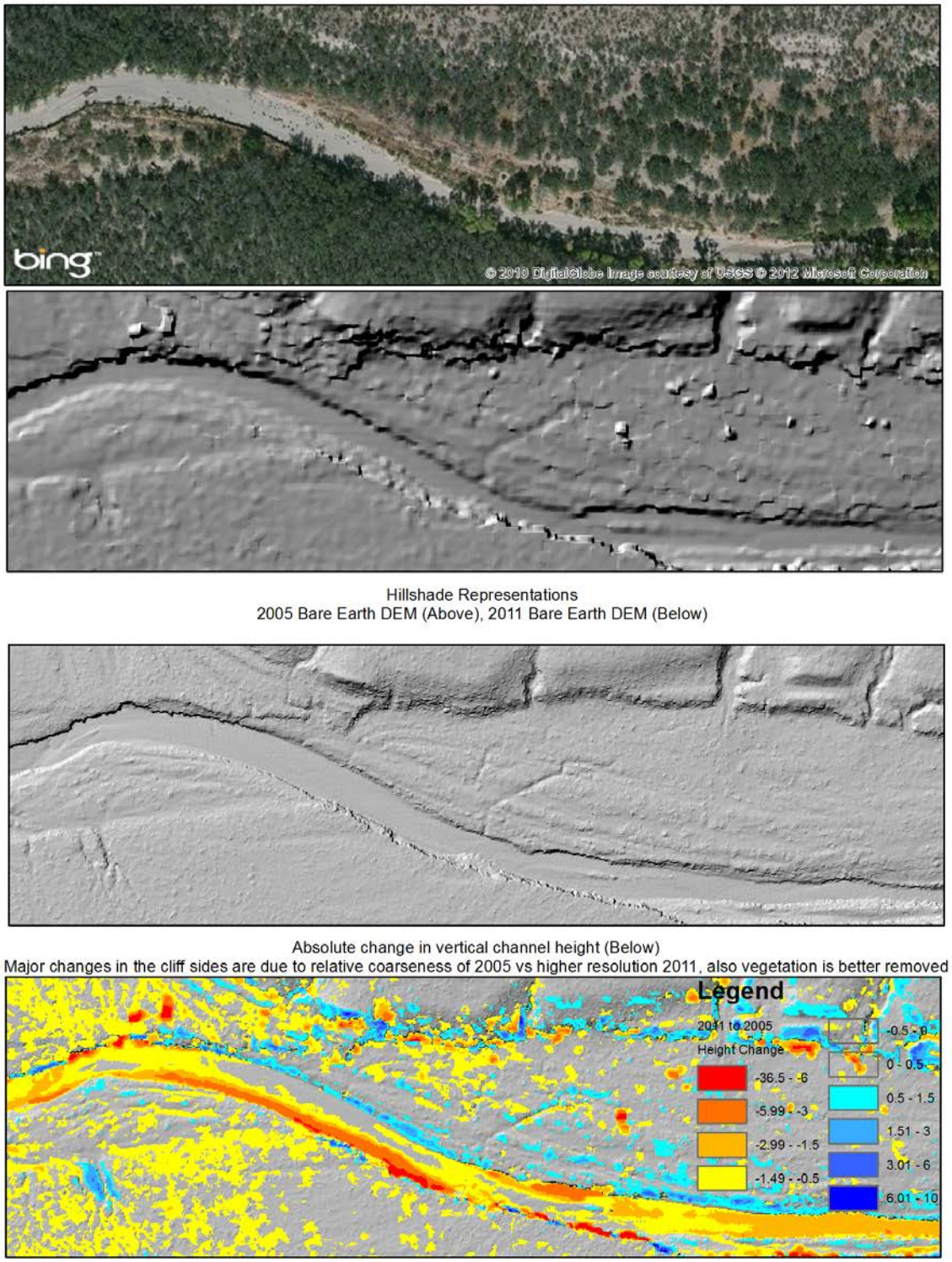

Fig. 5.3b: Example of the 2005 bare earth model (upper) and the 2011 bare earth model (lower) along Ciénega Creek. The total difference between 2005 and 2011 is shown on bottom.

Table 5.3 The cost and benefit of aerial LiDAR pulse densities.

Density	**High**	**Medium**	**Low**
Cost	$$$$	$$$	$
Point spacing	< 15 cm	30 – 60 cm	> 60 cm
Pulse Density	> 12 ppsm	4-12 ppsm	< 4 ppsm
Limitation	Cost	Cost	Surface and vegetation model accuracy
Benefit added	Individual vegetation discrimination, surface morphology under dense vegetation, replacement to TVV monitoring protocol	Most large plants will be identified, surface morphology possible in open cover areas.	Cost effective, a vast amount of relevant details gained over other remote sensing techniques
Recommendation	Collect in priority areas where vegetation monitoring is important and vegetation cover is generally high.	If high density is too costly collect in priority areas where vegetation monitoring is important.	Collect in low priority areas where vegetation monitoring is not important, or vegetation cover is in general low.

An important consideration of the costs of acquiring more dense data are the return on the investment. The benefit gained by gathering more dense data may begin to decrease and eventually the cost will outweigh the added benefit. It may not be economically practical to collect high density LiDAR data over areas for which there is no specified need.

For the vendor to generate a high density data set they must either (1) upgrade to the newest technology which has higher pulse rates and more sensitive equipment [passing that cost onto their customers], and/or (2) fly their plane at a lower elevation and slower air speed where the swath widths of flight lines are narrower and therefore require more passes to cover an area [where again they pass the added cost onto the customer]. Conversely, if they collect lower density data they can fly higher and faster with fewer flight lines and thus spend less time collecting, causing less wear to their aircraft and equipment, and spending less on fuel [allowing them to increase their profit margin]. Notably, there are also the additional costs to post-processing and storing more data for the flight.

Importantly, Moore's Law appears to still hold for most computing technology advancements; this means on average every two years the speed of computing power doubles, and the costs of computing decrease by ½. Whether Moore's Law is expressed in the capability and costs of acquiring LiDAR remains to be seen, but the authors consider it likely. Further, as additional

operators enter the market place competition for private and publically funded LiDAR contracts will likely help to drive acquisition prices lower.

5.4 Priority Coverage Areas

Based on our findings we suggest all waterways in Pima County with complex assemblages of vegetation [i.e. any mature mesoriparian mesquite bosques, hydroriparian Cottonwood-willow gallery forest, or effluent dependent hydroriparian Tamarix and willow bosque] be identified as future priority coverage areas. There are three primary reasons for acquiring a higher density LiDAR scan over riparian zones: (1) complex vegetation makes discrimination of the bare earth surface with low density LiDAR problematic, (2) characterizing dense vegetation accurately [e.g. TVV estimation] requires a high density of pulse returns from the canopy and inter-canopy space (Farid et al. 2006, 2008, James et al. 2007, Gatziolis and Anderson 2008, Evans et al. 2009, Mitchell et al. 2012) and (3) these are the most important habitat zones for migratory and endangered species of birds in the region (Webb et al. 2013). Further, these habitats are the most vulnerable to future disturbance events [e.g. a flood like observed in 2006 or a possible human-ignited wildfire].

The agency in charge of negotiating the acquisition areas should coordinate with the vendor to acquire the higher density LiDAR data over priority areas. We suggest using the 100-year flood plain boundary as the priority boundary line for monitoring vegetation in the effluent dependent zone, the Ciénega Creek, and any other hydroriparian zone in Pima County. This request should not be difficult to achieve along our rivers which tend to be mostly linear and less than ¼ mile wide. Importantly, in the past the vendor has defined the collection area on township and range section lines. The negotiation of high density coverage areas along defined polygons (provided by the agency in charge) will be key to this change in the contract. For the vendor determining the optimal flight planning is done in software so there should not be an additional cost associated in generating these targeted high density data collections other than paying for the area of the high density coverage.

5.5 Creation of a regional LiDAR Consortium

We also recommend state land-grant research institutions (e.g. University of Arizona, Arizona State University, and Northern Arizona University), as well as municipal, state, and federal government agencies, non-governmental organizations, and privately held utilities, corporations, or entities located in Arizona, and possibly New Mexico and West Texas establish a state-wide LiDAR working group, sometimes referred to elsewhere nationally as a consortium. The working group's job should be to (1) help identify and connect with all potential stakeholders of the existing and future LiDAR data collections, (2) foster awareness of national LiDAR standards, (3) determine what is affordable and how to maximize the value of new LiDAR, (4) help define where and at what scale new LiDAR should be collected, (5) determine if

specific projects can be expanded to find new stakeholders to help alleviate cost of carry, and (6) conduct Benefit-Cost analyses of the existing data collections.

A local LiDAR consortium can help local stakeholders develop single sets of purchase agreements and contracts, cutting down on duplicate work and ensuring data and price consistency. This also decreases the cost of carry, or opportunity cost, to individual groups looking to get LiDAR for a project. To date this job has been done, and will likely continue to be done by the Pima Association of Governments.

A first priority in establishing a local LiDAR Consortium should be to identify the inter-agency leaders who are willing to coordinate potential stakeholders and to identify how they can benefit from LiDAR. The leadership group might include local government staff, federal research scientists, university scientists, and private interests in Southeastern Arizona who have a need for geo-spatial data and products derived from the LiDAR. Second, ensure a collaborative environment is established for enabling the development of public-domain high-resolution LiDAR topography and derivative product data that are not duplicative and are suitable to the uses of as many consortium members as possible. Third, ensure the rapid dispersal of these data so the local users and authorities can benefit from them as soon as possible.

As a hypothetical case, let's assume the RFCD only requires Federal Emergency Management Agency (FEMA) grade point spacing of ~1 ppsm and a vertical uncertainty of ±30 centimeters for their long term flood monitoring; meanwhile a regional NGO conservation group along with the National Park Service (NPS) and Fish and Wildlife are interested in evaluating threatened and endangered species habitat [e.g. Southwestern Willow Flycatcher] along the riparian corridors of Rincon Creek, Ciénega Creek Nature Preserve, and the Las Ciénegas National Conservation Area, which requires vegetation grade LiDAR acquisition [8-12 ppsm]. The areas needed for identifying T&E habitat are known to reside within the 50-year flood plain while the area needed by the RFCD is wall-to-wall coverage. The consortium's role would be to find and negotiate with a vendor willing to fly the riparian corridors at high density and the rest of the area at low density. The vendor could parameterize their flight-plan to fly the entire area at low density for the FEMA grade LiDAR, and then fly an alternate programmed flight route along the riparian areas for the vegetation acquisition. The area of denser data should be established with the vendor not on a per-tile basis, but by the area of the polygons in which the high density data are required. An unintended consequence of not identifying the required flight area with a polygon covering the flood plain over the LSCR for the 2011 acquisition resulted in the vendor clipping the required area along a township and range section line; this caused several sections of the river channel to be clipped out of the delivered data. When these corner section data were requested post-hoc the vendor requested an additional payment

approximately twice the cost of the original 9 mi^2 acquisition area. The square blocks delivered by the vendor contained large areas [>40% of the total area] of urban setting which were not needed for our analysis of the LSCR and were essentially wasted area that could have been reallocated to allow more coverage of the riparian zone. The difference in a processed data product along a defined corridor versus a wall-to-wall tile area should be negligible; the excess cost in the vendor's proposed fee is assumed to have come from their stated need to reprocess all of the original raw data.

5.6 Benefit Cost Analysis

We suggest in future acquisition funding a small budget item be allocated for tracking and quantifying a benefit cost analysis (BCA) ratio of the newly acquired LIDAR data as well as the continuing benefits added from the older data (e.g. tracking long term changes in vegetation and channel morphology). An important consideration for continuing acquisitions is measuring the cost-savings and identifying the indirect benefits of the large scale acquisitions acquired by PAG and other agencies. Other BCA studies of aerial LiDAR have suggested large scale LiDAR acquisitions bring $3.50 and $5.00 in realized benefit for every dollar spent (Hallum and Parent 2009). The cost of acquiring aerial LiDAR in Pima County were quoted in 2011 to be: Low density [1 – 3 ppsm] = $360.00 / mi^2, Medium density [3 – 7 ppsm] = $461.00 / mi^2, High density [7 – 12 ppsm] = $869.00 /$mi^2$ (PAG personal communication). For a future 1,800 mi^2 acquisition, like those done in 2005 and 2008, the potential realized benefit is, on the low end $1.62 million, and on the high end $6.25 million dollars.

The utility of the 2005 and 2008 PAG LiDAR coverage over the entire Tucson basin has allowed multiple indirect parties that were not originally envisioned in the collection to produce beneficial study results and groundbreaking new science. To date the PAG LiDAR data has been used to: (1) rectify the ortho-imagery for the Department of Transportation, (2) develop FEMA-grade flood maps, (3) identify riparian vegetation (Carpenter 2012), (4) create an urban tree inventory (Pope 2013), (5) model impervious surfaces (Maits RFCD), (6) model urban shadows in downtown (Glenn 2012), (7) determine urban vegetation and irrigation location (Halper et al 2012), (8) urban mosquito abatement (Hartfield et al. 2011, Landau et al. 2012), (9) sediment transport (Hummel and Duan 2010, Hummel et al. 2012), and (10) landscape evolution modeling (Pelletier et al. 2009, Pelletier et al. 2013). The PAG LiDAR can also potentially help identify better locations for placement of wind farming, broad-band communication towers, and define where potential impacts of vegetation on power-lines may occur.

Digital technologies are revolutionizing the ways we view our world. LiDAR has many non-economic benefits [such as the recent rediscovery of lost cities in the jungles of Honduras, Nicaragua, and Cambodia]. Quantifying the economic impact of these scientific discoveries is a challenge, but can easily be appreciated for their effect on humanity as we increase in our

understanding of history. Disaster planning will likely continue to play a major role in determining where expanded LiDAR acquisitions are done. However, as has already been observed, benefits realized to the scientific community and to the public are likely to far out way the costs of acquiring new LiDAR. As is common in other fields of science, a small but significant contribution to a developing field often results in profound changes for humanity: the development of the personal computer [that this report was written on], and laser technology [e.g. LiDAR] are just two examples of countless technological innovations which have fundamentally changed human society.

5.7 Awareness of National Standards

It is important to understand standards by agency differ in regards to acceptable levels of pulse density and horizontal and vertical uncertainty. Here is a brief list of the agencies and societies that administer national LiDAR standards (Tables 5.6a – 5.6e). We also show several tables supporting agency standards and common deliverable products for a LiDAR acquisition.

The American Society for Photogrammetry and Remote Sensing (ASPRS) and National Digital Elevation Program (NDEP) described in the LAS v1.4 standard.
http://www.asprs.org/a/society/committees/standards/LAS_1_4_r12.pdf

National Digital Elevation Program (NDEP) Guidelines for Digital Elevation Data (2004):
http://www.ndep.gov/NDEP_Elevation_Guidelines_Ver1_10May2004.pdf

The Federal Emegerncy Management Agency (FEMA), and the United States Geological Survey (USGS) each released their own collection standards for discrete return LiDAR within the LAS format. These formats were updated to be standardized across agencies in 2010.

FEMA (2010) a memorandum on LiDAR standards:
http://www.fema.gov/library/viewRecord.do?id=4345

The FEMA specification for flood hazard mapping:
http://giscenter.isu.edu/pdf/FEMASpecsFloodHazardMapping.pdf

USGS LiDAR Base Specification Version 1.0 (2012): http://pubs.usgs.gov/tm/11b4/TM11-B4.pdf

Table 5.6a LiDAR Standards given by ASPRS, USGS, and FEMA

Item	NDEP/ASPRS LAS 1.4	USGS/FEMA
Multiple Discrete Returns	Up to 15	3+
Intensity	Optional, if available should be included Normalized to 16-bit	Required
DEM Nominal Point Spacing		<2 m
Spatial distribution (cells w/ >1 point)	Optional	95%
Scan Angle	Optional	Support horizontal + vertical accuracy
Vertical Accuracy Fundamental Consolidated Supplemental		<= 24.5 cm ACC_Z, 95% (12.5 cm RMSE) 36.3 cm, 95th percentile
Relative Accuracy Individual Swath Adjacent Swaths		<= 7 cm RMSE_z <= 10 cm RMSE_z
Flightline Overlap		>10%
Buffered edges		>100 m
File Formats	LAS 1.4 (backward compatible v1.2 or v1.3)	LAS v1.2 or v1.3
GPS Times		Adjusted GPS Time LAS v1.3
Datum Horizontal Vertical		NAD 1983 HARN NAVD 88 NGS-geoid
Coordinate Reference System	Required for all data. Either Variable Length Record (VLR), GEOTiff, or WKT	CONUS, UTM, NAD 83 HARN, Meters; NAVD88, Meters. State Plane / State Coordinate Reference System
Units of Reference	If geographic: horizontal = decimal degrees, vertical = meters.	'Feet' and 'Foot' must specify 'International', 'Intl', or 'US'.
Swath Size and Segmentation		<2 GB

Table 5.6b Pre-flight Operations Plan (from FEMA 2010).

Item	Contents	Format
Flight Operations Plan	• Planned flight lines • Planned GPS stations • Planned control • Planned airport locations • Calibration plans • Quality procedures for flight crew (project-related for pilot and operator) • Planned scan set (sensor settings and altitude) • Type of aircraft • Procedure for tracking, executing, and checking reflights • Considerations for terrain, cover, and weather in project	MS Word or PDF

Table 5.6c Post-flight Aerial Acquisition and Calibration Report (from FEMA 2010).

Item	Contents	Format
GPS Base station info	• Base station name • Latitude/Longitude (ddd-mm-ss.sss) • Base height (Ellipsoidal meters) • Maximum Position Dilution of Precision PDOP • Map of locations	Excel, TXT, MS Word, or PDF for data; ESRI shape file for map of locations (data and info may be in attribute table)
GPS/IMU processing summary	• Max Horizontal GPS Variance (cm) • Max Vertical GPS Variance (cm) • Notes on GPS quality (High, Good, etc.) • GPS separation plot • GPS altitude plot • PDOP plot • Plot of GPS distance from base station/s	MS Word or PDF with screenshots
Coverage	• Verification of project coverage	ESRI shape files reflecting the actual coverage area and not the applicable tiles.
Flights	• As-flown trajectories • Calibration lines	ESRI shape files
Flight logs	Incorporated as appendix Should include: • Job # / name • Lift # • Block or AOI designator • Date • Aircraft tail number, type • Flight line, line #, direction, start/stop, altitude, scan angle/rate, speed, conditions, comments • Pilot name • Operator name • AGC switch setting • Laser pulse rate • Mirror rate • Field of view • Airport of operations • GPS base station names or numbers • Comments	
Control	• Ground control and base station layouts	ESRI shape files
Data verification/QC	• Description of data verification/QC process • Results of verification and QC steps	MS Word, Excel or PDF

Table 5.6d Vendors may offer the option to classify the LAS data to the LAS 1.4 (ASPRS 2011) standard, each code is represented in this table.

Code	Description
0	Created, not classified
1	Processed unclassified
2	Bare Earth or Ground
3	Low Vegetation
4	Medium Vegetation
5	High Vegetation
6	Building
7	Noise (low point)
8	Model Key-point (mass)
9	Water
10	Ignored Ground (break line proximity)
11	Withheld
12	Overlap Points
13-31	Reserved for later definition

Table 5.6e Establishing what will be delivered is an important part of the contract. Typical data products from vendors now include:

Deliverables	Description
Project Report	Detailed report that includes: Acquisition, Data Processing, Accuracy Assessment, Projection/Datum Units.
Pulse Data	
.ASC or .CSV	ASCII files that contain columns for X,Y,Z, Intensity, etc.
.LAS	Most Common Discrete LiDAR data format
.LAZ	Loss-less Compressed .LAS file type
.LVIS	Full Waveform data format
.PLS	PuLSe file for Full Waveform PulseWaves format
.WVS	WaVeS file for Full Waveform PulseWaves format
.XYZ	ASCII data only for three axes in volume space
Vector Data	
Tile Index	of .LAS files in shapefile format
Area Perimeter	Polygon shapefile of total flight area
Flight Survey	Smoothed best estimated trajectory (SBET) of continuous aircraft positions and altitude.
Raster Data	
DEM	Ground point derived elevation model (typically 1 m resolution)
Spectral Intensity	High resolution image of laser spectral intensity, typically in a non-normalized 8-bit [0-255]format.

5.8 Software and Online Support Networks

There are many versions of software available for analyzing LiDAR data. Here we demonstrated a freely available software, FUSION (McGaughey 2012) for analyzing vegetation; there are multiple other software platforms (both commercial and open-source) for analyzing LiDAR data that users should be aware of.

Free Software

FUSION: http://forsys.cfr.washington.edu/fusion/fusionlatest.html

BCAL LiDAR Tools: http://bcal.boisestate.edu/tools/lidar/

SAGA: http://www.saga-gis.org/

MCC-LIDAR: http://sourceforge.net/apps/trac/mcclidar/

CloudCompare: http://www.danielgm.net/cc/

Commercial Software

ENVI: http://www.exelisvis.com/Home.aspx

MARS: http://www.merrick.com/Geospatial/Services/MARS-Software

Terrasolid/Terrascan: http://www.terrasolid.fi/

Rapidlasso: http://rapidlasso.com/

General Resources & Vendors

OpenTopography (NSF): http://www.opentopography.org/

National Center for Airborne Laser Mapping (NCALM – NSF): http://www.ncalm.cive.uh.edu/

USGS LiDAR for Science and Resource Management: http://ngom.usgs.gov/dsp/index.php

Sanborn Inc.: http://www.sanborn.com/

Watershed Sciences Inc.: http://www.watershedsciences.com/

Reigl: http://www.rieglusa.com/index.html

Leica: http://www.leica-geosystems.us/en/Airborne-LIDAR_86814.htm

Existing State Level LiDAR Consortiums

Puget Sound LiDAR Consortium: http://www.pugetsoundlidar.ess.washington.edu/

Oregon LiDAR Consortium: http://www.oregongeology.org/sub/projects/olc

Idaho LiDAR Consortium: http://www.idaholidar.org/

South Carolina LiDAR Consortium: http://www.dnr.sc.gov/GIS/lidar.html

6 Data

6.1 Acronym descriptions

Table 6.1 Acronyms used in this document

Acronym	Long Name	Acronym	Long Name
ASCII	American Standard Code for Information Interchange	LSCR	Lower Santa Cruz River
ALSM	Airborne Laser Swath Mapping	MSCP	Multi-Species Conservation Plan
AMSL	Above Mean Sea Level	NAD	North American Datum
BE	Bare Earth	NAD83	North American Datum 1983
CHM	Canopy Height Model	NAIP	National Agricultural Imagery Program
CSM	Canopy Surface Model	NAVD83	North American Vertical Datum 1983
CSV	Comma Separated Value	NDEP	National Digital Elevation Program
DEM	Digital Elevation Model	NDVI	Normalized Difference Vegetation Index
DTM	Digital Terrain Model	NIR	Near Infra-Red
EIS	Environmental Impact Statement	NVCS	National Vegetation Classification System
EPA	Environmental Protection Agency	PAG	Pima Association of Governments
ESA	Endangered Species Act	RFCD	[Pima County] Regional Flood Control District
EVI	Enhanced Vegetation Index	RMSE	Root Mean Square Error
EVT	Existing Vegetation Type	RRP	Reviving River Project
FEMA	Federal Emergency Management Agency	RWRD	Regional Wastewater Reclamation Department
FWS	Fish and Wildlife Service	SAVI	Soil Adjusted Vegetation Index
HARN	High Accuracy Reference Network	TLS	Terrestrial LiDAR Scan
HRMS	Horizontal root mean square	TSMS	Tucson Stormwater Management Study
HUC	Hydrological Unit Code	TVV	Total Vegetation Volume
GIS	Geographic Information System	USDA	United States Department of Agriculture
GPS	Global Positioning System	USFS	United States Forest Service
LANDSAT	NASA land-viewing imaging satellite	USCR	Upper Santa Cruz River
LANDFIRE	Nationally consistent vegetation mapping project	USGS	United States Geological Survey
LAS	Log ASCII Standard	WRF	Wastewater Reclamation Facility
LiDAR	Light Detection and Ranging	WSI	Watershed Sciences Incorporated

6.2 Definitions

***.ASC** – the ASCII file are text files that are useful for their ability to be ported directly into ArcGIS from FUSION outputs, ex. the products from GridMetrics, and DTM2ASCII.

***.BAT** – Windows batch command files, we use .BAT commands to run on select sets of files in FUSION.

***.CSV** – Comma Separated Value, basic text files that use commas as separator values. Can be used to support either grid or table data.

***.DTM** – Digital Terrain Models that are produced by FUSION. We produced *.dtm files for both the bare earth model and the canopy height modeling exercises.

***.EXE** – Windows executable commands, these are done mostly through the FUSION batch processing.

***.LAS** – the Log ASCII Standard file format for all LiDAR data products, see specifications in the ASPRS Guidelines (2011) and USGS (2010)

***.LDA** – the LiDAR Data file produced by FUSION, this file is indexed by the .LDI and .LDX file types.

***.TXT** – Text files that contain lists of file names (see below for tips on generating file lists).

6.3 File Tree

Bare earth

Bare earth models were produced at 2 ft resolution; this scale exceeded the ground return pulse density in locations with vegetation. All data were collected in Central Arizona State Plane, NAD89-92, NAVD88, International Feet.

To correct for no-data pixels we used a 5 x 5 smooth and median filter on the surface model. We were not interested in creating a hydrographically correct surface – this has already been done at 10m resolution by the PCRFD. Instead we were interested in capturing the finest scale variability in the surface as possible to assist in measuring vegetation amongst the riparian stream features. These variations are apparent when we create hill shades of the bare surfaces in ArcGIS (Fig. 3.1.1a – 3.1.1d).

The data are saved as *.ASC files in township and range section tiles. We do not mosaic these data in the deliverable files because the size of the mosaic dataset would far exceed what ArcGIS and many other spatial analysis software are capable of handling at one time in memory. These individual tiles can be mosaicked by users to create their own custom project areas with manageable file sizes.

Canopy Height Models

2 ft (0.6096 m) canopy height models (CHM) were generated for all years. All data were collected in Central Arizona State Plane, NAD89-92, NAVD88, International Feet.

The 2011 data in the Santa Cruz and Ciénega Creek sections were collected at higher densities that can support 1 ft (0.3048 m) CHM. We deliver only the 2 ft model so that the data can be pyramided on top of one another across all years. The BATCH folder contains the necessary

*.BAT code to reprocess the tiles at other resolutions. The CHM are saved as *.ASC in their individual township and range section tiles, for the same reasons as given for the bare earth.

Canopy Surface Model

A canopy surface model is produced when the maximum height value of the LiDAR pulse cloud is selected. We did not produce a surface model in this effort; however, a surface height model can be easily generated by adding the bare earth model to the canopy height model in ArcGIS Raster Calculator.

The *.LAS derivatives are saved into a file tree under the years they were collected [e.g. **PAG2005**, **RFCD2007**, **PAG2008**, and **PAG2011**]. The sub-folders in each directory are:

> **CHM** – the 2 ft canopy height models saved as .DTM [FUSION] *.ASC format files [ArcGIS]
>
> **DTM** – the 2 ft bare earth models saved as .DTM [FUSION] *.ASC format files [ArcGIS]
>
> **GRIDMETRICS** – Subfolders contain the 10M and 30M grid metrics saved as *.ASC format files, also all Statistics are saved as *.CSV and contains all of the metrics for each tile.
>
> **QA/QC** – results of the FUSION Catalog for each of the study areas in the report, for each year in which there were data.

BATCH - In this folder are all of the FUSION/LDV (McGaughey 2012) Batch files used to create the LiDAR data derivatives.

SHAPE – In the 2005, 2008, and 2011 folders are shape files that can be opened in ArcGIS which show the LiDAR coverage of each year.

FIGURES - In this folder are the high resolution maps (300dpi) produced over the project areas. The figures are reproduced in this report at page scale resolution.

DOCUMENTATION - In this folder are (1) the LiDAR Campaign Reports and associated meta-data products for the acquisitions (density maps, coverage, etc.); (2) National Standards for LiDAR data; (3) Hydrological research reports involving the Santa Cruz or similar systems with LiDAR; (4) Pima County vegetation monitoring reports reviewed for this study; and (5) the Historical Conditions report, and details of this projects source funding.

References

Asner, G. P., Flint Hughes, R., Varga, T. A., Knapp, D. E., & Kennedy-Bowdoin, T. 2009. Environmental and biotic controls over aboveground biomass throughout a tropical rain forest. *Ecosystems*, *12*(2), 261-278.

Asner, G. P., Powell, G. V., Mascaro, J., Knapp, D. E., Clark, J. K., Jacobson, J., ... & Hughes, R. F. 2010. High-resolution forest carbon stocks and emissions in the Amazon. *Proceedings of the National Academy of Sciences*, *107*(38), 16738-16742.

Asner GP, Hughes RF, Mascaro J, et al. 2011a. High-resolution carbon mapping on the million-hectare Island of Hawaii. Frontiers Ecology and Environment; doi:10.1890/100179.

Asner G.P., J. Mascaro, H.C. Muller-Landau, G. Vieilledent, R. Vaudry, M. Rasamoelina, J. Hall, and M. van Breugel. 2011b. A universal airborne LiDAR approach for tropical forest carbon mapping. Oecologia. 168:1147-1160.

Asner G.P., J.K. Clark, J. Mascaro, R. Vaudry, K.D. Chadwick, G.Vieilledent, M. Rasamoelina, A. Balaji, T. Kennedy-Bowdoin, L. Matoug, et al. 2012. Human and environmental controls over above ground carbon storage in Madagascar. Carbon Balance and Management. Vol. 7(1) 2012, 2, DOI: 10.1186/1750-0680-7-2.

Boryan, C., Yang, Z., Mueller, R., & Craig, M. 2011. Monitoring US agriculture: The US Department of Agriculture, National agricultural statistics service, cropland data layer program. *Geocarto International*, *26*(5), 341-358.

Carpenter, L. 2012. Use of LiDAR and Multi-spectral Imagery to Characterize Riparian Vegetation. MS-GIST Project Report. http://m.tucsonaz.gov/files/gis/P_Carpenter_LiDAR_1.2013.pdf

Drake JB, Knox RG, Dubayah RO, Clark DB, Condit R, Blair JB, Hofton M. 2003. Above-ground biomass estimation in closed canopy neotropical forests using lidar remote sensing: factors affecting the generality of relationships. Glob Ecol Biogeography 12:147–59.

Evans, J. S., Hudak, A. T., Faux, R., & Smith, A. 2009. Discrete return LiDAR in natural resources: recommendations for project planning, data processing, and deliverables. *Remote Sensing*, *1*(4), 776-794.

Farid, A., Goodrich, D. C., & Sorooshian, S. 2006. Using airborne lidar to discern age classes of cottonwood trees in a riparian area. *Western Journal of Applied Forestry*, *21*(3), 149-158.

Farid, A., Goodrich, D. C., Bryant, R., & Sorooshian, S. 2008. Using airborne lidar to predict Leaf Area Index in cottonwood trees and refine riparian water-use estimates. *Journal of Arid environments*, *72*(1), 1-15.

FEMA 2010, Procedure Memorandum No. 61 - Standards for Lidar and Other High Quality Digital Topography. p. 26. http://www.fema.gov/library/viewRecord.do?id=4345

Frazer, G. W., Magnussen, S., Wulder, M. A., & Niemann, K. O. 2011. Simulated impact of sample plot size and co-registration error on the accuracy and uncertainty of LiDAR-derived estimates of forest stand biomass. *Remote Sensing of Environment*, *115*(2), 636-649.

Fonseca, J. and J. Regan. 2002. Map revision for the riparian habitat mitigation ordinance. Memorandum to the Pima County Board of Supervisors.

Gatziolis, D., & Andersen, H. E. 2008. *A guide to LiDAR data acquisition and processing for the forests of the Pacific Northwest* (pp. 1-32). US Department of Agriculture, Forest Service, Pacific Northwest Research Station.

Glenn E. A demonstration and discussion of shadow analysis techniques applicable to Tucson's downtown. http://cms3.tucsonaz.gov/files/gis/p_glenn_shadow_1.13.2012.pdf

Griffiths, P. G., Magirl, C. S., Webb, R. H., Pytlak, E., Troch, P. A., & Lyon, S. W. 2009. Spatial distribution and frequency of precipitation during an extreme event: July 2006 mesoscale convective complexes and floods in southeastern Arizona. *Water Resources Research*, *45*(7).

Guo, L., Chehata, N., Mallet, C., & Boukir, S. 2011. Relevance of airborne lidar and multispectral image data for urban scene classification using Random Forests. *ISPRS Journal of Photogrammetry and Remote Sensing*, *66*(1), 56-66.

Hallum, D., S. Parent 2009. Developing a Business Case for Statewide Light Detection and Ranging Data Collection. http://watercenter.unl.edu/PRS/PRS2009/Posters/Hallum%20Doug.pdf

Halper, E. B., Scott, C. A., & Yool, S. R. 2012. Correlating Vegetation, Water Use, and Surface Temperature in a Semiarid City: A Multiscale Analysis of the Impacts of Irrigation by Single-Family Residences. *Geographical Analysis*,*44*(3), 235-257.

Hartfield, K. A., Landau, K. I., & Leeuwen, W. J. V. 2011. Fusion of high resolution aerial multispectral and LiDAR data: Land cover in the context of urban mosquito habitat. *Remote Sensing*, *3*(11), 2364-2383.

Huete, A. R. 1988. A Soil-Adjusted Vegetation Index (SAVI). Remote Sensing of Environment, vol. 25:295-309.

Huete, A.R., K. Didan, T.Miura, E.P. Rodriguez, X. Gao, L.G. Ferreira 2002. Overview of the radiometric and biophysical performance of the MODIS vegetation indices. Remote Sensing of Environment 83(2002) 195-213.

Huete, A., Didan, K., Miura, T., Rodriguez, E. P., Gao, X., & Ferreira, L. G. 2002. Overview of the radiometric and biophysical performance of the MODIS vegetation indices. *Remote sensing of environment*, *83*(1), 195-213.

Hummel, R., & Duan, J. G. 2010. Modeling Sediment Transport in the Pantano Wash, Tucson. In *World Environmental and Water Resources Congress 2011@ sBearing Knowledge for Sustainability* (pp. 4246-4254). ASCE.

Hummel, R., Duan, J. G., & Zhang, S. 2012. Comparison of Unsteady and Quasi-Unsteady Flow Models in Simulating Sediment Transport in an Ephemeral Arizona Stream1. *JAWRA Journal of the American Water Resources Association*, *48*(5), 987-998.

James, L. A., Watson, D. G., & Hansen, W. F. 2007. Using LiDAR data to map gullies and headwater streams under forest canopy: South Carolina, USA.*Catena*, *71*(1), 132-144.

Jenkins, J.C.; Chojnacky, D.C.; Heath, L.S.; Birdsey, R.A. 2004. A comprehensive database of biomass regressions for North American tree species. Gen. Tech. Rep. NE-319. Newtown Square, PA: U.S. Department of Agriculture, Forest Service, Northeastern Research Station. 45 p.

Jiang, Z., Huete, A. R., Didan, K. & Miura T. 2008. Development of a two-band Enhanced Vegetation Index without a blue band, Remote Sensing of Environment, 112(10), 3833-3845.

Ke, Y., Quackenbush, L. J., & Im, J. 2010. Synergistic use of QuickBird multispectral imagery and LIDAR data for object-based forest species classification. *Remote Sensing of Environment*, *114*(6), 1141-1154.

Kerr, J. T., & Ostrovsky, M. 2003. From space to species: ecological applications for remote sensing. *Trends in Ecology & Evolution*, *18*(6), 299-305.

Korhonen, L., Korpela, I., Heiskanen, J., & Maltamo, M. 2011. Airborne discrete-return LIDAR data in the estimation of vertical canopy cover, angular canopy closure and leaf area index. *Remote Sensing of Environment*, *115*(4), 1065-1080.

Landau, K. I., & van Leeuwen, W. J. 2012. Fine scale spatial urban land cover factors associated with adult mosquito abundance and risk in Tucson, Arizona.*Journal of Vector Ecology*, *37*(2), 407-418.

LANDFIRE: LANDFIRE 1.1.0 Vegetation Dynamics Models. 2010. [Homepage of the LANDFIRE Project, U.S. Department of Agriculture, Forest Service; U.S. Department of the Interior][Online]. Available: http://www.landfire.gov/index.php [2010, October 28].

Lefsky M.A., Cohen W.B., Harding D.J., Parker G.G., Acker S.A., Gower S.T. 2002a. Lidar remote sensing of above-ground biomass in three biomes. Glob Ecol Biogeogr 11:393–9.

Lefsky M.A., Cohen W.B., Parker GG, Harding DJ. 2002b. Lidar remote sensing for ecosystem studies. Bioscience 52:19–30.

Lefsky M.A., Harding D.J., Keller M., Cohen W.B., Carabajal C.C., Espirito-Santo F.D.B., Hunter M.O., Oliveira R. Jr. 2005. Estimates of forest canopy height and aboveground biomass using ICESat. Geophys Res Lett 32:L22S02. doi:10.1029/2005GL023971.

Levin, S.A. 1992. The problem of pattern and scale in ecology. Ecology 73: 1943-1967

Mascaro, J., Detto, M., Asner, G. P., & Muller-Landau, H. C. 2011. Evaluating uncertainty in mapping forest carbon with airborne LiDAR. *Remote Sensing of Environment*, *115*(12), 3770-3774.

McGaughey, R. 2012. FUSION / LDV: Software for LiDAR Data Analysis and Visualization. USDA Forest Service, Pacific Northwest Research Station.

Mitchell, B., Walterman, M., Mellin, T., Wilcox, C., Lynch, A. M., Anhold, J., ... & Fisk, H. 2012. Mapping vegetation structure in the Pinaleno Mountains using lidar-phase 3: Forest inventory modeling. *Notes*.

Nordkvist, K., Granholm, A. H., Holmgren, J., Olsson, H., & Nilsson, M. 2012. Combining optical satellite data and airborne laser scanner data for vegetation classification. *Remote Sensing Letters*, *3*(5), 393-401.

Pelletier, J. D., Engelder, T., Comeau, D., Hudson, A., Leclerc, M., Youberg, A., & Diniega, S. 2009. Tectonic and structural control of fluvial channel morphology in metamorphic core complexes: The example of the Catalina-Rincon core complex, Arizona. *Geosphere*, *5*(4), 363-384.

Pelletier, J. D., Barron-Gafford, G. A., Breshears, D. D., Brooks, P. D., Chorover, J., Durcik, M., ... & Troch, P. A. 2013. Coevolution of nonlinear trends in vegetation, soils, and topography with elevation

and slope aspect: A case study in the sky islands of southern Arizona. *Journal of Geophysical Research: Earth Surface*.

Pope, J. 2013. Presentation to Stormwater Management Working Group: http://www.pagnet.org/documents/committees/SWMWG/2013/SWMWG-2013-02-12-Presentation-2-PopePAG--PresentationHowGISAndPAGLidarCanHelpLID-Applications.pdf

RFCD 2010. Regulated riparian habitat mitigation standards and implementation guidelines. Supplement to Title 16 Chapter 16.30 of the Watercourse and Riparian Habitat Protection and Mitigation Requirements Ordinance No. 2005-FC2 January 2010

RECON 2009. Standard Operating Procedure: Quantitative Methods for Regulated RiparianHabitat Boundary Modification and On-Site Vegetation Surveys. Submitted to Pima County Regional Flood Control District, June 10 2009. 34 pages with appendices.

RECON. 2011. Requisition #1100233-Pantano at Melpomene HMMP Annual Vegetation

Ridd, M. K. 1995. Exploring a VIS (vegetation-impervious surface-soil) model for urban ecosystem analysis through remote sensing: comparative anatomy for cities†. *International Journal of Remote Sensing*, *16*(12), 2165-2185.

Rollins, M. G. 2009. LANDFIRE: a nationally consistent vegetation, wildland fire, and fuel assessment. *International Journal of Wildland Fire*, *18*(3), 235-249.

Sanborn Inc. 2007. LiDAR Campaign Final Report For Pima County Regional FCD Topographic Mapping of the Santa Catalina Mountains, May 2007.

Sanborn Inc. 2009. Pima Association of Governments 2008 Digital Orthophotography and LiDAR Project LiDAR Campaign Report, July 08, 2009.

Sanborn Inc. 2011. Pima Association of Governments (PAG) LiDAR Campaign (Pima County, AZ) Report of Survey, August, 2011.

TSMS 2013. http://cms3.tucsonaz.gov/transportation/wp-habitat-class

Ustin, S. L., & Gamon, J. A. 2010. Remote sensing of plant functional types.*New Phytologist*, *186*(4), 795-816.

Van Leeuwen, M., & Nieuwenhuis, M. 2010. Retrieval of forest structural parameters using LiDAR remote sensing. *European Journal of Forest Research*, *129*(4), 749-770.

Westland Resources, Inc. 2009. Pantano Wash Permanent Bank Stabilization and Channelization Project Habitat Mitigation.

Webb, R.H., C.S. Magirl, P.G. Griffiths, D.E. Boyer. 2008. Debris Flows and Floods in Southeastern Arizona from Extreme Precipitation in July 2006: Magnitude, Frequency, and Sediment Delivery. USGS Open-file Report 2008-1274

Webb. R.H, J.L. Betancourt, R.M. Turner, R.R. Johnson. 2013.The Santa Cruz River Near Tucson: Historic Change of an Arid-region River. University of Arizona Press. pp. 501.

White, M.S. 2011. Effluent-dominated waterways in the Southwestern U.S.—Advancing Water Policy through Ecological Analysis. Ph.D dissertation, Arizona State University, Tempe, Arizona.